

In Vivo ^{13}C Stable Isotope Tracing of Single Leaf Development in the Cold

Dipl.-Biologe Frederik Dethloff

25. Oktober 2013

Dissertation zur Erlangung des akademischen Grades
Doctor rerum naturalium (Dr. rer. nat.) im Fach Biologie

eingereicht an der
Mathematisch-Naturwissenschaftlichen Fakultät der
Universität Potsdam

This work is licensed under a Creative Commons License:
Attribution - Noncommercial - Share Alike 3.0 Germany
To view a copy of this license visit
<http://creativecommons.org/licenses/by-nc-sa/3.0/de/>

Published online at the
Institutional Repository of the University of Potsdam:
URL <http://opus.kobv.de/ubp/volltexte/2014/7048/>
URN <urn:nbn:de:kobv:517-opus-70486>
<http://nbn-resolving.de/urn:nbn:de:kobv:517-opus-70486>

This thesis was prepared at the

Max Planck Institute of Molecular Plant Physiology

Am Mühlenberg 1

14476 Potsdam – Golm

in the research group "Applied Metabolome Analysis" of Dr. habil. Joachim Kopka between April 2010 and October 2013.



Declaration

I hereby declare that the work presented in this thesis has been carried out by myself and does not incorporate any material previously submitted for another degree in any university. To the best of my knowledge, it does not contain any material previously written by another person, except where reference is made in the text.

Erklärung

Ich erkläre hiermit, die für diese Dissertationsschrift angefertigten Arbeiten selbst ausgeführt zu haben. Die Dissertationsschrift beinhaltet kein Material, das für andere Abschlüsse an dieser oder einer anderen Universität eingereicht wurde. Ich habe für diese Dissertationsschrift keine anderen als die angegebenen Hilfsmittel und Quellen verwendet.

Potsdam, October 25, 2013

Frederik Dethloff

Acknowledgement

A lot of people supported me during my PhD and made it a wonderful time.

The first and biggest thanks go to Joachim Kopka, my direct supervisor. We had a lot of extensive and fruitful discussions, which not least contributed to the success of this work. Moreover the whole Kopka group deserve my thanks for providing a pleasant and productive environment. My special thanks go to Ines and Alex who were always there for me with advice and support when I needed help with the GC-MS.

My very special thanks are due to my family for supporting me not only during the last 3 years, but during a whole lifetime. This also goes to Dr Heribert Steinmetz and my two grandmothers. A very important person who deserves a big thank you is Lena, who supported me the most during the time of writing.

Furthermore, I want to thank my friends, especially in Berlin, who culinarily and musically upgraded my PhD time.

Finally, I want to thank the Max Planck Society for funding, and the IMPRS for a great education with special thanks to Ina Talke.

Last but not least I want to thank the whole MPI-MP Institute and especially Kerstin Otto.

Table of Contents

Acknowledgement	II
Abstract	VI
Zusammenfassung.....	VII
1 Introduction.....	1
1.1 Carbon isotope tracing	1
1.2 Feeding methods	3
1.3 Leaf growth.....	3
1.3.1 The role of carbon in leaf growth	4
1.3.2 The growing leaf.....	5
1.4 Growth in cold	7
1.5 What is known about the reil genes	8
1.6 Aim and structure.....	10
2 Materials and methods	11
2.1 Plant cultivation	11
2.1.1 Optimal plant cultivation for controls.....	11
2.1.2 Plant cultivation in the cold	11
2.2 Molecular biological material for <i>in situ</i> expression with promotor-GUS studies..	12
2.2.1 Generation of promotor-GUS plants.....	12
2.2.2 <i>Agrobacterium</i> transformation.....	13
2.2.3 <i>Arabidopsis</i> transformation.....	13
2.2.4 Extraction of genomic DNA from plant	13
2.2.5 PCR.....	14
2.2.6 Electrophoresis of DNA.....	14
2.2.7 GUS staining.....	15
2.3 Measurements and documentation.....	16
2.3.1 Morphometric measurements for growth and documentation.....	16

2.3.2	Documentation of carboxyfluorescein diacetate (CFDA)	17
2.3.3	Gravimetric measurements	17
2.3.4	Visualisation of feeding	17
2.3.5	Solutions for stable isotope tracing.....	18
2.4	Labelling and harvesting approach	18
2.4.1	<i>Arabidopsis</i> plant labelling with a petiole or hypocotyl feeding assay	18
2.4.2	Leaf harvesting.....	19
2.5	Sample preparation for GC-MS analysis	20
2.5.1	Sample extraction.....	20
2.5.2	Metabolite profiling	21
2.5.3	Exact quantification of metabolites with GC-MS.....	22
2.6	Processing of GC-MS data from ¹³ C-isotope tracing studies	22
2.7	Statistical analysis.....	28
3	Results.....	30
3.1	Development of isotope tracing assays for single leaves.....	30
3.1.1	Metabolic analysis of single leaves – choice of harvesting procedure and assessment of size limitations	30
3.1.2	Downscaling of the conventional GC-MS-based metabolite profiling.....	33
3.1.3	Petiole feeding assay – stable isotope tracing for <i>in vivo</i> primary metabolites ...	34
3.1.4	Hypocotyl feeding assay – for homogeneous feeding	48
3.2	The single leaf metabolism of sequential developmental stages in an <i>Arabidopsis</i> rosette	57
3.2.1	Metabolic pool size differences between single leaf positions in <i>Arabidopsis</i> rosettes	57
3.2.2	Metabolic differences of single leaves between cold and warm development....	62
3.2.3	Hypocotyl feeding of ¹³ C-sucrose and stable isotope tracing in single leaves of plants grown under control conditions.....	64
3.2.4	Relative ¹³ C composition under cold development	67

3.3	First analysis of <i>REIL1</i> and <i>REIL2</i>	70
3.3.1	Promoter-GUS studies for <i>in situ</i> expression analysis.....	70
3.3.2	Single leaf metabolic analysis of <i>reil2</i> grown in the cold.....	73
4	Discussion.....	75
4.1	Metabolic inactivation harvest of multiple single leaves from a whole rosette.....	75
4.2	Determination of sample amount.....	76
4.3	Fast extraction of metabolites	76
4.4	Feeding methods	77
4.4.1	Feeding solution distribution in the rosette is dependent on connectivity of the vascular tissue in the shoot	77
4.4.2	Metabolic changes caused by the feeding.....	79
4.5	¹³ C-quantification for net isotope flow calculations	80
4.6	Metabolic differences between single leaves of an <i>Arabidopsis</i> rosette.....	82
4.6.1	Metabolite pool sizes mark developmental stages.....	82
4.6.2	Carbon allocation from ¹³ C-sucrose in primary metabolites between different developmental leaf stages reveals pronounced differences	83
4.7	Metabolic differences between single leaves of an <i>Arabidopsis</i> rosette in cold-grown plants.....	85
4.7.1	Single leaves adjust metabolites differently during cold growth.....	85
4.7.2	Carbon allocation from ¹³ C-sucrose differs in primary metabolites of different developmental leaf stages in cold-grown plants	86
4.8	Expression of <i>REIL</i> genes and single leaf metabolism of <i>reil2</i> in the cold	86
5	Outlook	89
6	Abbreviations.....	90
7	List of figures and tables.....	91
8	Supplemental.....	94
8.1	Supplemental figures	95
9	Literature.....	102

Abstract

Measuring the metabolite profile of plants can be a strong phenotyping tool, but the changes of metabolite pool sizes are often difficult to interpret, not least because metabolite pool sizes may stay constant while carbon flows are altered and vice versa. Hence, measuring the carbon allocation of metabolites enables a better understanding of the metabolic phenotype. The main challenge of such measurements is the *in vivo* integration of a stable or radioactive label into a plant without perturbation of the system.

To follow the carbon flow of a precursor metabolite, a method is developed in this work that is based on metabolite profiling of primary metabolites measured with a mass spectrometer preceded by a gas chromatograph (Wagner *et al.* 2003; Erban *et al.* 2007; Dethloff *et al.* submitted). This method generates stable isotope profiling data, besides conventional metabolite profiling data. In order to allow the feeding of a ^{13}C -sucrose solution into the plant, a petiole and a hypocotyl feeding assay are developed. To enable the processing of large numbers of single leaf samples, their preparation and extraction are simplified and optimised. The metabolite profiles of primary metabolites are measured, and a simple relative calculation is done to gain information on carbon allocation from ^{13}C -sucrose.

This method is tested examining single leaves of one rosette in different developmental stages, both metabolically and regarding carbon allocation from ^{13}C -sucrose. It is revealed that some metabolite pool sizes and ^{13}C -pools are tightly associated to relative leaf growth, i.e. to the developmental stage of the leaf. Fumaric acid turns out to be the most interesting candidate for further studies because pool size and ^{13}C -pool diverge considerably. In addition, the analyses are also performed on plants grown in the cold, and the initial results show a different metabolite pool size pattern across single leaves of one *Arabidopsis* rosette, compared to the plants grown under normal temperatures. Lastly, *in situ* expression of *REIL* genes in the cold is examined using promotor-GUS plants. Initial results suggest that single leaf metabolite profiles of *reil2* differ from those of the WT.

Zusammenfassung

Messungen des pflanzlichen Metaboloms können ein hilfreiches Werkzeug sein, um Pflanzen zu phänotypisieren. Jedoch sind die Änderungen der Poolgrößen teilweise schwer zu interpretieren, weil sich nicht nur die Poolgrößen sondern auch die Kohlenstoffflüsse unabhängig voneinander ändern können. Werden nun zusätzlich Informationen über die Flüsse ermittelt, kann der pflanzliche Phänotyp deutlich genauer beschrieben werden. Die größte Herausforderung für diese Messungen ist die *In-vivo*-Integration einer stabilen oder radioaktiven Markierung in einer Pflanze, ohne das System dabei zu stören.

In dieser Arbeit wird ein Verfahren entwickelt, um die Verteilung von Kohlenstoffen aus einer gefütterten Vorstufe zu messen. Die Messung basiert dabei auf einem Primärmetabolitenprofil, das mit Hilfe eines Massenspektrometers mit vorgeschaltetem Gaschromatographen erstellt wird (Wagner *et al.* 2003; Erban *et al.* 2007; Dethloff *et al.* eingereicht). Mit dieser Methode ist es einfach möglich, stabile Isotopenprofilaten neben herkömmlichen Metabolitprofilaten zu erzeugen. Die Vorstufe, in diesem Fall ¹³C-Saccharose, wird dazu mit Hilfe eines neuen Petiolen- und Hypokotyl-Fütterungs-Assay in die Pflanze gefüttert. Um die große Menge an Einzelblattproben aufzuarbeiten, die dabei anfallen, wird eine vereinfachte und optimierte Extraktion angewendet. Mit Hilfe einer einfachen Berechnung kann aus den Messdaten eine relative Verteilung des Kohlenstoffs aus ¹³C-Saccharose bestimmt werden.

Die Funktionalität dieses Verfahrens wird an Einzelblättern von *Arabidopsis*-Rosetten gezeigt, wobei sowohl Primärmetabolitenprofile als auch stabile Isotopenprofile erzeugt und untersucht werden. Es kann hierbei gezeigt werden, dass konventionelle Poolgrößen und ¹³C-Poolgrößen einiger Metaboliten eng mit dem relativen Wachstum einzelner Blattpositionen bzw. mit dem jeweiligen Entwicklungsstadium der Blätter zusammenhängen. Anders als bei den meisten anderen Metaboliten zeigen die konventionellen Poolgrößen und ¹³C-Poolgrößen von Fumarsäure ein unterschiedliches Verhalten in den einzelnen Blättern, was Fumarsäure zum interessantesten Kandidaten für weitere Studien macht. Die beschriebenen Untersuchungen werden weiterhin an in Kälte gewachsenen Pflanzen durchgeführt, wobei erste Ergebnisse ein verändertes Metabolitenprofil in den einzelnen Blättern zeigen. Des Weiteren wird die *In-situ*-Expression von *REIL*-Genen mit Hilfe von Promotor-GUS-Reportern untersucht. Erste Ergebnisse von Einzelblatt-Metabolitenprofilen der *reil2* zeigen einen deutlichen Unterschied zum WT.

1 Introduction

1.1 Carbon isotope tracing

Isotope tracing is a fundamental technique in plant science and helps to acquire knowledge in many research areas. Isotope tracing can be distinguished into the analysis of naturally occurring isotopes and the analysis of artificially induced isotopes. There are four naturally occurring isotopes of carbon which are used for investigations: the stable isotopes, ^{12}C and ^{13}C , and the non-stable isotopes, ^{11}C and ^{14}C . Of the naturally occurring stable carbon isotopes ^{13}C represents only 1.07% of all carbon (Audi *et al.* 2003). Besides these, known carbon isotopes range from ^8C to ^{22}C , but they are not of interest for the following work. With the analysis of stable isotope tracing different questions can be addressed that concern plant function, growth, distribution and the biogeochemical cycle in which plants participate (Dawson *et al.* 2002). Measurements can be done on the isotope fraction (partitioning between heavy and light isotopes) between source and product substrate, because physical and chemical processes influence the representation of each isotope in a particular phase (liquid vs. gas) and are proportional to their mass (Dawson *et al.* 2002). Another effect of the chemical property is the strength of bonds: light isotopes form weaker bonds than heavy isotopes, therefore heavy isotopes are discriminated by enzymes and the isotope ratio of substrate and product is different (Dawson *et al.* 2001). In the past this ratio was used to perform ecological studies (Peterson *et al.* 1987), and to investigate photosynthetic activity across ecological gradients in space and time (Wickman 1952; Craig 1953). With the introduction of artificial ^{13}C isotopes a ratio between ^{12}C and ^{13}C is created that exceeds the naturally occurring ratio and makes measurements easier. The application of artificial $^{13}\text{CO}_2$ enables investigations concerning quantity and fate of carbon to various plants, organs, tissues and compounds or the surrounding soil. Photosynthetic labelling of paper birch and Douglas fir seedlings revealed that half of the ^{13}C was quickly lost via shoot and root respiration, root exudation and tissue death (Simard *et al.* 1997). In an earlier study the carbon allocation in the plant was investigated. It could be shown in chestnut coppice that carbon was first allocated to the growing shoot and leaves and later in the season the root became a major sink (Mordacq *et al.* 1986). To make such an allocation possible a transport system for carbon is necessary. With a radio label it has been demonstrated that minor veins of leaf discs are actively loaded with ^{14}C -sucrose. This was shown for soybean, pea and *Solenostemon scutellarioides* (“painted nettle”) (Sovonick *et al.* 1974; Turgeon *et al.* 1988).

However, not only the allocation in the plant can be traced; metabolic pathways can also be studied. Soybean ovules incubated with labelled CO₂ enabled a quality estimation of sugar metabolism. Further the synthesis rate of lipids and the distribution of labelled C in the lipids could be determined (Schaefer *et al.* 1975). Moreover, a measurement of the ratio of ¹²C/¹³C in sucrose in a time series with different O₂ concentrations showed the rate of photorespiration to be higher in soybean than in corn leaves (Schaefer *et al.* 1980), demonstrating the benefits of C4-plants.

A lot of achievements could be made by isotope tracing, such as the unravelling of a biosynthesis pathway of proline, a metabolite that was already known to accumulate in plants under drought stress (Morris *et al.* 1969). With the use of ¹⁴CO₂ it was shown that radioactivity appears rapidly in the vacuole of protoplasts incorporated in sucrose in barley, wheat and spinach (Giersch *et al.* 1980; Kaiser *et al.* 1982; Kaiser and Heber 1984). Ground-breaking biological insights into photosynthetic carbon assimilation and photorespiration metabolism were gained by Calvin and Benson. The work they did with ¹⁴CO₂ yielded fundamental knowledge about how photosynthetic organisms incorporate CO₂ to build up carbohydrates with the additional use only of water and light energy (Calvin 1956; Calvin 1964).

Recently, isotope tracing has gained new attention in systems biology for estimating metabolic fluxes (Fornie *et al.* 2005; Baxter *et al.* 2007). Measuring and interpretation of flux data is quite complex and needs to cope with the problem of compartmentation in the cell (Allen *et al.* 2009). To solve this problem different labelling strategies have been developed, using specifically labelled precursors (Roscher *et al.* 2000). These precursors have been verified and optimised by modelling approaches (Nargund *et al.* 2013). Others have used these labelling strategies in experiments (Junker *et al.* 2007).

In order to determine real fluxes, kinetic labelling is used, i.e. samples are labelled for various time intervals (Roessner-Tunali *et al.* 2004), or plants are fully photosynthetically labelled and the chase is measured at different time intervals when the plants are exposed to normal air (reverse kinetic labelling) (Huege *et al.* 2007). Most recently, measurements have been combined with the strength of modelling to get more detailed flux information in cell cultures (Masakapalli *et al.* 2010) and even in whole *Arabidopsis* rosettes (Szecowka *et al.* 2013).

1.2 Feeding methods

Besides the elegant way of photosynthetic labelling with isotopes of CO₂ (Huege *et al.* 2007; Szecowka *et al.* 2013), a lot of different feeding methods for non-photosynthetic labelling have been used in the past for a range of purposes. For sufficient labelling *Arabidopsis* cell cultures have been grown on media containing labelled compounds (Masakapalli *et al.* 2010). In addition whole seedlings or prepared embryos have been grown further in liquid cultures (Geigenberger *et al.* 1991; Junker *et al.* 2007) with media containing labelled compounds. Other *in vitro* approaches used leaf discs (Timm *et al.* 2008) or potato tuber discs (Roessner-Tunali *et al.* 2004) that were incubated in labelling solution. Similar to the disc feeding assay is a petiole feeding assay where detached leaves are placed in a labelling solution (Zook *et al.* 1997). Some less common methods have also been reported, such as the cotton wick method, where a labelling solution is transported through a small hole in the stem of pea via a cotton wick (Wichern *et al.* 2010). In 1972, Morris described how droplets of labelling solution were applied to leaves with scraped surfaces (Morris *et al.* 1972) to increase a foliar uptake. Even more direct is the injection of labelling solution into tobacco leaves with a syringe (Jamet *et al.* 1985).

Although a lot of different feeding methods to integrate isotopes for different purposes are known, an easy and reproducible method to apply a labelled precursor metabolite that is distributed in a whole plant to investigate carbon allocation is still lacking.

1.3 Leaf growth

Growth and gain of biomass is, besides reproduction, a major task of plants, and of high agricultural interest. This process has been studied for decades, even before photosynthesis as the foundation of plant life growth was unravelled (Calvin 1956). The studies of plant growth cover a lot of different aspects of plant physiology. The following text provides a partial overview of the current knowledge about leaf growth.

The growth of a leaf is dependent on cell proliferation, expansion and differentiation and on the final size of the leaf (Mizukami 2001). Leaves emerge as primordia from the shoot apical meristem and develop into very small leaves by cell division and proliferation. A phase of cell division is followed by a phase of mainly cell elongation. Leaf growth can be divided into structural growth (increase in dry matter) and expansive growth (increase in volume). In order to maintain structural growth, a substantial supply of carbon is necessary to build up

new structures in the cell wall, like cellulose and hemicellulose. Additionally, more photosynthetic products are necessary to keep processes like the cell cycle, protein synthesis and active transports running. It is assumed that leaf growth is mainly limited by the supply of carbon and water (Kriedemann 1986; Dale 1988; Walter *et al.* 2009) and is highly influenced by temperature (Parent *et al.* 2012). It has also been shown that leaf growth takes place mainly during the night and growth rates are low during the day (Pantin *et al.* 2011).

The fundamentals of expansive growth on the cellular level are described by the well-established Lockhart model (Lockhart 1965). An increase in cell turgor pressure leads to tensional stress in the cell wall. When a threshold pressure is exceeded the cell wall stretches irreversibly. This deformation is accompanied by a water flow that feeds the cell to maintain the turgor. An active adjustment of the osmotic potential in the cell is necessary to reach this water flow. The Lockhart model is supported by a range of experiments (Bunce 1977; Bouchabké *et al.* 2006; Ehlert *et al.* 2009; Ehlert *et al.* 2011; Zhang *et al.* 2011). The model accounts for reduced leaf growth under water deficit, as well as under high transpiration rates, although only 1-2% of transpiration water is needed to maintain growth (Fricke 2002).

1.3.1 The role of carbon in leaf growth

As mentioned before, photosynthesis provides energy and building blocks for leaf growth. Recent studies show that leaf growth or shoot biomass correlate with net photosynthesis, with the activity of carbon metabolism or with the level of carbon metabolites (Cross *et al.* 2006; Sulpice *et al.* 2009; Sulpice *et al.* 2010). The carbohydrates produced by photosynthesis are stored during the day in form of starch and are mobilised during the night (Stitt *et al.* 2012), which provides one explanation for the higher growth rates at night. The degradation of starch is regulated by the circadian clock, which indicates that leaf growth is also regulated by the clock in a direct or indirect way. Although carbohydrates are the major source of growth, detailed information on the process is still missing because carbohydrates and sugars also play an important role in signalling for a broad range of developmental processes and stress responses (Rolland *et al.* 2006). In addition they are difficult to measure locally.

In order to coordinate growth, a crosstalk between carbon and cell wall material deposition should exist, to prevent a thinning of the cell wall during low carbon availability. Evidence of this crosstalk was first presented in 2000. It has been reported that the expression or activity of enzymes supporting cell wall expansion is tightly associated with growth changes (Cho *et al.* 2000; Muller *et al.* 2007). In addition their expression and activity are also affected by

water deficits (Muller *et al.* 2007; Harb *et al.* 2010). More recently, it has also been proposed that cell expansion and carbohydrate metabolism are under the control of a cell wall-sensing machinery, which is able to detect changes in turgor pressure. Under osmotic stress biosynthesis of cellulose is inhibited and causes transcriptional and enzymatic changes in the central carbon metabolism (Wormit *et al.* 2012). Furthermore, cell wall-associated kinases regulate vacuolar invertases that act as contributors to osmotic pressure (Kohorn *et al.* 2006). The osmotic pressure is dependent on sugars, organic acids, proline and other amino acids and only to less than 50% dependent on inorganic osmotica (Hummel *et al.* 2010).

The rheological properties of the cell wall also respond to other stimuli, such as: pH, reactive oxygen species and abscisic acid (ABA). ABA regulates water flux and mediates growth responses to various stresses. Two targets are stomata and aquaporins that do not just regulate the water flux but also the availability of CO₂. Thus, ABA interferes with the energy, carbohydrate and water supply that is needed for growth. The hormone is further connected to growth because it interferes with sugar sensing. It is linked to sugar phosphate intermediates (notably trehalose-6-phosphate) and coordinates metabolic stress signalling (Delatte *et al.* 2011; Ma *et al.* 2011). In addition it has been shown that ABA inhibits cell division (Wang *et al.* 1998).

1.3.2 The growing leaf

During the development from young to mature leaf, the leaf area increases in a sigmoidal manner. The absolute expansion rate peaks at around 50% of the final leaf area, accompanied by a carbon import peak (Figure 1).

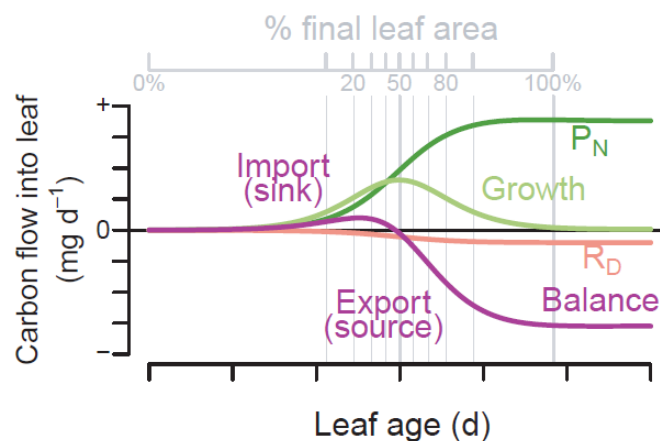


Figure 1: Carbon flow into the leaf at relative final leaf sizes. Rd-dark/night respiration; P = net photosynthesis; Growth = absolute growth; modified after Pantin *et al.* 2012

In contrast the relative expansion rate is at its highest in the earliest leaf stage and decreases towards the mature leaf stage. During this growth process the leaf undergoes a conversion from a net sink to a net source leaf. This conversion starts from the tip of the leaf, followed by a basipetal progression during leaf development, and the leaf base is converted last (Figure 2). The relative cell division rate is at its highest shortly before relative leaf expansion starts to decrease. The control of leaf expansion is predominantly metabolic in early stages and the hydraulic influence develops along with leaf development (Pantin *et al.* 2011). The net sink to net source transition is defined as the moment when a leaf becomes a net carbon exporter (Figure 1). This rapid transition is caused by an increase in carbon supply through enhanced photosynthesis and a decrease in carbon demand by growth and respiration (Figure 1) (Turgeon 1989). The sink-to-source transition occurs when leaves reach 30-60% of their final size (Turgeon 1989). It is accompanied by various changes in central carbon metabolism, enzymatic machinery, phloem structure and other anatomical changes that favour CO₂ assimilation and carbohydrate export. The photosynthesis rate increases strongly during the early expansion and reaches a peak between 25 and 100% of final leaf size (Pantin *et al.* 2012). Photorespiration follows this trend and dark respiration decreases. In addition the CO₂ flux via stomata and mesophyll increases and is followed by an increase of chloroplast number and volume (Pantin *et al.* 2012).

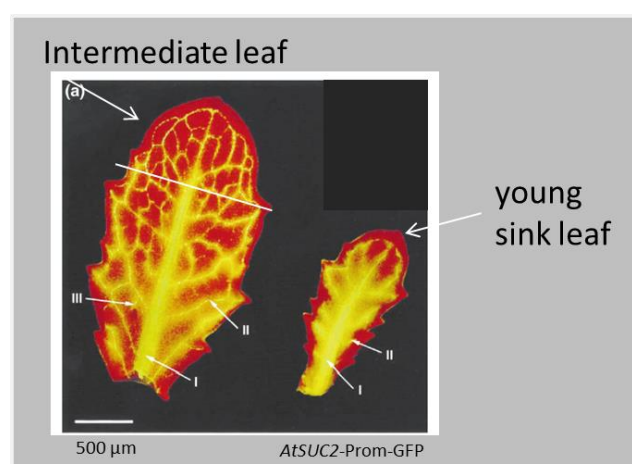


Figure 2: Visualisation of the sink-to-source border in *Arabidopsis* leaves. An *ATSUC2*-Prom-GFP fusion protein is expressed. Sink tissues are indicated by a diffuse pattern where the GFP protein is symplastically unloaded; source tissues are indicated by a clear pattern of fully developed leaf veins. Typical veins of classes I, II, and III where the unloading happens are marked with arrows; modified after Imlau *et al.* 1999.

In further studies it could be shown that carbohydrate supply affects cell division but not cell expansion because the carbohydrate requirements are very low compared to the amount maintained by the leaf's own photosynthesis (Kriedemann 1986). Very young and small leaves make an exception (Pantin *et al.* 2011). Sink tissues are also able to partly control photosynthesis of source tissues. When sink tissues only have a low carbohydrate demand, carbohydrates accumulate in the phloem loading site and lead to a downregulation of photosynthesis in the source tissues (Paul *et al.* 2001).

1.4 Growth in cold

A broad range of plants germinate in late summer or autumn and grow during wintertime till spring to flower and propagate, for example northern European accessions of *Arabidopsis*. As of yet, not much is known about the development in the cold (Shindo *et al.* 2007). Most studies investigate the short-term adaptation to cold. The adaptation can be distinguished into cold hardening, where plants are shifted from normal conditions to temperatures below 0 °C, and cold acclimation, where plants are shifted from normal conditions to temperatures between 10 – 0 °C (Hannah *et al.* 2005). A lot of publications describe the regulation of cold-induced responses in plants (Graham *et al.* 1982; Chinnusamy *et al.* 2007; Heidarvand *et al.* 2010), and especially changes of primary metabolism (Kaplan *et al.* 2004; Guy *et al.* 2008).

However, this work concentrates on the germination and cultivation of plants below 15 °C without a shift, which is termed cold growth (Strand *et al.* 1999; Gorsuch *et al.* 2010).

Cold growth is accompanied by strong morphological changes of leaves, which in the following will be compared to the morphology of leaves grown under normal conditions. The major photosynthetic tissue, the palisade parenchyma, changes from a mono cell layer to a multiple cell layer tissue. The photosynthesis rate is at the same level. In cells the ratio of cytosol and vacuole increases, however, because vacuoles get smaller (Strand *et al.* 1999). In addition cells show reduced water content and an increased fresh and dry weight, as well as an increase in protein and chlorophyll content. Moreover, the ratio between sucrose and starch changes in favour of sucrose (Strand *et al.* 1999). Besides these physiological changes biochemical changes occur. Among others the activity of enzymes in the Calvin cycle and in sucrose biosynthesis increases. In addition the expression of known cold-induced genes (*cbf1*, *cbf2*, *cbf3*) stays high in cold-grown plants (Lee *et al.* 2009).

Recently, attempts to model temperature-dependent growth revealed that the growth rate increases 1.5-fold at 20 °C to a maximum at 28 °C and decreases by 50% at 10 °C. It has also been reported that growth is highly temperature-dependent and similar across different plant species (Parent *et al.* 2012).

1.5 What is known about the reil genes

The *REIL* (Rei1-like) genes were found as homolog candidates of *Rei1*, which was first observed in experiments with yeast, performed in the Kopka group (Strassburg *et al.* 2010). The initial work dealt with the response of yeast to temperature changes at the level of the transcriptome and the metabolome. At the transcriptome level a number of genes that showed a temperature-reciprocal transcriptional response could be identified. From this set the gene *Rei1* (*Ybr267w*) was selected as a gene with an exemplary, temperature-reciprocal behaviour but exhibiting the most extreme and early responses (Strassburg *et al.* 2010). The yeast *Rei1p* was found to belong to the maturation machinery of the 60S-ribosomal subunit by Lebreton and co-authors (Lebreton *et al.* 2006). Comprising evidence from yeast two hybrid screening, where *Rrl24Bp* acted as bait and *Rei1p* was identified as prey, led to this assumption. *Rei1p* was found to represent an important ribosomal maturation factor. More precisely, the authors deduced that *Rei1p* is a factor involved in the recycling of the 60S-ribosomal subunit shuttling factors *Tif6*, *Arx1* and *Alb1*. These factors bind to the 60S subunit and are necessary for the export out of the nucleus. While *Rei1p* is central in this maturation process, its paralog *Reh1p* (*Ylr387c*) that appears to stabilize the 60S subunits in the absence of *Rei1p* may have a partially redundant function.

In the *Arabidopsis thaliana* genome two orthologous genes, namely *REIL1* (At4g31420) and *REIL2* (At2g24500), have been identified (Schmidt 2013; Schmidt *et al.* 2013). Their proteins *REIL1p* and *REIL2p* have four conserved zinc finger domains. The genes are the product of gene duplications that took place in yeast and *Arabidopsis thaliana* independently from each other (Schmidt *et al.* 2013). It has been reported that the *REIL* are required specifically for growth in the cold (10 °C), but not for growth at normal temperatures. A *reil1-1 reil2-1* double mutant shows a growth-arrest at 10 °C prior to the emergence of the first rosette leaf. The knockout mutant of *REIL2* forms small spoon-shaped leaves and shows a significant growth reduction at 10 °C. The phenotype reverts after emergence of the

inflorescence in the cold or upon a shift to 20 °C. Until now no phenotype for *reil1* could be observed.

Table 1: Shown are partial results of transcript profiling of *reil1* and *reil2* rosettes in a vegetative state compared to WT. It shows the numbers of probes that differ significantly based on transcription analysis performed with Agilent chips. Significances of comparisons were calculated by a Student's *t*-test (modified after Schmidt 2013).

Significance value	1 [^] 10 ⁻ 5	1 [^] 10 ⁻ 4	1 [^] 10 ⁻ 3	1 [^] 10 ⁻ 2
Significant <i>reil2.1</i> vs WT:	10	67	548	2920
Significant <i>reil2.2</i> vs WT:	7	37	213	1277
Significant in both:		6	64	649
^ more than 2.0-fold			2	8
^ more than 1.5-fold		1	5	19
Significant <i>reil1.1</i> vs WT:	3	6	18	91
Significant in all				10

Due to the emergence of the inflorescence, *Arabidopsis* plants undergo a transition from a vegetative to a generative state. With this transition it has been reported that the primary, secondary and lipid metabolisms change in the WT and in *reil1*, as does the transcriptional profile (Schmidt 2013). However, these changes have not been found in *reil2*, where primary metabolism and transcript profile in the generative state stay similar to the vegetative state. Lipid and secondary metabolisms move to an intermediate state between vegetative and generative, indicating that *reil2* does not fulfil a full transition to a generative state (Schmidt 2013). It has been reported that besides the morphological differences between WT and *reil2* no major changes are found in a vegetative state. In a vegetative state the physiology (transcriptome and metabolome) of *reil2* and WT is very similar on the rosette level; only in a generative state differences are found between the two.

A transcription analysis of vegetative rosettes grown in the cold revealed that only a minor number of genes are changed robustly, which leads to the assumption of either a gene regulation in a specific tissue or a regulation on a higher level than the transcriptome. Only 649 out of over 44000 probes consistently differed significantly from WT in the intersection of both lines of *reil2* (Table 1). Of this number only nineteen probes were changed 1.5-fold and eight probes 2-fold with a significance value of $p \leq 0.01$ for each (Schmidt 2013).

In summary, it can be stated that the strong changes in leaf morphology of the *reil2* are not accompanied by obvious differences in the transcriptome and the metabolome. As the morphological changes can be caused by changes during leaf development, an examination of the metabolism of single leaves in an early developmental stage might help to understand how metabolism and morphology are connected.

1.6 Aim and structure

The aim of this work is to combine a classical approach of isotope tracing (using a non-photosynthetic labelling) with a metabolite profiling, so as to gain information not only on a metabolic phenotype, but also on carbon distribution from a specific precursor. The method should comprise a fast and efficient labelling leading to a screening that reveals pool size changes and altered carbon distribution.

In the first part of this work the method development will be presented. In the second part the method is tested examining *Arabidopsis* single leaf metabolism of plants grown in normal conditions and plants grown in the cold.

Lastly, *reil* are examined. The results indicate altered single leaf metabolites and altered carbon allocation, making these genes interesting candidates for further studies.

2 Materials and methods

2.1 Plant cultivation

2.1.1 Optimal plant cultivation for controls

Seeds of *Arabidopsis thaliana* Columbia-0 (Col-0) were stored dry at 4 °C before use. If not described differently, all seeds were sterilized with an ethanol solution and germinated without further stratification on MS agar plates, i.e. (MS: 36 mM MS; 2.5 mM MES; 2% sucrose; 0.8% Select Agar (Murashige *et al.* 1962)) under long day conditions; 16 h light with an intensity of 120 $\mu\text{mol m}^{-2} \text{s}^{-1}$ and a constant temperature of 22 °C. After germination for 10 days the seedlings were picked and transferred to soil, standard compost Stendererde (Stender AG, <http://www.stender.de>, Schermbeck, Deutschland) in 6 cm or 10 cm plastic pots. Seedlings were kept under a transparent plastic hood for one week to guarantee a maximum humidity. The plants were grown for a total of 5 weeks in a growth chamber with short day conditions; 8 h light with an intensity of 120 $\mu\text{mol m}^{-2} \text{s}^{-1}$ and a temperature of 20 °C at day and 18 °C at night, to a 7-9 leaves stage before they were used for experiments.

Ethanol sterilisation:

- Fill some seeds into a 1.5 ml Eppendorf tube
- Add 1 ml of EtOH-Mix (70% EtOH, 0,5% Triton X-100)
- Shake 3-15 min
- Substitute with 95% EtOH, vortex
- Dry on EtOH sterilized filter tissue
- Collect in new Eppendorf tube

2.1.2 Plant cultivation in the cold

Seeds were sterilized and transferred on MS agar plates as described above. Further plates were transferred to a phytotron with long day conditions and a temperature regime of 10 °C / 8 °C (day / night) for germination and 16 h light with an intensity of 100 $\mu\text{mol m}^{-2} \text{s}^{-1}$. After 4 weeks seedlings were transferred to soil as mentioned above and put back into the phytotron and grown for a total of 10 weeks to a 7-9 leaves stage before they were treated.

2.2 Molecular biological material for *in situ* expression with promotor-GUS studies

Finished Promotor-GUS-constructs were provided by Stefanie Schmidt from the Kopka group. Constructs were transformed in *Agrobacterium tumefaciens*. Successful transformations were selected on media containing the appropriate antibiotics. With the use of the floral dip method (Clough *et al.* 1998) *Arabidopsis* plants were transformed. Successful transformations were selected on media plates containing the appropriate antibiotics. Selected plants were transferred to soil and the presence of constructs was confirmed by PCR. From each construct five or more clones were selected, propagated and used for the analysis of Promotor-GUS studies. DR5::GUS plants were provided by Jens Schwachtje from the van Dongen group.

2.2.1 Generation of promotor-GUS plants

Table 2: Table of promotor-GUS constructs and plants

Name (GMO-Name)	Construct-Number:	Agro-number	Plant
pREIL1::GUS_pKGWFS7	325834	880164	880174
pREIL2::GUS_pKGWFS7	325835	880187	880191
pDREB1A::GUS_pKGWFS7	325836	880188	880192
pDREB2A::GUS_pKGWFS7	325837	880189	880193
p35S::GUS_pKGWFS7	325838	880190	880194
DR5::GUS			902176

primer name	Forward 5'--> 3'	size (bp)	temperature (°C)
ATH_1_1000for	GCGTCGACGTACAAACCTGAAGATGAATCC	1000	46.4(45-55.8)
ATH_2_1000for	GCGTCGACGTCCTCGGGATTTTAAAGGTA	1000	46.4(45-55.8)
DREB1A_for	GCGTCGACGTgcatccgatctacaatta	1023	46.4(45-55.8)
DREB2A_for	GCGTCGACGTtctggctgacacatttatg	1012	46.4(45-55.8)
35S_for	GCGTCGACGTtcgacgaattaattccaat	1346	(45-65.6)

Reverse Primer for PCRs was: GACTTGAAGAAGTCGTGCTG

2.2.2 *Agrobacterium* transformation

- Thaw competent cells on ice (50 µl per transformation).
- Add plasmid DNA (1 µl of *E. coli* miniprep or 1-5 µg of CsCl-purified plasmid DNA) to the cells, and mix them together on ice.
- Transfer the mixture to a pre-cooled electroporation cuvette. Carry out electroporation as recommended for *E. coli* by the manufacturer of the chosen electroporator. For example, when using a Bio-Rad electroporator with a 2-mm cuvette, use the following conditions:
 - o Capacitance: 25 µF
 - o Voltage: 2.5 kV (for 2mm cuvetts)
 - o Resistance: 200 Ω
 - o Pulse length: 5 msec
- Immediately after electroporation, add 1 ml of LB to the cuvette, and transfer the bacterial suspension to a 15-ml culture tube. Incubate for 4 hours at 28 °C with gentle agitation.
- Collect the cells by centrifugating briefly, and spread them on an LB agar plate containing the appropriate antibiotic. Include the antibiotic for the T-DNA vector.
- Incubate the cells for 3-4 days at 28 °C.
- Restreak colonies on a new LB agar plate. Incubate this plate at 28 °C, and, when the colonies have grown, seal the plate with Parafilm. Keep it at 4 °C as a stock plate.
- Grow small liquid cultures of the restreaked colonies, and carry out minipreps and/or PCR to verify the presence of plasmid DNA.
- Make glycerol stocks of the appropriate clones, and store them at -20 °C.

(Shen *et al.* 1989; Mersereau *et al.* 1990)

2.2.3 *Arabidopsis* transformation

- Grow transformed *Agrobacterium* on YEB agar plates containing Gentamycin (25 mg/l), Rifampicin (100 mg/l) and Kanamycin (50 mg/l) at 28 °C for 48 h.
- Resuspend cells in liquid YEB medium.
- Mix 200 ml of resuspended cells with 100 ml of infiltration medium and add 500 µl Silwet L-77.
- Dip *Arabidopsis* flowers into the solution for 2 – 5 sec.
- Take plants out of the solution, cover them and put them into the green house.
- Culture till seeds are ripened.

(Bechtold *et al.* 1998; Bent *et al.* 1998)

2.2.4 Extraction of genomic DNA from plant

- Pestle in liquid nitrogen frozen plant material, put the powder in a 2 ml tube (ca 50 mg).
- Add the same volume CTAB-buffer to the frozen material and mix carefully.
- Incubate 30 min at 65 °C.
- Add one volume phenol/chloroform (PCI also works), mix well.

- Centrifuge 5 min / 14000 rpm / room temperature.
- Put out the tubes carefully of the centrifuge and collect the upper phase in a new tube.
- Ad 1/10 volume 3 M sodiumacetat.
- Ad 0.7 volume isopropanol mix with caution.
- Incubate 30 min on ice.
- Centrifuge 10 min / 14000 rpm / room temperature.
- Remove carefully the supernatant.
- Wash the pellet with 500 µl 70% ethanol, centrifuge 10 min / 14000 rpm / room temperature.
- Resuspend the pellet in water with RNase.

(Doyle *et al.* 1987)

2.2.5 PCR

For a normal polymerase chain reaction (PCR) a Taq-polymerase can be used with the following reaction batch and settings.

5 µl	10x PCR-Buffer	94 °C	2 min
1.5 µl	50 mM MgCl ₂	94 °C	30 sec
1 µl	10 mM dNTPs	55 °C	30 sec*
2 µl	Primermix (each 10 µM)	72 °C	2 min
1 µl	Taq-polimerase	→ repeat from step 2 29 times	
1 µl	DNA	72 °C	10 min
<u>38.5 µl</u>	H ₂ O	4 °C	forever
50 µl			

*the annealing temperature and time depend upon the primer pair and the length of the amplification product. For a length of 1kbp 1-2 min are recommended. (Saiki *et al.* 1988)

2.2.6 Electrophoresis of DNA

2.2.6.1 Gel loading buffer

0.25%	bromphenol blue
0.25%	xylem cyanol
40% (w/v)	sucrose

For use dilute 1:2 with 60% glycerol, ad 1/6 volume to the sample and load on a gel

2.2.6.2 TAE electrophoresis buffer

50x stock solution

242 g	tris base
57.1 ml	glacial acetic acid
37.2 g	Na ₂ EDTA•2H ₂ O

Adjust to 1 litre with H₂O, for use dilute 1:50.

2.2.6.3 Agarose gel electrophoresis

For agarose gel electrophoresis you have to prepare a gel. Therefore you have to solve the agar in TAE-buffer, a list of gel percentage for separation of the respective fragment sizes are shown in the following table.

Size estimation of DNA fragments in agarose gels

% agarose	Fragment size (bp)
0.4	3000-2500
0.8	1500-1000
1	1000-500
1.25	500-250
1.5	500-250
2	250-100
3.5	1000-100
5	500-75
8	500-50
12	250-25
15	100-25

2.2.7 GUS staining

Reference: Dominique Bergman

- Make up staining solution as outlined below. Make **10 ml of staining solution** for every 48-well plate. **X-Gluc, potassium ferricyanate, and ferrocyanate stocks must be made fresh** every time. It is possible to store these three stock solutions in the dark at 4 °C for a few days without loss of staining. However, check that stock solutions have not gone bad by making sure the yellow ferricyanate stocks have not faded and that the X-Gluc is not reddish in colour.
- Aliquots 150 – 200 µl staining solution to every well in a 48-well plate.
- Add bits of tissue to assay for GUS activity. Make sure tissues are in solution, not floating on the surface.
- Cover plate with lid and parafilm.
- Incubate at 37 °C, overnight
- Check for blue staining colour. Be careful of misleading punctuated-looking, dense deposits. These may not be due to actual GUS expression and X-Gluc cleavage, but instead to a precipitation of the X-Gluc.
- Should green or other coloured pigments interfere, clear tissue preps by **pipetting off staining solution, adding 100% EtOH, and incubating at 37 °C for 1-2 hours**

- Tissue was rehydrated in reverse ethanol series (95%; 80%; 70%; 50%) each for 5 min.
- Tissue was cleared using 1 M NaOH solution overnight.

Solutions:

1 M Na₂HPO₄, pH 7

1 M NaH₂PO₄, pH 7

25 mg/ml X-Gluc (cyclohexamodium salt) made up in DMF (or DMSO)

100 mM potassium ferricyanate (32.9 mg/ml in H₂O)

100 mM potassium ferrocyanate (42.2 mg/ml in H₂O)

Table 3: Components to generate a GUS staining solution

Experiment	High Stringency		Low Stringency
	For 5mM Fe	For 2,5 mM Fe	For 1 mM Fe
1M Na ₂ HPO ₄	577 µl	577 µl	577 µl
1M NaH ₂ PO ₄	423 µl	423 µl	423 µl
20% Tween	500 µl	500 µl	500 µl
0,5M EDTA	20 µl	20 µl	20 µl
25 mg/ml X-Gluc	400 µl	400 µl	400 µl
100 mM K Ferri-(CN ₆)	500 µl	250 µl	100 µl
100 mM K Ferro-(CN ₆)	500 µl	250 µl	100 µl
H ₂ O	7,08 ml	7,58 ml	7,88 ml
Total volume	10 ml	10 ml	10 ml

2.3 Measurements and documentation

2.3.1 Morphometric measurements for growth and documentation

Digital pictures were taken of the plants with a 6 cm size reference. Pictures were taken with a resolution of 4288 x 2848 pixels with a SLR Nikon D5000 Camera and an AF-S DX Nikkor 18-55mm f/3.5-5.6G VR lens (Nikon Cooperation, Tokio, Japan). Leaf length was

afterwards calibrated to the size reference and determined with the software ImageJ (<http://rsbweb.nih.gov/ij/index.html>). Length was measured from shoot rosette centre to leaf tip. Leaf growth was determined as difference (absolute) and ratio (relative) per day of two measurements within five days.

If not described differently, documentations were done with the same camera.

2.3.2 Documentation of carboxyfluorescein diacetate (CFDA)

The documentation of plants fed with CFDA were performed with a Leica Stereo-Fluorescence microscope motorized MZ 16FA with a DC FL 300 camera and the software LAS (Leica Mikrosysteme Vertrieb GmbH Mikroskopie und Histologie, Wetzlar, Germany). A GFP-filter with an excitation wave length of 470 ± 40 nm and a barrier filter starting at a wave length of 525 ± 50 nm were used. Pictures of one plant were all done with the same microscope and camera adjustments.

Pictures were assembled using the software Adobe Photoshop CS4 Extended (Adobe Photoshop Version 11.0, Adobe Systems, San Jose, California, USA). All pictures of one plant were corrected with the same adjustments in contrast and brightness, to visualise the plant edges and the stain in one picture.

For confocal analysis a Spectral Laser Scanning Confocal Microscope Leica TCS SP5 (Leica Mikrosysteme Vertrieb GmbH Mikroskopie und Histologie, Wetzlar, Germany) was used, with the adjustments reported in the respective dye publication (see 2.3.4).

2.3.3 Gravimetric measurements

Fresh weight of frozen plant material was determined gravimetrically with a Mettler analytical balance XS105 Dual Range (Mettler-Toledo GmbH, Ockerweg 3, 35396 Gießen, Deutschland; www.mt.com). The balance had a specific error of 0.1 mg.

2.3.4 Visualisation of feeding

Tracing dyes were used to test the labelling system and the distribution of labelling solution (Table 5). Dye distribution was documented at different indicated points in time.

Table 4: The different dyes that were used for plant labelling

Dye	λ excitation	λ emission	λ absorption	reference
CFDA	492 nm	517 nm		(Oparka 1994)
Calcofluor White	355 nm	433 nm		(Zaas <i>et al.</i> 2008)
Fast Green FCF			625 nm	(Wood <i>et al.</i> 2009)
Brilliant Blue FCF			628 nm	(Flury <i>et al.</i> 1994)

Dyes were prepared as described in references. Calcofluor White was detected with a confocal microscope with adjustments described in the publication.

2.3.5 Solutions for stable isotope tracing

For stable isotope tracing studies a 20 mM or 100 mM [UL-¹³C₁₂]-sucrose (in the following ¹³C-sucrose) solution in tap water was applied to the plants. These concentrations were chosen to stay below the natural sucrose concentration in the phloem of *Arabidopsis* of ca. 350 mM (Deeken *et al.* 2002). After three to four hours of incubation time single leaves were harvested. Labelled sucrose was purchased from Omicron Biochemicals Inc. (South Bend, Indiana, USA) with a purity of 99%.

2.4 Labelling and harvesting approach

2.4.1 *Arabidopsis* plant labelling with a petiole or hypocotyl feeding assay

- Bottoms of black, 0.5 ml Eppendorf tubes were cut off to 4-5 mm in size and used as disposable reservoirs of labelling solution. Wells were taken from a fresh unpacked package.
- Labelling solution was prepared as stock solution. If possible labelled metabolites and dyes were dissolved in tap water, to avoid contaminations that influence the plant metabolism. A defined volume of labelling solution was filled into the well (30 μ l for petiole feeding; 100 μ l for hypocotyl feeding).
- Petiole feeding assay: Leaf lamina was cut off the “feeding” leaf and the well was placed on the section of the remaining petiole that was still attached to the plant, so that the solution covers the cutting side and could enter the plant via the petiole. The solution stayed

in the well because of the adhesion of the small volume, although it was placed upside down on the petiole. The total amount of the solution was not taken up during the labelling time.

- Hypocotyl feeding assay: The well was placed in the soil close to the remaining root. Care was taken that no soil parts contaminated the solution and no soil fibres were in contact with the solution. Solution would otherwise be lost via these fibres by capillary forces. The root was cut off and the plant was placed in the well with the hypocotyl. Placing plant in the solution took around 1 to 2 seconds, as the plant was immediately transferred into the solution after cutting off the root.
- Plants were incubated for a fixed time (around 1 hour was needed to reach a good distribution of dye in a plant), 3 or 4 hours were used as standard feeding time for ^{13}C -sucrose.
- Leaves were harvested and immediately shock-frozen in liquid nitrogen (2.4.2), to stop metabolism.
- Samples were extracted and prepared for measurements (see 2.5).

2.4.2 Leaf harvesting

Except for some special *Arabidopsis* mutant phenotypes, new leaves of a rosette appear within an angle of 137.5° , fixed in meristem development. Neighbouring leaves should be at an angle around 137.5° and be larger than the younger one (for young leaves). *Arabidopsis* rosettes can turn clockwise and anti-clockwise but they keep the turning direction within one rosette. The youngest leaf was harvested at first. The youngest leaf is determined as the first leaf where a part of the petiole is visible; in younger leaves a visible petiole will be absent. First all leaf positions were determined and then harvested one by one. The leaf was cut off with clean scissors and put into a 2 ml round bottom micro vial and shock frozen immediately in liquid nitrogen. Then the next leaf was harvested and so on, following the scheme in Figure 3.

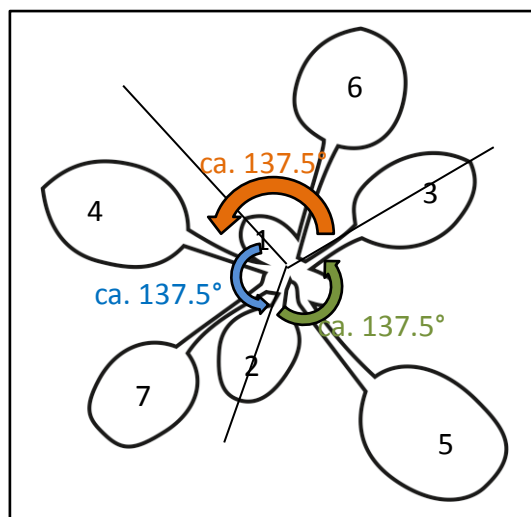


Figure 3: Determination of leaf positions and harvesting scheme. Shown is a scheme of an *Arabidopsis* rosette at a 7 leaf stage. Numbers indicate the sequence of leaf appearance from last-appearing leaf to oldest leaf. Leaf 1 is in this study defined as the youngest leaf with a visible petiole in overhead view. Younger leaves are not considered in this study. Leaf 2 and subsequent leaves have an offset of approximately 137.5° anti-clockwise (can be clockwise in other rosettes).

If necessary samples were stored below -60 °C in a freezer until further processing. The fresh weight of the samples was determined (see 2.3.3).

2.5 Sample preparation for GC-MS analysis

2.5.1 Sample extraction

Leaves were weighed in the frozen state and ground pre-cooled with liquid nitrogen. After grinding samples were extracted with methanol, modified after Roessner *et al.* (Roessner *et al.* 2000). The extraction amount was individually adapted to the fresh weight of each sample (Table 5).

Table 5: The extraction volume of methanol is adapted to the fresh weight.

fresh weight	volume of methanol mix
0-10 mg	400 µl
10-20 mg	800 µl
20-30 mg	1200 µl
30-40 mg	1600 µl

For the extraction a methanol mix was prepared with 398 µl methanol, 1µl of a 0.2 mg/ml uniformly labelled U-¹³C₆-sorbitol (in the following ¹³C-sorbitol) solution and 1µl of a

2 mg/ml (CHCl₃) nonadecanoic acid methyl ester. Samples were extracted for 15 min at 70 °C in a thermo shaker. Aliquots of a total volume of 350 µl were taken after centrifugation, avoiding cellular debris. The aliquots were dried by vacuum concentration and stored dry under inert gas at -20 °C until further processing.

2.5.2 Metabolite profiling

Metabolite profiling was performed as detailed previously (Wagner *et al.* 2003; Erban *et al.* 2007) by gas chromatography coupled to electron impact ionization/time-of-flight mass spectrometry (further GC-MS) using an Agilent 6890N24 gas chromatograph (Agilent Technologies, Böblingen, Germany; <http://www.agilent.com>) with split and splitless injection onto a FactorFour VF-5ms capillary column, 30-m length, 0.25-mm inner diameter, 0.25-µm film thickness (Varian-Agilent Technologies), which was connected to a Pegasus III time-of-flight mass spectrometer (LECO Instrumente GmbH, Mönchengladbach, Germany; <http://www.leco.de>).

Dried metabolites were methoxyaminated and trimethylsilylated manually prior to GC-MS analysis (Fiehn *et al.* 2000; Roessner *et al.* 2000; Wagner *et al.* 2003; Lisec *et al.* 2006; Erban *et al.* 2007). Retention indices were calibrated by addition of a C₁₀, C₁₂, C₁₅, C₁₈, C₁₉, C₂₂, C₂₈, C₃₂, and C₃₆ n-alkane mixture to each sample (Strehmel *et al.* 2008).

GC-MS chromatograms were acquired, visually controlled, baseline-corrected and exported in NetCDF file format using ChromaTOF software (Version 4.22; LECO, St. Joseph, USA). GC-MS data processing into a standardized numerical data matrix and compound identification were performed using the Tagfinder software (Luedemann *et al.* 2008; Allwood *et al.* 2009). Compounds were identified by mass spectral and retention time index matching the reference collection of the Golm metabolome database (GMD, <http://gmd.mpimpgolm.mpg.de/>; (Kopka *et al.* 2005; Schauer *et al.* 2005; Hummel *et al.* 2010) and the mass spectra of the NIST08 database (<http://www.nist.gov/srd/mslist.htm>). Guidelines for manually supervised metabolite identification were the presence of at least 3 specific mass fragments per compound and a retention index deviation < 1.0% (Strehmel *et al.* 2008).

All mass features of an experiment were normalized by sample fresh weight, internal standard and maximum scaled. For quantification purposes all mass features were evaluated for the best specific, selective and quantitative representation of observed analytes. Laboratory and reagent contaminations were evaluated by non-sample control experiments.

Metabolites were routinely assessed by relative changes expressed as response ratios, i.e. x-fold factors in comparison to a control condition or in comparison to the overall median of each metabolite measure

2.5.3 Exact quantification of metabolites with GC-MS

For exact quantification the recovery of each compound has to be determined by adding specific amounts of reference substances to the material before extraction; usually the amount of reference compound is 3 times higher than the natural concentration in the sample or an equal amount of a labelled reference compound is used (Roessner *et al.* 2000). Further quantification of molar amounts and concentrations was done by measuring exact calibration curves of reference substances (Roessner *et al.* 2000). Due to the measuring method of a TOF detector every calibration curve has a sigmoidal shape. Because all measurements were in the linear range of the calibration curve, the quantification could be calculated with a function based on a linear regression.

2.6 Processing of GC-MS data from ¹³C-isotope tracing studies

The following paragraph describes the measurement and calculation steps that are required to convert mass spectrometric data of ¹³C-isotope tracing studies into measures that can be used to analyse the absolute or relative changes of metabolite pool sizes and the proportion of ¹³C-atoms relative to all carbon atoms in the metabolite pool.

Mass spectrometric technologies ionize compounds and determine the mass of resulting molecular ions and of fragment ions that result from rapid breakdown reactions of the molecular ions following ionization (Figure 4). The molecular ions and fragment ions can contain naturally occurring heavy isotopes of carbon, namely ¹³C, and of any other element that is present in the molecular structure, such as H, O, N, S, P in metabolites. Due to the chemical derivatization that is required for GC-MS profiling of polar metabolites the isotopomer analysis also needs to consider the atoms that are chemically added and cannot be labelled *in vivo*, i.e. the methoxyamine moiety, =N-O-CH₃, and the trimethylsilyl moiety, –Si(CH₃)₃. The ¹³C-isotope feeding studies introduce C-atoms with a nominal mass shift of +1 per atom into metabolite pools that have natural isotope composition, for example, 1.07% of naturally occurring carbon atoms are ¹³C-atoms. As a consequence the composition of

abundance for the isotopomers of a molecular ion or fragment ion changes (Figure 4) according to the probability that one or more of the carbon atoms are labelled.

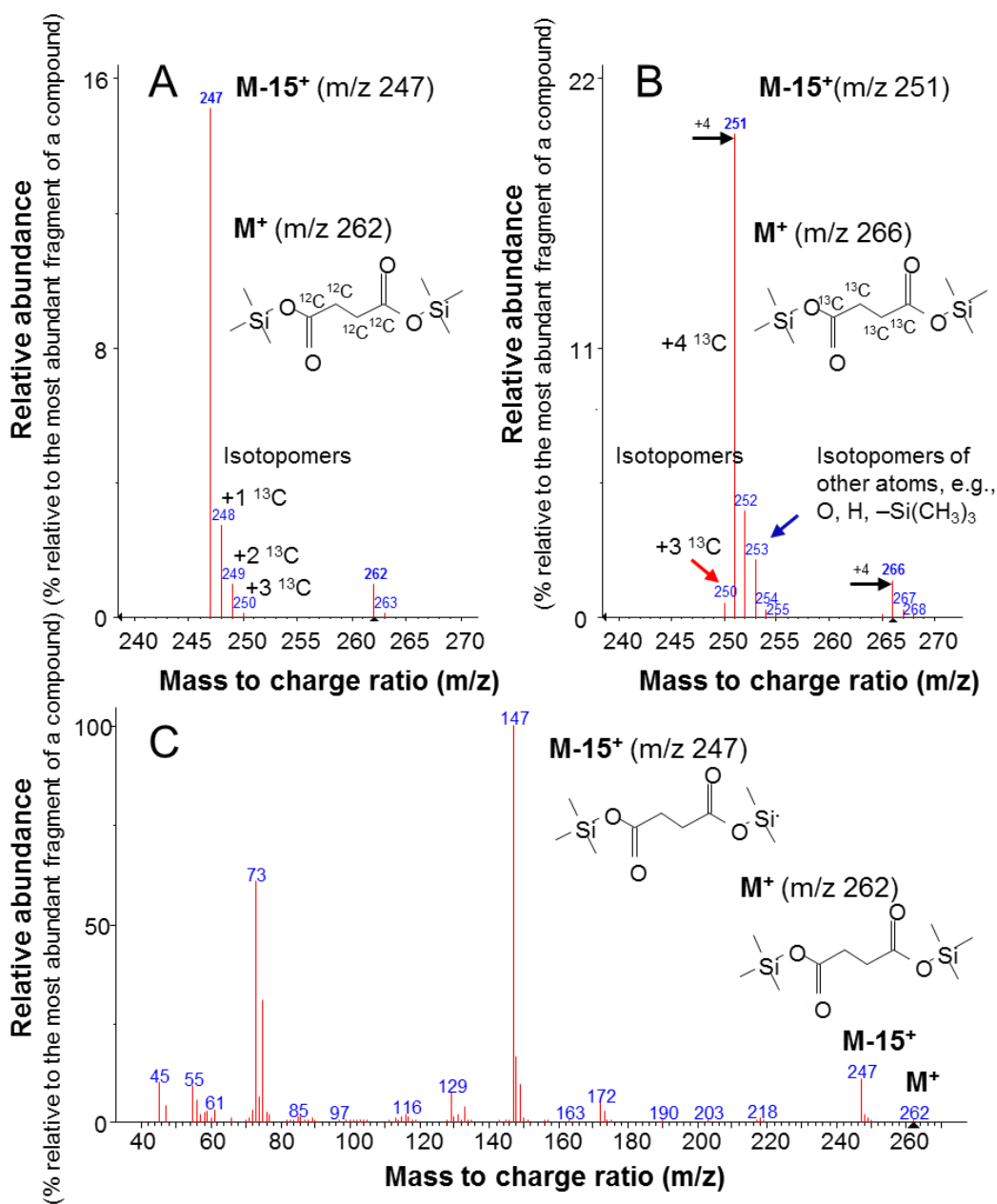


Figure 4: Molecular ion, fragment ion, and respective isotopomers of trimethylsilylated succinic acid with (A) natural isotope composition and (B) of uniformly labelled U-¹³C-succinic acid. Only a part of the complete mass spectrum (C) of the succinic acid di-(trimethylsilylester), cf. inserted structure, is shown in (A, B). The zoom-in shows the molecular ion (M⁺) and the fragment ion after loss of a methyl group (M-15⁺), cf. inserted structure, with respective isotopomers. The mass shift of M⁺ and of M-15⁺ is +4 (black arrows) due to the presence of 4 carbon atoms in succinic acid. Note that U-¹³C-succinic acid was not completely ¹³C-labelled (red arrow). Also note that additional isotopomers (blue arrow) are present which are caused by naturally occurring isotopes of other elements, i.e., O, H, and Si, and by non-labelled carbon atoms of the -Si(CH₃)₃ moiety of the trimethylsilylation reagent. The relative abundance of mass isotopomers is dependent on the probability of the presence of 1 or more heavy isotopes of carbon or any other element that is part of the molecule.

For the absolute or relative quantification of non-labelled metabolite pools the percentage of ^{13}C and of heavy isotopes of other elements can be assumed constant. As a consequence the most abundant, so-called monoisotopic isotopomer of a molecular or fragment ion can be used for quantification. In ^{13}C -feeding studies the isotopomer composition varies depending on the percentage of labelled carbon that is present in the metabolite pool. To quantify metabolites with variable isotopomer compositions the abundance of the sum of all isotopomers of a molecular or fragment ion can be calculated and used for quantification. This procedure assumes that the influence of the isotope on the measured abundance of a compound can be neglected. To quantify the metabolite pools the sum of isotopomers of molecular and fragment ions have to be calculated first.

To monitor the ^{13}C -enrichment that is experimentally introduced by *in vivo* stable isotope feeding into a metabolite pool a correction of the influence of naturally occurring heavy isotopes is required. This correction needs to consider the number of carbon atoms and of all other elements in the molecular or fragment ion. In addition the correction needs to consider the natural abundance of heavy isotopes of these elements. In GC-MS based studies this also includes the atoms that are added by chemical derivatization.

The following procedure is designed to use pre-existing software tools, namely Tagfinder (see 2.5.2) and Corrector (Huege *et al.* 2012) for basic chromatography data processing steps and for the calculation of corrected ^{13}C -enrichments of selected metabolite pools.

This study developed an experimental design which co-processes (1) non-labelled control samples of single leaves or rosettes from non-treated plants, (2) leaves from plants treated with non-labelled sucrose and leaf samples from plants fed with identical concentrations of ^{13}C -sucrose. A procedure for data processing was developed that includes significance and selectivity tests to validate the calculation results of the automated software tools and that takes into account that the feeding procedure delivers variable amounts of ^{13}C -sucrose to each single leaf (Figure 14, Figure 24). The role and interpretation of the respective tests and controls is reported in the following together with respective processing steps.

Step 1: Comprehensive retrieval of mass features responses from GC-MS chromatography files.

Step 2: Metabolite-targeted selection of recorded molecular or fragment ions with the Tagfinder tool.

Recorded mass fragments were grouped into time groups of co-eluting mass fragments (Luedemann *et al.* 2008; Allwood *et al.* 2009). Isotopomer data was annotated within time groups. Electron-impacted fragments and all isotopomers of these fragments (Figure 5) were collated into one Tagfinder output table. Isotopomers were sorted for compound and mass. Typically more than one compound was annotated in one time group, so isotopomers had to be allocated to the compounds. This was done by matching the measured elution retention index frame to the retention index of reference substances from the GMD.

Step 3: Retrieval of isotopomer responses (I_1 , I_2 , etc.).

For each analyte only identified fragments were selected, because the exact structure and number of carbons is needed for ^{13}C -enrichment calculations (Huege *et al.* 2011; Huege *et al.* 2012). For example glucose has the mass fragment 205 m/z that consists of 2 carbon atoms and has 3 isotopomers: both ^{12}C = mass 205 m/z, mix of ^{12}C and ^{13}C = mass 206 m/z and both ^{13}C = mass 207 m/z. Each fragment and their isotopomers can be determined in this manner when the structure is known. Typically three mass fragments and their isotopomers were processed for one compound (Figure 5).

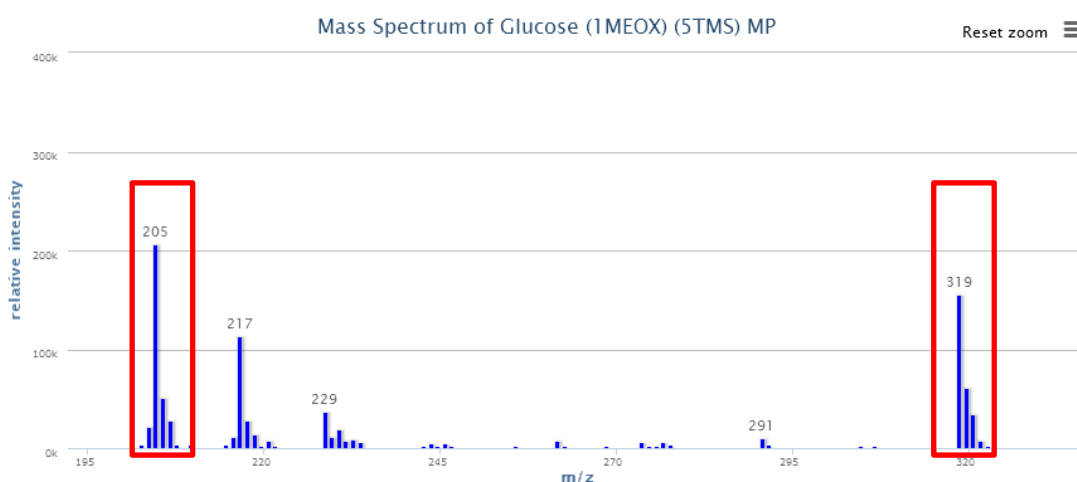


Figure 5: Partial mass spectrum of glucose. Mass fragments and their isotopes are shown in the graph as relative intensities. Fragment 205 consists of 2 carbon atoms, fragment 319 consists of 5 carbon atoms (graph: GMD).

Step 4: Processing data with the CORRECTOR tool; calculation of ^{13}C -enrichments and correction of isotopomer responses.

After fragments and respective mass isotopomers had been selected, data was reformatted into an input file for the CORRECTOR (Huege *et al.* 2011) software tool. The tool was used

for the allocation of the naturally occurring isotope distribution (Wittmann *et al.* 1999; Van Winden *et al.* 2002). In addition to the correction of intensities, the isotopomer ratio (^{13}C -enrichment = $^{13}\text{C}/(^{12}\text{C}+^{13}\text{C})$) was calculated. The CORRECTOR (v1.91) was used (http://www.mpimp-golm.mpg.de/10871/Supplementary_Materials).

Step 5: Calculation of the isotopomer sums (I_{1-x}) (pool size).

Step 6: Selectivity test by correlation analysis of the isotopomer sums.

After a first allocation and selection, the quality of identification was tested, to decrease the probability of artefacts caused by co-elution of fragments from different analytes or contaminations. A quality test for the selectivity of the chosen fragments is possible by correlation analysis. Specific fragments that originate from electron-impacted ionisation of a compound are generated in fixed and highly repeatable ratios. The sum of the isotopomers of a fragment is constant independently of the fractional ^{13}C -enrichment by ^{13}C . Therefore, the sum of mass isotopomers of different fragments must be highly correlated across samples with changing concentrations, if they represent the same compound (Figure 6a).

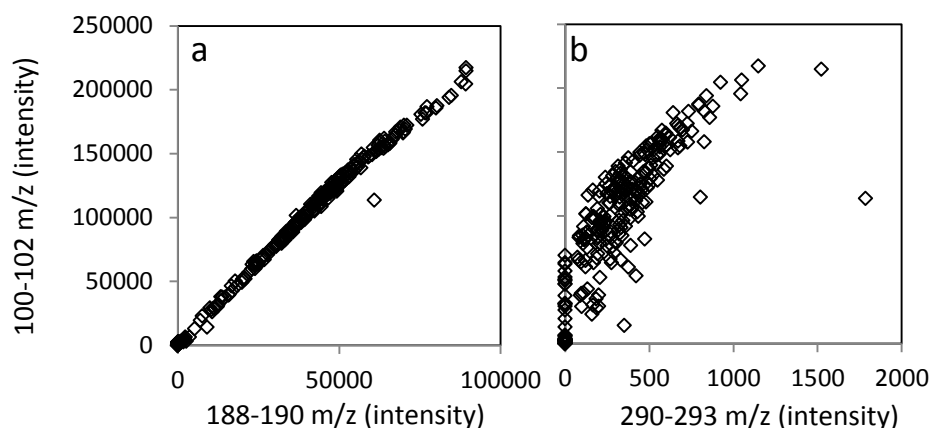


Figure 6: Correlation analysis of isotopomer sum. Alanine (3 TMS) as example; correlation of isotopomer sum 100-102m/z vs. 188-190m/z (a) and vs. 290-293m/z (b). Correlation of isotopomer sums in plot a shows an example for a good correlation and in plot b for a bad correlation.

If such fragment sums do not correlate at least one of the fragments does not represent the same analyte, thus is generated by a different co-eluting compound (Figure 6b). The evaluation of correlation analysis was done by eye because the isotopomer sums of fragments

with intensities at the edge of the linear detector response can be misleading because the correlation is not linear anymore.

Step 7: Normalization of isotopomer sums (N_{1-x}) (by fresh weight and internal standard).

Step 8: Calculation of corrected ^{13}C -enrichments.

Step 9: Testing for significant ^{13}C -enrichment in comparison to non-labelled control samples.

A second selection round was done on the level of the ^{13}C -enrichment. The ^{13}C -enrichment is expressed as the percentage of the mass fragment. Mass fragments for each compound were selected for a minor labelling in the non-labelled fraction of the dataset. If the previous selection was more or less successful, there was either no labelling in the non-labelled fraction (Figure 7a) or typically a low constant background labelling (Figure 7b).

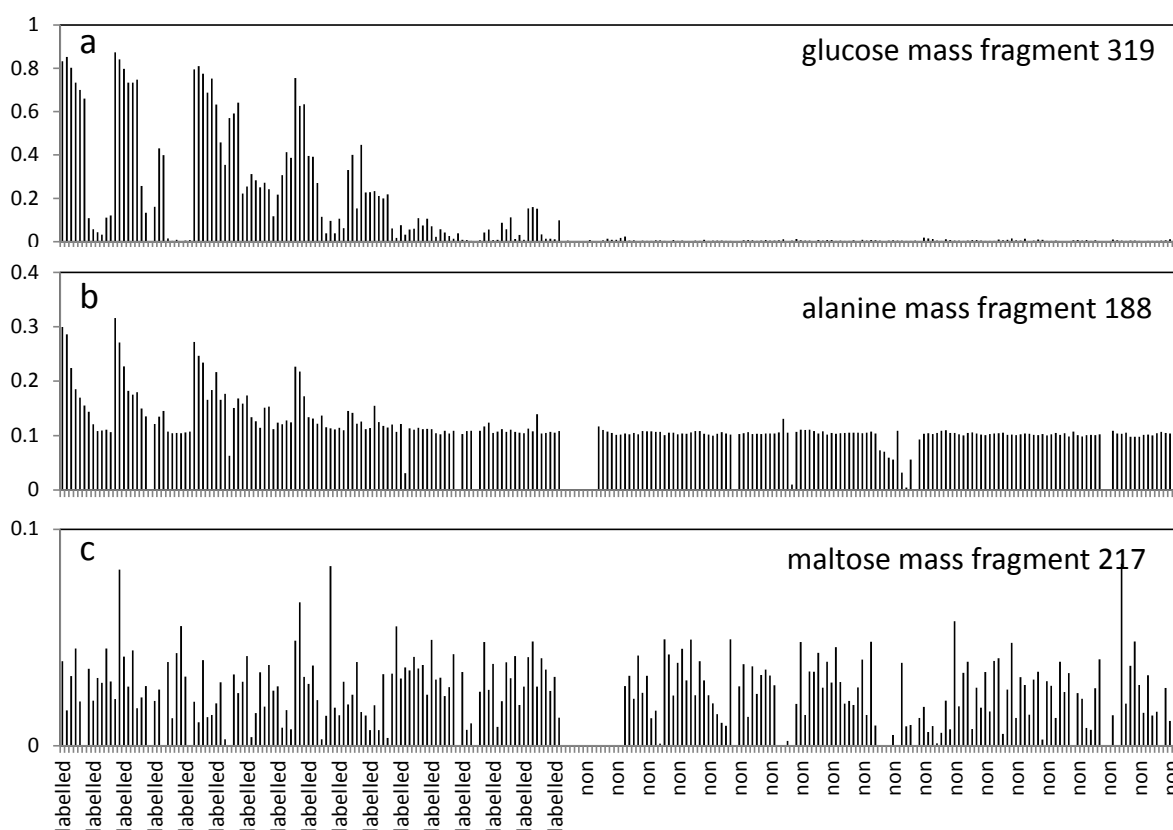


Figure 7: ^{13}C -enrichment of all samples for the selected mass fragments. Percentage is normalized to 1.

This constant background is likely created by interfering mass fragments from the same compound. For other fragments the specific labelling seemed to be random across all samples

including the non-labelled controls; these fragments were removed from the analysis (Figure 7c).

Step 10: Baseline subtraction of residual correction errors.

After the general mass fragments selection, a background correction was done on the samples for each fragment. Therefore a signal-to-noise threshold was calculated (the average ^{13}C -enrichment over the non-labelled fragment plus two times standard deviation). The signal-to-noise threshold was subtracted from the values. All values that were below the signal-to-noise threshold were further replaced with “NA”. After final selection of the data, two different values were calculated.

Step 11: Calculation of ratios of ^{13}C -enrichment relative to the ^{13}C -enrichment of sucrose in each sample.

Step 12: Calculation of the estimated ^{13}C -labelled pool size (^{13}C -pool).

Pool size: The sum of all isotopomers of one mass fragment was normalized to fresh weight and internal standard and further used as pool size.

^{13}C -pool: Selected ^{13}C -enrichments were normalised to the ^{13}C -enrichment of the precursor metabolite, sucrose (relative ^{13}C -enrichment). The final calculation step was the multiplication of the pool size by the relative ^{13}C -enrichment. This value represents the pool size of the metabolite, if all C-atoms originated from the total precursor pool at the specific time in point.

The ratio between the ^{13}C -enrichment of a compound and the precursor should not exceed a maximum of 2. These values were further used to search for outliers.

2.7 Statistical analysis

For statistical analysis the data was transformed from a non-parametric distribution to a Gaussian distribution. Therefore data was centred to the median and logarithmized. All statistical tests were performed on the transformed data.

Unless indicated otherwise all statistical analyses and calculations were performed with Microsoft Excel from the Office Professional Plus 2010 package (Microsoft Corporation,

Redmond, Washington, USA). Typical calculations are transformations, simple calculations and Student's *t*-tests.

All ICAs and PCAs were calculated with the online tool MetaGeneAlyse (<http://metagenealyse.mpimp-golm.mpg.de>).

All hierarchical cluster analyses were done with a Pearson correlation and an average linkage. All correlations matrices were also based on a Person correlation with an average linkage. Both were calculated with MeV v4.2; ANOVA and non-parametric equivalents were calculated with MeV v4.7.4 (Multiexperiment Viewer; (<http://www.tm4.org/mev>) with a critical α -value of $\alpha = 0.01$. All shown significance values are named after the output nomenclature of MeV, i.e. α -values are p-values.

3 Results

3.1 Development of isotope tracing assays for single leaves

3.1.1 Metabolic analysis of single leaves – choice of harvesting procedure and assessment of size limitations

The *Arabidopsis* rosette consists of leaves in a range of different developmental stages. Very young leaves that import carbohydrates, i.e. net sink leaves, and mature leaves that provide the supply of carbohydrates, net source leaves (see 1.3). To capture the metabolic differences between net sink and net source leaves of one rosette, the single leaves in different developmental stages of an *Arabidopsis* rosette needed to be analysed. After some preliminary harvesting tests for this purpose, the following harvesting procedure was designed and further used. Before leaves were harvested the leaf positions were determined, to make measurements of biological replicates possible. The determination and counting starts with the youngest leaf, because rosettes differed in their total leaf number between 7 and 9 leaves. When the determination started with the oldest leaf, young leaves of a specific position varied in their relative size and thus in their developmental stage, which was not intended. The leaf position 1 (leaf 1) of the analysis was determined as the youngest leaf with a visible petiole in an overhead view. Younger leaves could not be considered in this study because of the sample weight limitations (see below 3.1.1).

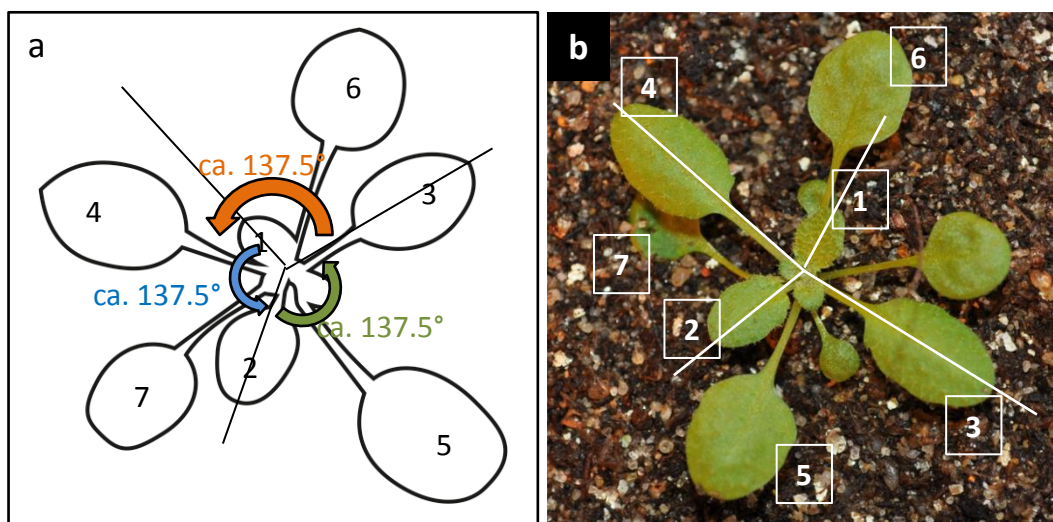


Figure 8: Determination of leaf position in *Arabidopsis* rosettes. Harvesting scheme of an *Arabidopsis* rosette (a) and leaf positions of a representative *Arabidopsis* plant (b). Numbers indicate the leaf age or developmental stage of the leaf. Leaf 1 is the youngest leaf (net sink) of the rosette where a part of the petiole is visible, followed by leaf 2 in an angle of 137.5° anti-clockwise (in this case, but can also be clockwise). Next leaves follow in the same direction each after an angle of 137.5° to leaf 7, the oldest leaf (net source).

For determining further leaf positions, leaves of a rosette were counted sequentially from leaf 1 to leaf 7, the oldest, most mature leaf of the study. Older leaves were not analysed, because they were shaded or partly shaded most of the time. The analysis of shaded leaves should be avoided because they have an altered metabolism. Sequential leaves were found by following the spiral leaf phyllotaxy of *Arabidopsis* with a divergence angle between successive leaves of 137.5° (Callos *et al.* 1994). After leaf positions were determined they could be harvested successively from leaf 1 to leaf 6/7, one by one following the scheme in Figure 8 (see 2.4.2). To inactivate the metabolism, each leaf was instantly frozen in liquid nitrogen. By following this harvesting procedure single leaves could be harvested within 2 to 10 seconds and all leaves of a rosette in less than 1 minute.

In an earlier test harvesting, whole rosettes were frozen in liquid nitrogen and single leaves cut off in a frozen state. Because frozen plant material is extremely brittle and leaves often broke due to the vibration caused by the cutting, this harvesting procedure was rejected. In another approach leaf positions were harvested randomly, resulting in a much longer harvesting time. For each harvested leaf the correct classification of leaf position had to be re-examined. This procedure was therefore also rejected.

For analysing primary metabolites the harvested plant material was extracted in methanol (see 2.5.1). Extracts were derivatized and measured with a GC-MS-based metabolite profiling method (see 2.5.2). For the purpose of making the resulting data comparable, a normalisation to fresh weight was chosen. The fresh weight had to be determined of the still frozen, metabolically inactive plant material (Fiehn *et al.* 2000; Roessner *et al.* 2000). As the sample material derived from a single leaf was rather small, the sample preparation had to be miniaturised. The exact gravimetric determination of small samples was complicated. The samples were weighed differentially as pre-cooled tube and pre-cooled tube with sample. For very small leaves the displayed weight was zero or negative sometimes. To find the lower limit of a minimum sample weight, the following experiment was performed.

Test weights of aluminium foil were weighed in different approaches: weight solo, as differential weight in a 2 ml tube and as differential weight in 2 different tubes; everything pre-cooled in liquid nitrogen. Test weights of aluminium foil were used because they have a similar surface-to-weight ratio as leaves, which helps making any condensation processes comparable. In addition, aluminium has a higher heat conductivity than plant material and

needed to be handled faster, to be kept in a frozen state. Therefore all big mistakes due to handling were taken into account.

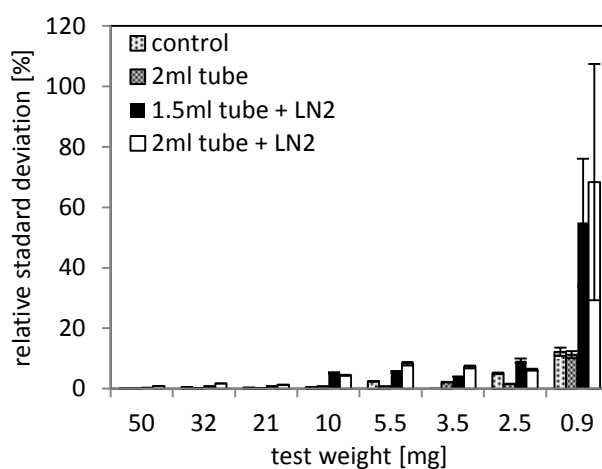


Figure 9: Determining the quality of normalisation by fresh weight. Diagrammed is the relative standard deviation based on the calculated average. The measurements were done 6 times on the same balance that was also used to measure any other fresh weight. Measured was the weight solo (control), 2 ml tube with weight, both at room temperature (2ml tube), and 1.5 ml tube with weight, both cooled in liquid nitrogen and remained frozen while weighing (1.5ml tube + LN2), 2 ml tube with weight, both cooled in liquid nitrogen and remained frozen while weighing (2ml tube + LN2). Averages of 6 replica measurements are shown; error bars represent the standard deviation.

To quantify the influence of the weighing procedure, the relative standard deviation was calculated out of 6 replica measurements for each condition (Figure 9). The relative standard deviation of the control and the 2 ml tube for 0.9 mg was around 11-12% which reflects a standard deviation of around 0.1 mg and thus is in the range of the specified error of the balance (see 2.3.3). The pre-cooled samples 1.5 ml + LN2 and 2 ml + LN2 showed a relative error of more than 50%.

Unless indicated otherwise, fresh weight was chosen rather than dry weight or leaf area. The error of the fresh weight was in a range of 4.5% for 10 mg and 7% to 8% for 2.5 mg to 5.5 mg. On top of the increasing relative error, the fresh weight was constantly underestimated for the 2 ml tube by 0.5 mg approximately. Therefore samples with a fresh weight smaller than 2 mg could not be accurately determined. Experiments with smaller samples were in the following normalised to the sum of all observed metabolites and specifically indicated as such. Sum-normalised data needs to be interpreted in terms of changes in composition rather than changes in pool size.

Alternatively to the normalisation to fresh weight, a normalisation to dry weight or volume is possible for a normalisation of GC-MS metabolite profile data. Both were rejected beforehand. Dry weight was rejected because of the very small weights after drying. Weights

are around 100-fold smaller than fresh weight, which leads to various complications related to the handling of very precise balances that can accurately weigh 0.02 mg, such as the influence of electrostatic charge (see 4.2). The leaf volume was rejected because of the three-dimensional shape of a leaf, which can be markedly different in various genotypes. In addition measurements of leaf thickness are difficult to perform without perturbation of the leaf metabolism (see 4.2).

3.1.2 Downscaling of the conventional GC-MS-based metabolite profiling

The conventional metabolite profiling with GC-MS is a well-established method and has been used routinely for more than a decade (Fiehn *et al.* 2000; Roessner *et al.* 2000; Wagner *et al.* 2003). It is usually done with samples in a range of sizes of 60-120 mg fresh weight (*Arabidopsis*), but depends on organism and tissues. The problem in this setting is the range of fresh weight that can vary between 2 and > 50 mg, thus 25- to even 100-fold in some cases. The performance of the extraction is dependent on the ratio between solvent and sample. When this ratio is changed extremely the composition of metabolites in the sample will change. To deal with this fact and with the wide range of fresh weights, the extraction volume was adapted to reduce the range to a 2-fold variation; in extreme cases a 10-fold variation. For this a fixed amount of methanol was added to samples in the range of 2 to 10 mg and the double amount to samples in a range of 10 to 20 mg and so on (see 2.5.1). After extraction and centrifugation a fixed amount of all extracts was transferred and used for the measurements (see 2.5.1).

The routinely used extraction method in our group is a mix of water, methanol and chloroform that leads to a phase separation into polar and non-polar solvents, thus providing the opportunity to analyse polar and non-polar metabolites separately in specific analyses. The solvents are added in three steps and the number of samples that can be extracted in one day usually ranges from 30 to 60 samples. The number of samples for a single leaf analysis was increased 6- to 7-fold compared to full rosette analysis and ranged from 400 to > 800 samples. The extraction method was therefore optimised to deal with the large number of single leaf samples by using a single step methanol extraction (see 2.5.1).

After establishing a method for the analysis of single leaf primary metabolism on the basis of the existing GC-MS method, the next step was the development of a stable isotope feeding and tracing method.

3.1.3 Petiole feeding assay - stable isotope tracing for *in vivo* primary metabolites

3.1.3.1 Developing the feeding technique

For the purpose of stable isotope tracing in single leaves a feeding method had to be developed. Dyes were used that visualise the distribution of the fed solution, to qualify the success of feeding. The focused precursor metabolite was ^{13}C -sucrose, which should be translocated in the plant on a natural way via the phloem. To this end in the beginning carboxyfluorescein diacetate (CFDA) was used because it has been reported to act as a phloem marker (Oparka 1994; Wright *et al.* 1997). However, to capture whole plants (Figure 12b) up to 20 single pictures had to be taken with an Epifluorescence microscope (see 2.3.2) and assembled afterwards with Photoshop (see 2.3.2). Since this turned out to be a very time-consuming process to qualify the feeding performance of various feeding methods, Fast Green FCF and later Brilliant Blue FCF (Figure 12a) were used, two dyes visible by eye. Both dyes showed a similar distribution pattern in the rosette like CFDA, but Brilliant Blue FCF could be detected more easily than Fast Green FCF in the green leaves. In addition it has been reported as a tracer dye for feeding plants via the petiole (Lin *et al.* 2010; Lin *et al.* 2011). Different attempts of plant feeding keeping the balance between efficient uptake of labelling solution and minimum influence were not satisfying. Cutting in the middle of a leaf lamina and adding an agar block on top seemed to strongly influence the plant (see 4.4.2). Infiltration of leaf stomata led to a patchy distribution of the dye (Figure 10). After testing different feeding methods, the method described by Lin *et al.* was adapted from bigger plants like Soybean and Tomato to *Arabidopsis*.

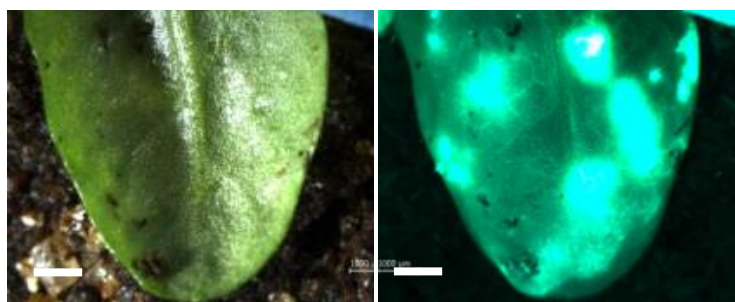


Figure 10: Attempt of Stomata feeding. Brij 30 was added to a CFDA solution to increase cuticle permeability and overcome water tension to make the entrance into the stomata available. After 1 hour of labelling. White bar represents a size of 1 mm. Solution could only penetrate in a few spots and was not distributed in the whole leaf.

The petiole feeding assay that has been described by Lin *et al.* was developed to characterise a nodulation suppressor molecule that is synthesised in the shoot and transported to the root

in Soybean. The solution is fed into the plant via a petiole like an intravenous infusion. As the feeding has been reported to distribute in the root and in different leaves, the method was adapted to feed solutions of stable isotopes into *Arabidopsis* as described in the following.

To provide enough feeding solution to the plant a reservoir with 20 to 30 μ l was prepared. For the petiole feeding the whole leaf lamina of one leaf was cut off at the transition from leaf lamina to petiole, to reduce the induced wound response in the plant (see 4.4.2). The reservoir with labelling solution was instantly placed on the freshly cut petiole that was still attached to the plant, to enable a direct uptake into the plant (Figure 11) and to prevent desiccation (see 2.4.1). To control how the solution was distributed in the plant, the feeding was tested with Brilliant Blue FCF (Figure 12a). This showed that the distribution was uneven in the rosette, as it has also been reported by Lin *et al.* (Lin *et al.* 2010; Lin *et al.* 2011).

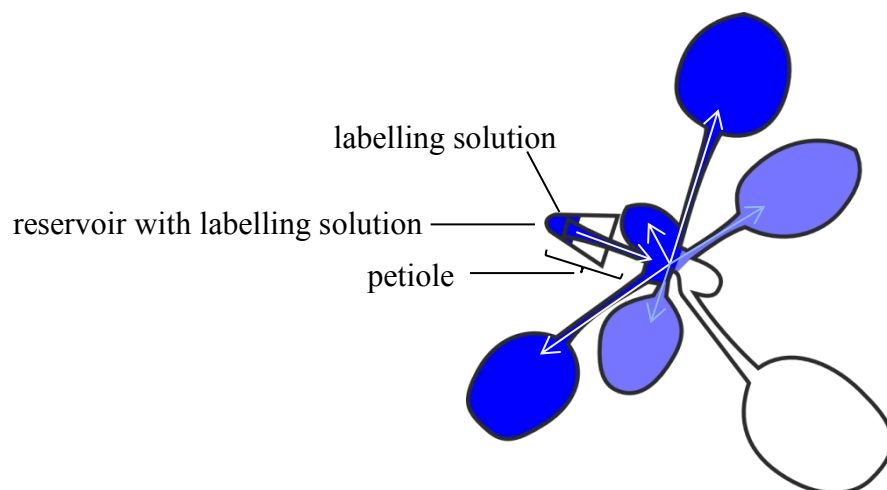


Figure 11: Scheme of the petiole feeding assay. Distribution of the labelling solution is indicated by the blue colour and the arrows. The leaf lamina is cut off the petiole and a reservoir with labelling solution is put on the freshly cut petiole.

In addition, differences in labelling efficiency could be observed, represented exemplarily by the two depicted plants (Figure 12a). To confirm the observed uneven distribution pattern, the distribution was tested in addition with CFDA (Figure 12b). Although the distribution was uneven in the rosette, it was observed to be even in single leaves (Figure 12). To further investigate via which transportation system the solution is taken up into the plant, a mix of Calcofluor White and CFDA was fed. The feeding petiole was cut off close to the shoot after 15 min of feeding and longitudinal sections were examined with a confocal microscope (see 2.3.2). Calcofluor White has been reported to stain cellulose of cell walls (Zaas *et al.* 2008) and CFDA has been reported to mark the phloem (Oparka 1994; Oparka *et al.* 1995). The

examination revealed that stain was found in and around the xylem (Calcofluor White) as well as in the phloem (CFDA) (Figure 13).

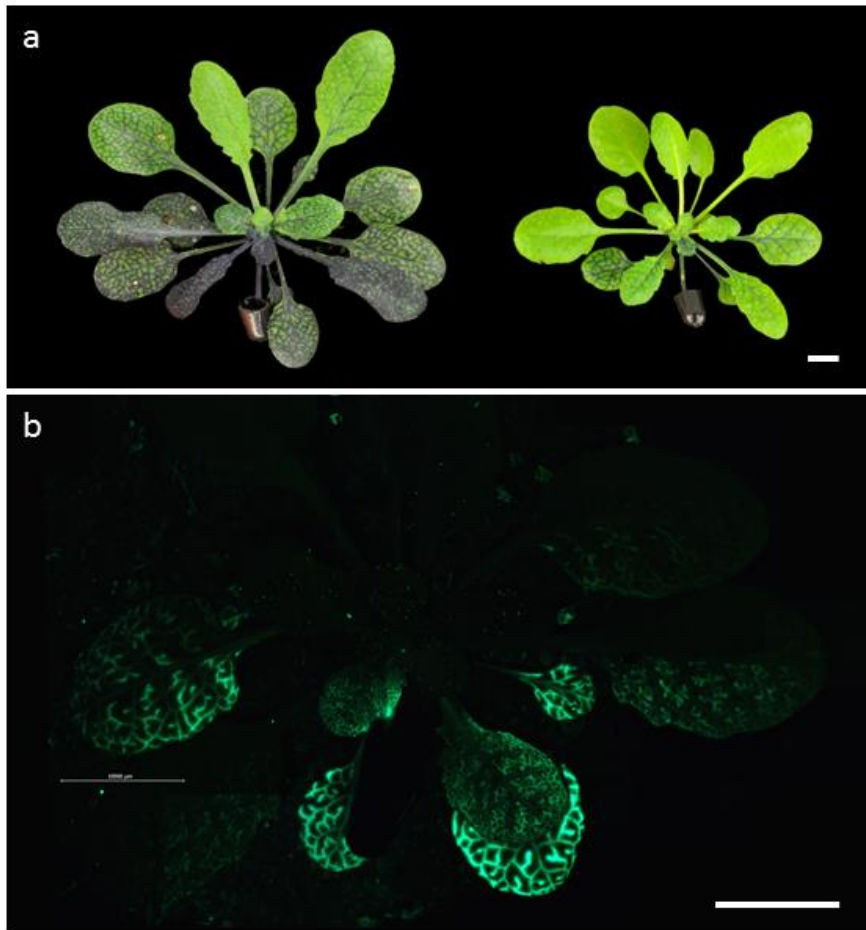


Figure 12: Distribution of dye in *Arabidopsis* rosettes after petiole feeding. The uptake of Brilliant Blue into two different plants from one population is shown (a). The applied labelling solution was taken from the same stock solution. The labelling solution was applied at the same time for both plants, and the pictures were taken at the same time. Additionally a feeding with CFDA was performed (b). White scale bars represent 1 cm in size.

After visualisation of the distribution in the rosette and in the vessel tissues of a feeding with dyes, the distribution of ^{13}C -sucrose was examined. Therefore plants in a 7-9 leaf stage were fed with ^{13}C -sucrose with the petiole feeding approach. Besides a control with unfed plants, two batches of plants were fed for 3 hours, one with a 20 mM and one with a 100 mM ^{13}C -sucrose solution. Metabolite profiles of primary metabolites of single leaf methanol extracts were analysed. Sucrose was selected and further processed with the CORRECTOR software (Huege *et al.* 2011) (see 2.6). The software tool corrects the measured responses of the fragment isotopomers for naturally occurring ^{13}C and afterwards calculates the ^{13}C -enrichment (specific labelled pool size of metabolite A = S_A) as a percentage value for

the selected metabolite. The ^{13}C -enrichment is defined as the share of ^{13}C -atoms from all C-atoms ($S_A = \frac{^{13}\text{C}}{^{12}\text{C}+^{13}\text{C}}$; 2.6).

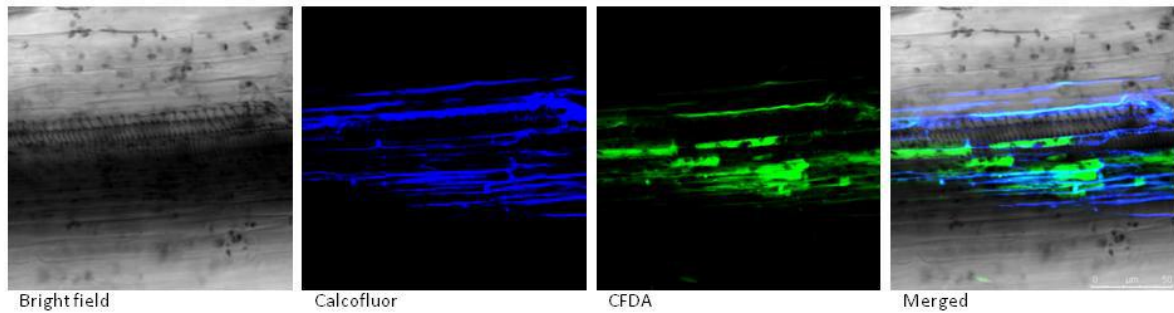


Figure 13: Longitudinal section of a feeding petiole after feeding with a mix of Calcofluor White and CFDA. Sections were cut after 15 min of incubation. Calcofluor White-stained material appears in blue and CFDA stain appears as yellowish green. The length of one edge of the squared pictures represents 150 μm . Phloem cells and cell walls of surrounding tissue shows a staining. No clear staining of only one transportation system.

The measured ^{13}C -enrichments of sucrose are diagrammed in Figure 14. A high ^{13}C -enrichment in the plant was found in leaf 1 and leaf 7, a low ^{13}C -enrichment in leaf 3 and leaf 5 and an intermediate ^{13}C -enrichment in leaf 2 and leaf 6 for the 100 mM ^{13}C -sucrose feeding (Figure 14a). Thus, the ^{13}C -sucrose distribution was similar to the previously shown distribution of the dyes. The ^{13}C -enrichment distribution of the 20 mM ^{13}C -sucrose solution was slightly different and showed a constant decrease, starting from leaf 1. That was to be expected as ^{13}C -sucrose is metabolised over time. By calculating the average sucrose ^{13}C -enrichment of each plant the uneven distribution in a plant gets obvious by the size of the error bars (Figure 14b). The ^{13}C -enrichment averages vary between 10% and 55% for the 100 mM feeding and between 4% and 25% for the 20 mM feeding, reflecting the interplant variation. Although the ^{13}C -enrichment of sucrose is only an estimation of the ^{13}C -sucrose distribution, it clearly shows the uneven distribution in the plant rosette.

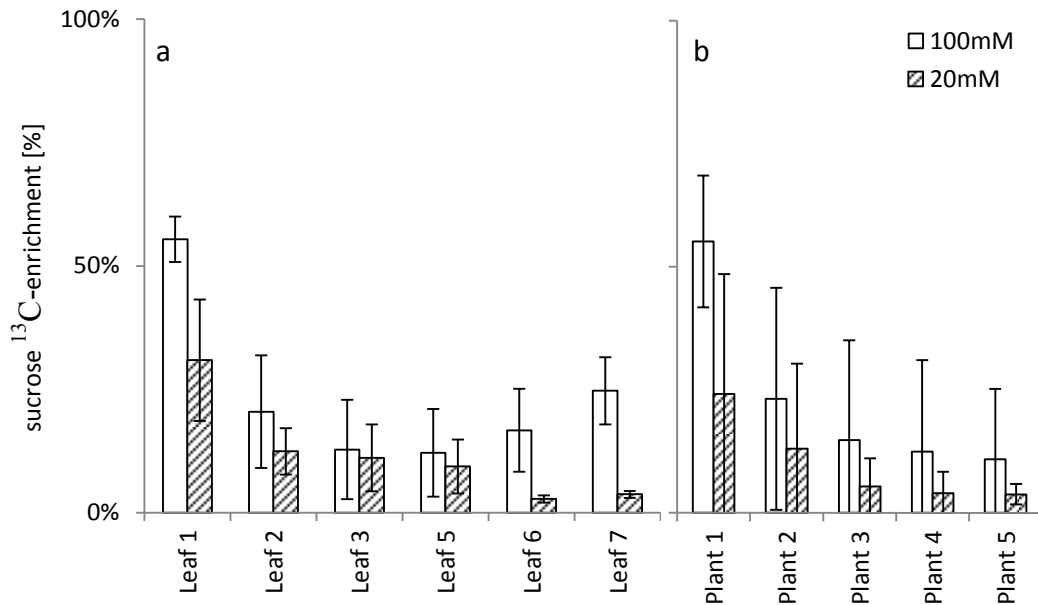


Figure 14: Distribution of ^{13}C -sucrose in *Arabidopsis* rosettes after a petiole feeding assay. The ^{13}C -sucrose in different leaf positions after feeding with a 20 mM and a 100 mM ^{13}C -sucrose solution is shown as the sucrose ^{13}C -enrichment. Diagrammed are averages of 4-5 replicates; error bars represent the standard error (a). Distribution of ^{13}C -sucrose is shown in single plants. Diagrammed are averages of 5-6 leaf positions; error bars represent the standard error (b).

For a precise ^{13}C measurement a quantification method was sought. A stable isotope ratio mass spectroscopy of samples for quantification had to be rejected due to sample size. For measurements samples between 0.1 mg and 0.5 mg dry weights were needed (Cabello *et al.* under submission), which matches the total sample size of most of the samples. Dry weight of samples after an estimated water loss of 95% would range between 0.1 mg and 0.5 mg, but would need to be split into one sample for isotope ratio measurements and one for GC-MS measurements. Therefore an alternative approach to estimate the ^{13}C amount was tested.

3.1.3.2 Internal standard for quantification of fed ^{13}C -sucrose in each leaf

To calculate an average uptake rate of ^{13}C -sucrose and an average net carbon flow into different metabolite pools, the total amount of ^{13}C needed to be determined for each leaf. ^{13}C -sucrose is metabolised over time and therefore does not allow a direct conclusion about the total amount of ^{13}C in a single leaf.

An easy solution would be the estimation of the total amount of ^{13}C -sucrose (or other compounds) applied, using a metabolically inert internal standard co-fed together with ^{13}C -sucrose. Assuming that both compounds are taken up in the same manner, the amount of the inert internal standard would be an estimation of the total ^{13}C -sucrose uptake.

To test this potential standardisation strategy, lactulose, a sugar structurally similar to sucrose, and the sugar alcohol ^{13}C -sorbitol were used for co-feeding. A population of 5-week-old *Arabidopsis* plants in a 7-9 leaf stage were split into 7 groups and fed with different feeding solutions shown in Table 6. All used mixes were prepared as equimolar solutions, to provide an equal amount of molecules for the feeding.

Table 6: labelling test solutions for ^{13}C -sucrose quantification with internal standards

solution	lactulose	^{13}C -sucrose	^{13}C -sorbitol
suc		20 mM	
lact	20 mM		
sorb			20 mM
suc+lact	20 mM	20 mM	
suc+sorb		20 mM	20 mM
suc+sorb+lact	20 mM	20 mM	20 mM
control			

After feeding plants for 3 hours single leaves were harvested in liquid nitrogen. The methanol extracts were measured by GC-MS and the primary metabolism was captured. Exact molar amounts were determined for ^{13}C -sucrose, ^{13}C -sorbitol and lactulose (see 2.5.3).

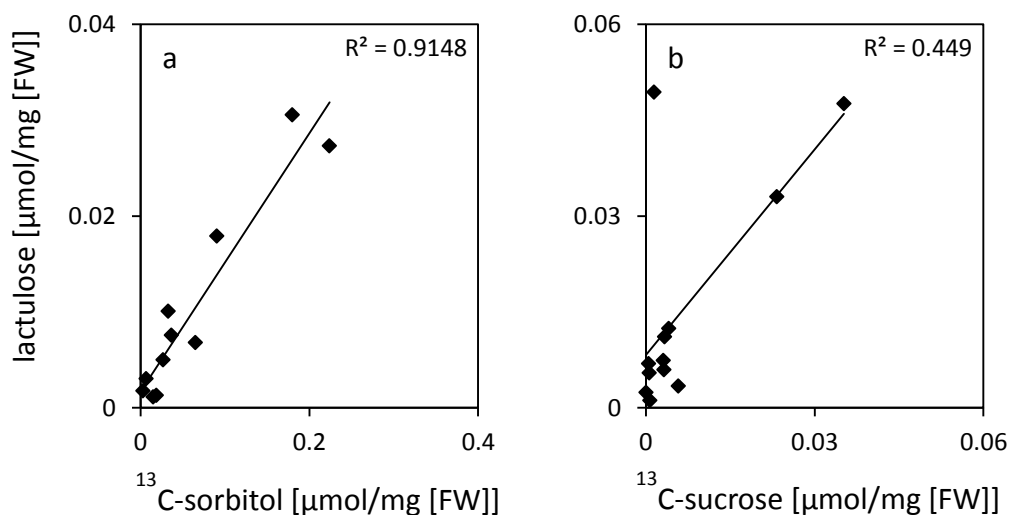


Figure 15: Testing distribution of internal standards in a co-feeding. Correlation plot of molar amounts of lactulose against molar amounts of ^{13}C -sorbitol of the samples taken from the suc+sorb+lact-feeding (a); correlation plot of molar amounts of lactulose against molar amounts of ^{13}C -sucrose of the samples taken from the suc+lact-feeding (b).

The molar amounts of the co-feeding of ^{13}C -sorbitol, lactulose and ^{13}C -sucrose (suc+sorb+lact) were plotted against each other to test if the compounds distribute in the rosette in a similar way. The R^2 -value of the linear fitting of the correlation between ^{13}C -sorbitol and lactulose was 0.94 (Figure 15a). The molar amount of lactulose plotted against the molar amount of ^{13}C -sucrose resulted in a linear fitting with an R^2 -value of 0.45 for the co-feeding of ^{13}C -sucrose and lactulose (suc+lact). These correlations are shown as an example (Figure 15b).

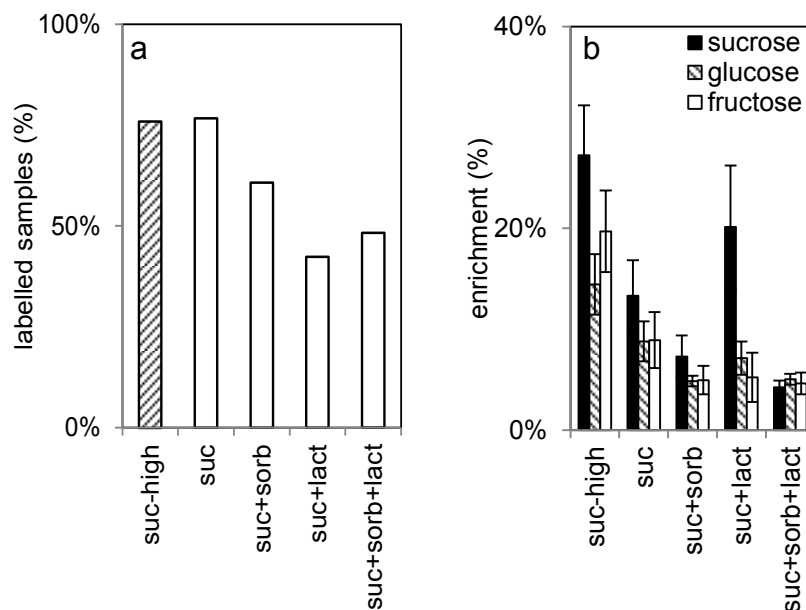


Figure 16: ^{13}C -enrichment measurements in co-fed plants. Shown are the per cent of samples that were labelled after correcting for the background labelling (a). Measured was the sucrose ^{13}C -enrichment for different feeding solutions. 20mM ^{13}C -sucrose (suc), 20mM ^{13}C -sucrose/ ^{13}C -sorbitol (suc+sorb), 20mM ^{13}C -sucrose/lactulose (suc+lact), 20mM ^{13}C -sucrose/ ^{13}C -sorbitol/lactulose (suc+sorb+lact), 100mM ^{13}C -sucrose (suc-high). Samples consist of all leaf positions from leaf-1 to leaf-7. Total number of samples ranges from 26 to 30. Average ^{13}C -enrichment of sucrose, fructose and glucose were calculated (b); error bars represent the standard error.

The correlation between lactulose and ^{13}C -sorbitol showed the similar distribution of these compounds in the plant. Nonetheless, the molar amounts of lactulose and ^{13}C -sorbitol differed considerably, indicating that the amount reaching the target tissue is highly dependent on the added standard. The amounts of ^{13}C -sucrose and lactulose were in the same range, but as expected the amounts of lactulose exceed the amounts of ^{13}C -sucrose, especially in low amounts. The amount of ^{13}C -sucrose is constantly underestimated because it is metabolised over time.

The amount of labelled sucrose is expressed as the ^{13}C -enrichment of sucrose. To distinguish between background noise and true ^{13}C -enrichments, a signal-to-noise threshold was

calculated. The threshold was determined as the sum of the average plus two times standard deviation of the ^{13}C -enrichment of the control samples (unlabelled). The percentage of samples with a detectable ^{13}C -enrichment was calculated to determine the influence of the co-feeding of standards on the feeding procedure (Figure 16a). Feeding a pure ^{13}C -sucrose solution led to a total of 75% labelled samples, which means 75% of harvested leaves of one rosette showed a labelling on the average. This was supported by a 100 mM ^{13}C -sucrose feeding, which led to a similar percentage, which indicates a kind of maximum number of rosette leaves that can be labelled by petiole feeding. The addition of sorbitol reduced this to 60% of samples with label. The addition of lactulose led to an even stronger decrease to 40% of samples with label. When a mixture of all three was added, approximately 42% of all samples showed a detectable label. This illustrates that adding a standard to the sucrose feeding leads to fewer samples with a detectable ^{13}C -enrichment and therefore reduces the labelling efficiency.

To verify the influence of co-feeding on the carbon allocation, the average ^{13}C -enrichments for sucrose, glucose and fructose were calculated (Figure 16b). As a control the two differently concentrated ^{13}C -sucrose solutions were analysed (20mM and 100mM). In all cases the average ^{13}C -enrichments were 2-fold higher when the higher concentrated sucrose solution was fed. The average ^{13}C -enrichment of sucrose decreased in the co-feeding with ^{13}C -sorbitol and ^{13}C -sorbitol and lactulose but slightly increased in the co-feeding with lactulose. The average ^{13}C -enrichment of glucose and fructose decreased in all co-feedings compared to the control. The co-feeding of an additional substance seems to interfere with the ^{13}C -sucrose translocation and uptake into the plant as well as its metabolic conversion into glucose and fructose. Although the co-feeding with sorbitol or lactulose had a strong effect on the ^{13}C -sucrose feeding, the feeding with all three compounds did not show a stronger effect, indicating that ^{13}C -sorbitol may have the dominant effect on the co-feeding.

3.1.3.3 Testing the influence of petiole feeding on the plant metabolism

For the purpose of method validation a control feeding experiment was performed to test how the petiole feeding assay influences the metabolite pool sizes. A population of 5-week-old *Arabidopsis* plants in a 7-9 leaf stage was split into two groups. One group was fed with a 20 mM ^{12}C -sucrose solution and one group neither cut nor fed was used as a control. After four hours single leaves were harvested from the plants for a GC-MS analysis of primary

metabolites. The labelling time was increased compared to the one mentioned above to enable a tracing of carbon in more metabolite pools in later experiments. Five replicates were harvested from each leaf position and each condition.

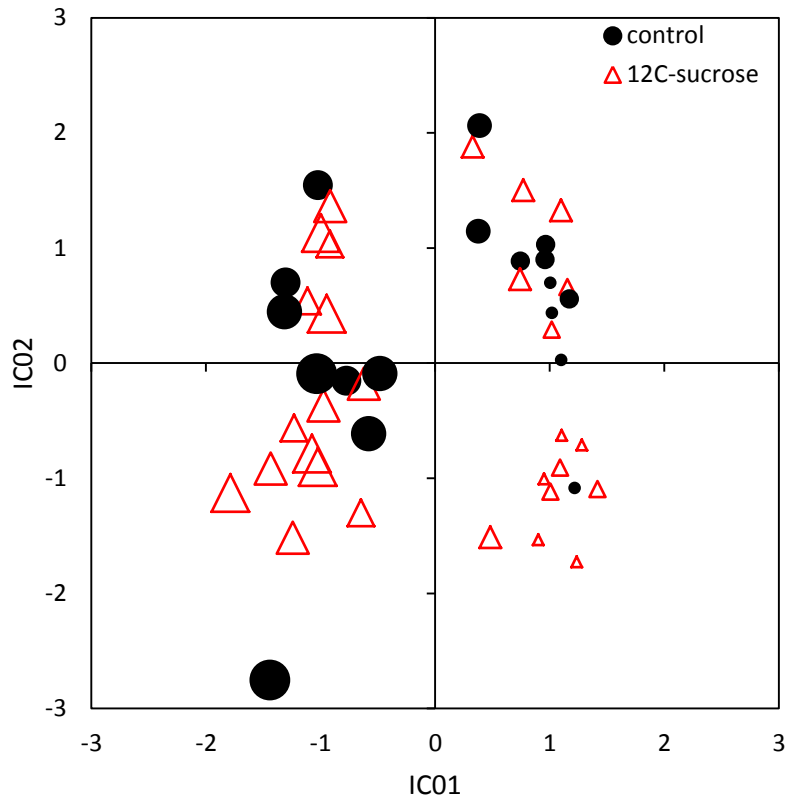


Figure 17: Global differences in primary metabolites of a petiole feeding test and a control; ICA of control against 20 mM ^{12}C -sucrose feeding. Calculation based on 2 PCs covering 54% of total variance. Single leaf positions are represented by different sizes from young = small to old = large. Each data point represents GC-MS profile data of primary metabolites of a single leaf.

Around 100 analytes were annotated in the GC-MS analysis of the methanol extract of single leaves. In order to get a first insight into the obvious global metabolic changes between the different feedings, a principal component analysis (PCA) was performed. The first two principal components (PCs) covering 54.4% of the total variance in the data set were subjected to an independent component analysis (ICA) for the detection of sample distribution within the dataset (Figure 17). The metabolic information of leaf position four did only exist for the control and was therefore disregarded in the following analysis. The ICA shows a clear separation between young and mature leaves. The data points of single leaf positions describe a continuous curve from young to mature leaves. The differences in the data of the control and the ^{12}C -sucrose feeding seemed to be minor as the data matches the control data.

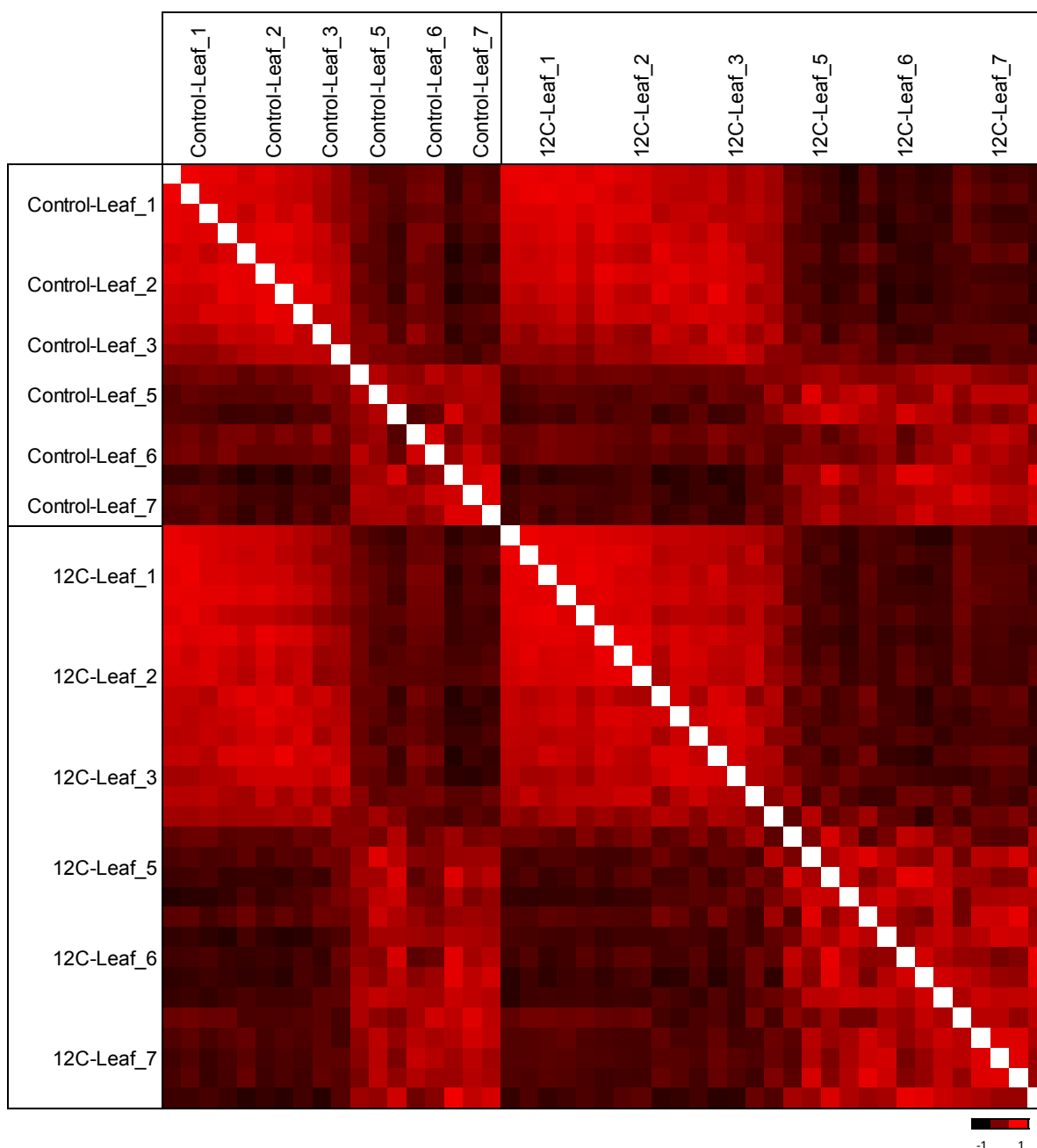
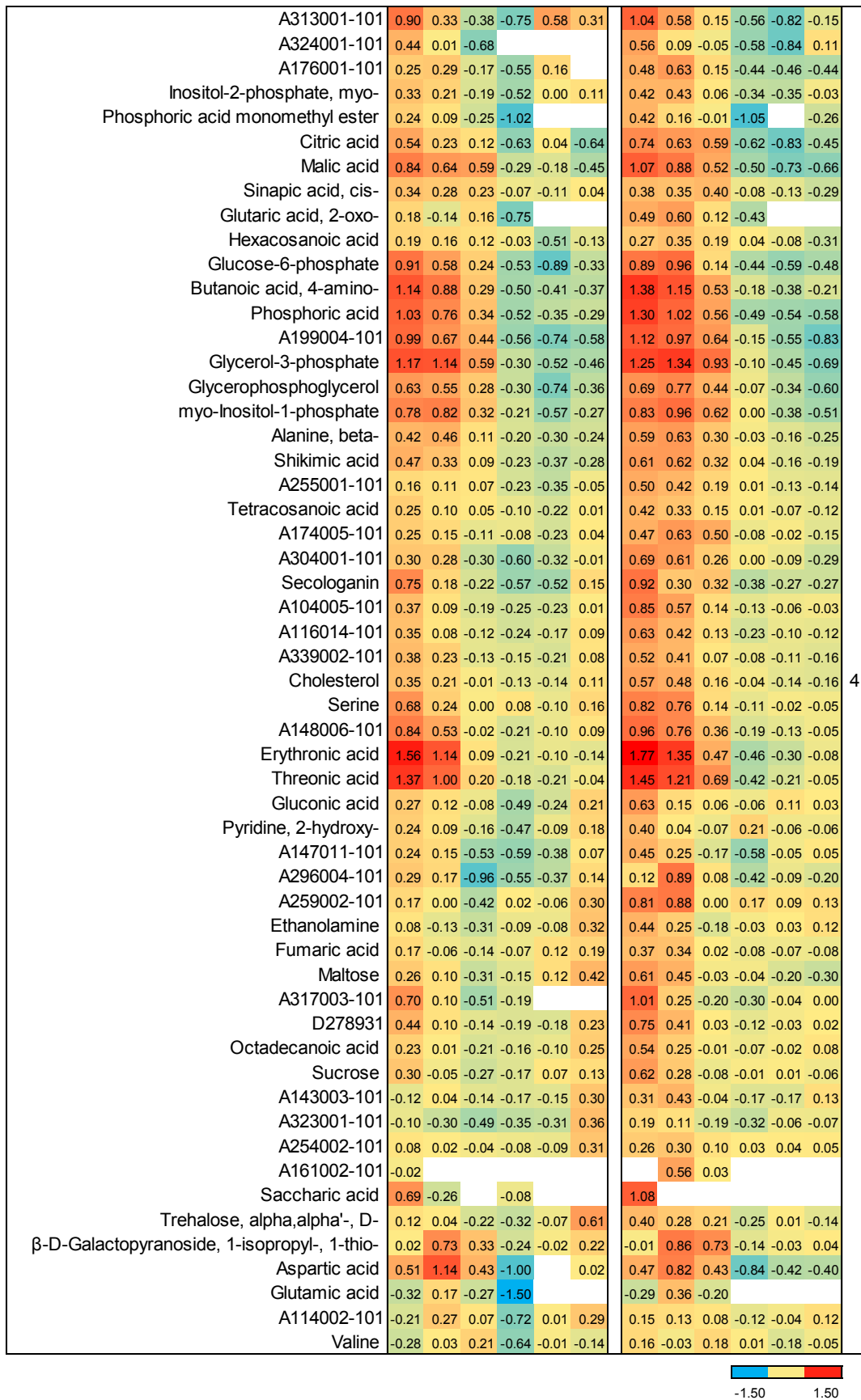


Figure 18: Correlation of the single leaf position samples of control and ^{12}C -sucrose (12C) fed plants. The calculations are based on a Pearson correlation of annotated metabolites with an average linkage. Bright red indicates a high correlation (1); dark red indicates an anti-correlation (-1); red indicates no correlation (0). Each column; row represents GC-MS primary metabolite data of annotated analytes.

To confirm the metabolic similarities which were observed in the ICA, samples were correlated to each other. A correlation matrix based on a Pearson correlation with an average linkage revealed that leaf positions 1 to 3 as well as leaf positions 5 to 7 were highly correlated to each other (Figure 18). These similarities were found for the 20 mM ^{12}C -sucrose feeding, for the control and between both feedings. This supported that the feeding had no global effect on the single leaf metabolites (Figure 18). In addition to the sample correlation

single metabolites were clustered to each other with a hierarchical clustering (HCL), to get a more detailed analysis of the response of single metabolites to the feeding.

	Control-Leaf1	Control-Leaf2	Control-Leaf3	Control-Leaf5	Control-Leaf6	Control-Leaf7	12C-SUC-Leaf1	12C-SUC-Leaf2	12C-SUC-Leaf3	12C-SUC-Leaf5	12C-SUC-Leaf6	12C-SUC-Leaf7	Cluster
A221004-101	0.00	0.02	0.18	-0.06	-0.24	-0.12	0.14	0.12	0.10	0.05	-0.10	-0.55	1
Alanine	-0.81	0.37	0.60	0.21	-0.12	-0.40	-0.54	-0.12	0.37	0.33	0.09	-0.10	
Threonine	-0.56	0.44	0.49	0.04	-0.22	-0.37	-0.41	-0.04	0.33	0.26	0.02	-0.27	
Dehydroascorbic acid dimer	-0.28	-0.25	0.14	0.02	-0.13	0.35	-0.07	0.14	0.18	0.19	-0.05	-0.17	2
A214004-101	0.09	-0.05	0.10	-0.01	-0.05	0.42	-0.16	0.08	0.06	0.15	0.13	0.06	
A143002-101			-0.11	-0.19		0.49				0.03	-0.01	0.12	
Caproic acid, 6-amino-	0.77			-0.63				0.03	0.48			-0.09	
Glucose	0.07	-0.05	-0.11	0.15	0.18	0.69	-0.26	-0.11	-0.22	0.14	0.08	-0.06	
Mannose	0.09	-0.06	-0.02	0.12	0.05	0.52	-0.08	0.05	-0.04	0.26	0.11	-0.05	
A216006-101	-0.49	-0.34	-0.02	0.06	0.07	0.35	-0.39	-0.14	-0.09	0.27	0.29	0.26	
Fructose	-0.38	-0.26	-0.34	0.20	0.28	0.73	-0.29	-0.25	-0.27	0.35	0.26	0.10	
Glycerol	-0.40	-0.59	-0.51	0.18	0.10	0.44	-0.05	-0.20	-0.42	0.22	0.26	0.22	
A203009-101	-0.53	-0.59	-0.37	0.14	0.47	0.61	-0.18	-0.32	-0.37	0.09	0.36	0.63	
Hexadecanoic acid	-0.15	-0.24	-0.25	0.04	0.18	0.34	0.12	-0.15	-0.10	0.06	0.11	0.22	
Octadecadienoic acid, 9,12-	-0.41	-0.44	-0.17	0.11	0.14	0.31	-0.16	-0.66	-0.20	0.07	0.18	0.26	
Octadecatrienoic acid, n-	-0.44	-0.50	-0.12	0.24	0.29	0.46	-0.09	-0.71	-0.19	0.19	0.34	0.45	
Fructose-6-phosphate	0.08	-0.32	-0.27	-0.19	-0.03	0.47	0.15	0.11	-0.14	0.02	0.07	0.26	
A211001-101	-0.15	-0.16	-0.02	-0.05	-0.10	0.44	-0.07	0.11	0.02	0.03	0.14	0.14	
A236005-101	-0.07	-0.11	-0.03	-0.08	-0.04	0.37	0.06	0.14	0.01	0.03	0.11	0.13	
Galactose	-0.16	-0.26	-0.13	0.04	0.01	0.44	0.20	0.02	-0.05	0.29	0.22	0.09	
A250001-101	-0.26	-0.25	-0.23	-0.08	-0.05	0.37	-0.13	0.03	-0.12	0.07	0.14	0.15	
similar to Glycerolaldopyranosid	-0.18	-0.38	-0.32	-0.06	0.03	0.44	0.05	-0.03	-0.15	0.14	0.17	0.23	
Melibiose			-0.58	-0.24	0.09	0.13	0.36		-0.22	0.13	0.36	0.07	
Putrescine	-0.36	-0.17	-0.59	-0.12	0.12	0.05	0.02	-0.04	-0.22	0.34	0.47	0.51	
Raffinose	-0.36	-0.69	-0.79	-0.40	-0.30	-0.30	-0.16	-0.18	-0.07	0.25	0.03	-0.26	
Kestose, 1-	-0.28	-0.39	-0.09	-0.15	-0.05	-0.42	0.45	0.13	-0.26	0.18	0.21	-0.35	
A251003-101	-0.06	-0.06	-0.11	-0.18	-0.39	0.04	0.20	0.33	0.03	0.05	0.06	0.08	
Glyceric acid	0.02	-0.06	-0.11	-0.21	-0.26	-0.11	0.50	0.79	0.46	0.31	0.12	0.10	
Galactinol	-0.52	-0.49	-0.51	-0.23	-0.37	-0.04	0.67	0.47	0.20	0.15	0.06	-0.09	
Glycine	-0.64	-0.33	-0.29	-0.49	-0.30	-0.54	0.25	0.35	0.13	0.11	0.12	0.04	
A300001-101	0.30	0.08	-0.41	-0.23	-0.60	-0.34	0.54	0.47	0.19	0.32	-0.07	-0.37	
A311002-101	0.11	-0.04	-0.64	-0.16	-0.06	-0.18	0.29	0.27	-0.07	0.08	0.00	-0.44	
A158017-101	0.14	-0.17	-0.15	-0.02	-0.22	-0.01	0.35	0.19	-0.13	0.11	0.09	-0.02	
Campesterol	0.23	0.09	-0.12	-0.04	-0.24	0.18	0.41	0.37	0.06	0.04	-0.06	-0.11	
Sitosterol, beta-	0.20	0.08	-0.16	0.03	-0.22	0.20	0.38	0.34	0.02	0.08	0.01	-0.13	
A106004-101	0.33	0.01	-0.23	-0.15	0.07	0.17	0.70	0.32	-0.01	-0.01	-0.05	-0.06	
Fumaric acid, 2-methyl-										0.75	-0.17		
Inositol, myo-	0.37	0.06	-0.18	-0.04	0.02	0.21	0.66	0.38	0.02	0.12	0.09	0.01	
Tocopherol, alpha-	0.36	0.06	-0.32	-0.04	-0.22	0.04	0.57	0.28	-0.04	0.10	-0.07	-0.06	



4

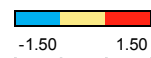


Figure 19: Heat map of annotated analytes of petiole feeding and control data. Clusters of a HCL are shown; analytes were clustered with a Pearson correlation and an average linkage; tree distance threshold was set to -0.295. Values are average response ratios.

The analysis revealed four clusters of metabolites (Figure 19). The behaviour of the majority of metabolites across the different leaf positions found in cluster 1, 2 and 4 seemed to be very similar between the control and the 20 mM ¹²C-sucrose feeding (Figure 19). Only in cluster 3 the behaviour of some metabolites differed between the control and the feeding (Figure 19). To support these observed different behaviours, metabolites were further investigated by an analysis of variances (ANOVA). To this end the data was subjected to a 2-way-ANOVA and a Mack-Skillings test to find the robust changes in metabolite pool size due to the petiole feeding. A parametric and a non-parametric test were used to find only robustly changed metabolites. The critical p-value was $p \leq 0.001$ for both tests to guarantee a significant change by keeping a false discovery rate at one of a thousand. Significance was tested for the feeding and the different leaf positions.

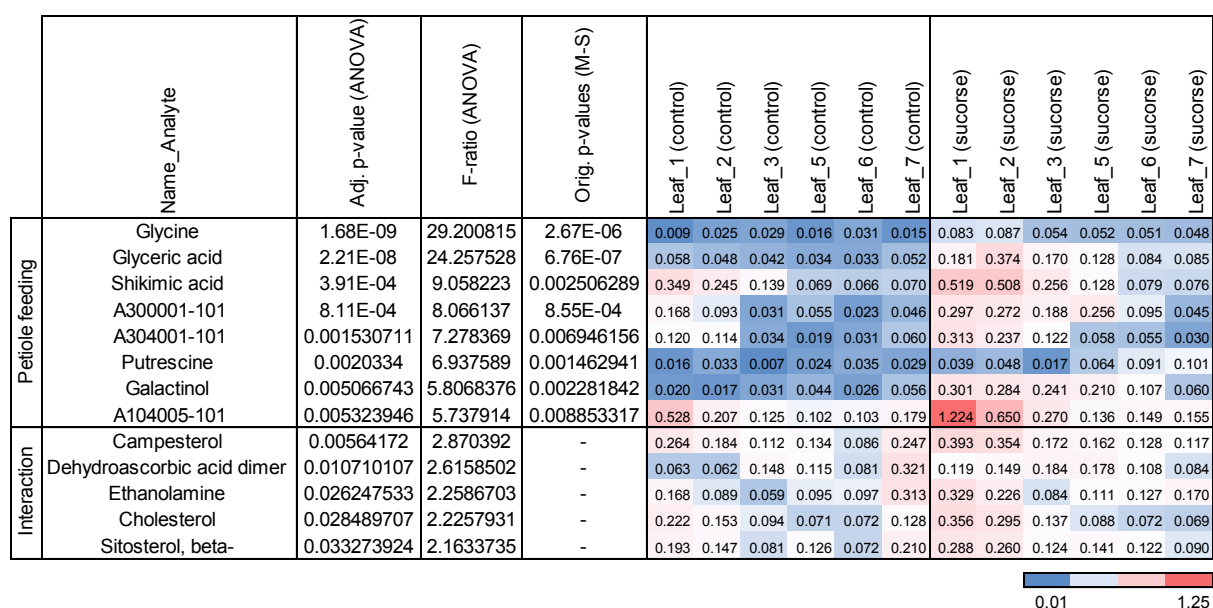


Figure 20: Heat map of significantly changed analytes after petiole feeding with a 20 mM ¹²C-sucrose solution. Shown are the top ten analytes that change significantly in the different categories. Significance was tested with a 2-way-ANOVA (ANOVA) and a Mack-Skillings test (M-S). Different feedings (petiole feeding) were tested as well as different leaf positions (development). Analytes are sorted by F-ratio top-down and cut off at a critical p-value of $p \leq 0.01$. In the interaction section analytes are shown with p-values of $p \leq 0.05$. Values of the heat map are averages of normalized responses of 3-5 replicates.

Only four analytes were found to be changed significantly for the petiole feeding: glycine, glyceric acid, shikimic acid and an unknown analyte (A300001-101) (Figure 20). By setting the p-value to $p \leq 0.01$, four more analytes could be found, namely putrescine, galactinol and two unknown analytes (A304001-101, A104005-101) (Figure 20). For the purpose of finding

analytes that do not only change in pool size but also in their pattern across leaf positions, metabolites changed in the interaction of both categories were selected with a p-value of $p \leq 0.05$. Changes could be found for sterols, lipid related compounds and dehydroascorbic acid dimer. Nevertheless a p-value of $p \leq 0.05$ has a false discovery rate of 5 out of 100 analytes and only indicates metabolites that could possibly be changed.

The galactinol increase indicates an activation of the stachyose pathway, supported by similar but less significant pool size changes for raffinose ($p = 0.025$). Furthermore putrescine, glycine and glyceric acid were increased (Figure 21).

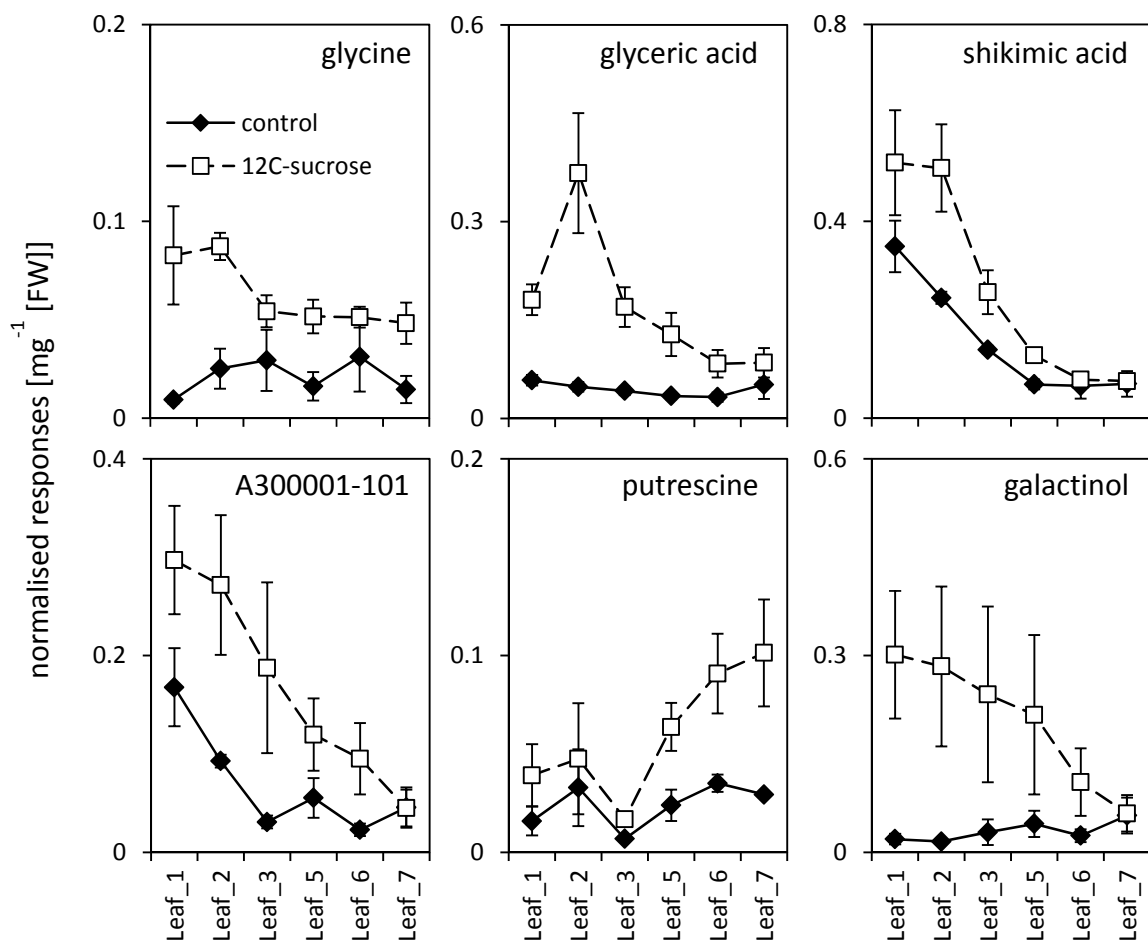


Figure 21: Selection of analytes changed due to petiole feeding. Shown are analytes that changed significantly for the petiole feeding (see heat map (Figure 20)). Significance was tested with a 2-way-ANOVA and a Mack-Skillings test. Shown are averages of 3-5 replicates; error bars represent the standard error.

3.1.4 Hypocotyl feeding assay – for homogeneous feeding

3.1.4.1 Development of a hypocotyl feeding method

The petiole feeding that was investigated above can be applied to analyse the carbon allocation between different single leaf positions and the root system. However, for analysing the carbon allocation in each leaf of a rosette a different feeding approach was necessary. For a more general analysis of all leaves of a shoot the hypocotyl feeding method was developed.

To reach an even distribution in the rosette, a labelling solution was fed into the plant via the hypocotyl. Therefore a whole plant was cut off at the root and the freshly cut hypocotyl placed in a reservoir with a labelling solution. The solution could then translocate into the plant (Figure 22).

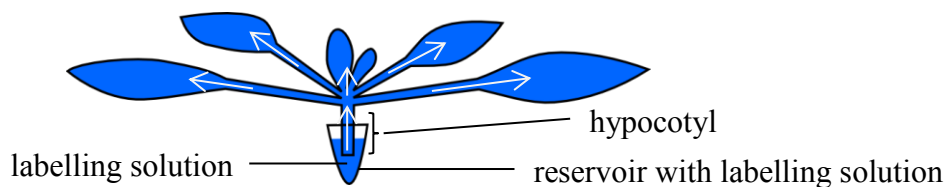


Figure 22: Scheme of the hypocotyl feeding assay. The distribution of the labelling solution is indicated by the blue colour and the arrows. The plant is cut off the root and the hypocotyl is put in a reservoir with labelling solution.

The distribution of the labelling solution was first tested in the plant by feeding the dye Brilliant Blue FCF (see 2.3.4). The feeding resulted in an equal distribution of the dye in the rosette (Figure 23), suggesting a uniform distribution for labelling solutions. A ^{13}C -sucrose solution was fed to test its distribution.



Figure 23: Testing the distribution of a dye by a hypocotyl feeding assay. Picture shows a control plant (A) and a plant fed with Brilliant Blue FCF via the hypocotyl for 1 hour (B).

The distribution of ^{13}C -sucrose was captured by measuring the sucrose ^{13}C -enrichment in single leaf positions of a rosette. Since the petiole feeding showed a high variation in feeding efficiency, the number of replicates was increased for further investigations. Plants in a 7-9 leaf stage were fed with a 20 mM and a 100 mM ^{13}C -sucrose solution with the hypocotyl feeding approach for 4 hours and each leaf position was harvested directly in liquid nitrogen. The methanol extracts were measured by GC-MS and the resulting data further processed. To analyse the ^{13}C -sucrose distribution in the rosette the average sucrose ^{13}C -enrichment was calculated for each harvested leaf position (Figure 24a) and each harvested plant (Figure 24b).

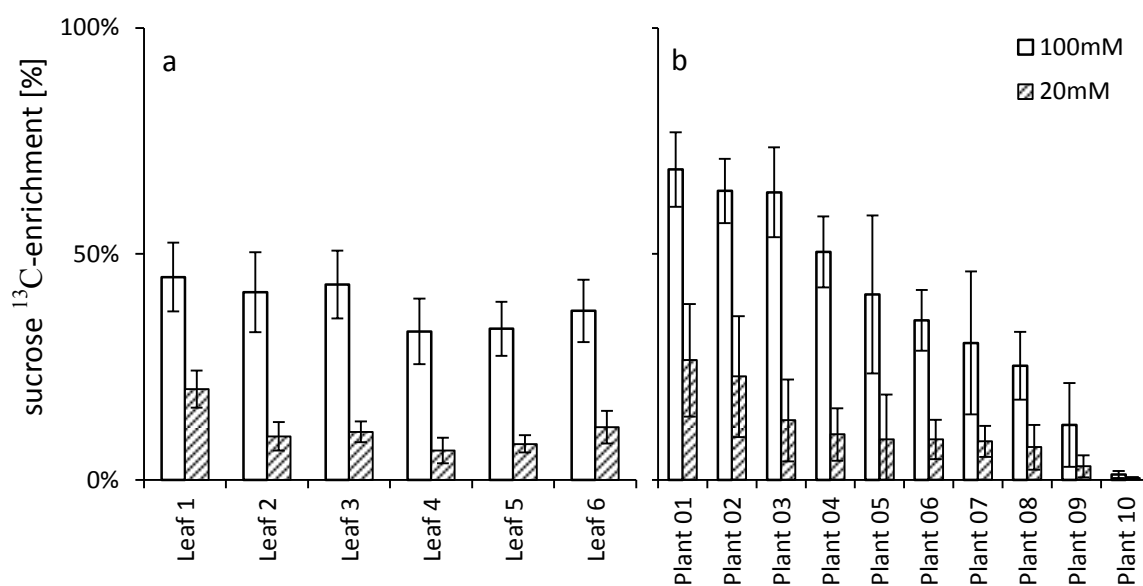


Figure 24: Distribution of ^{13}C -sucrose in *Arabidopsis* rosettes fed by a hypocotyl feeding. The average sucrose ^{13}C -enrichment is diagrammed for each leaf position (a) and each plant (b). Calculations were based on two experiments, one where plants were fed with a 100 mM (100mM) and one where plants were fed with a 20 mM (20mM) ^{13}C -sucrose solution. Averages of leaf positions were calculated out of 9-10 replicates; error bars represent the standard error. Averages for each plant were calculated out of 5-6 leaves; error bars represent the standard deviation.

The 100 mM ^{13}C -sucrose solution led to an average sucrose labelling between 69% and 1% and a 20 mM ^{13}C -sucrose solution revealed a range from 26% to 0.4% (Figure 24b). Although the range of labelling is quite wide over the different replicates, the standard deviation indicates that the variation of labelling in the different leaves of one plant seemed to be small for both labelling experiments (Figure 24b). The average ^{13}C -enrichment of the different leaf positions showed a nearly constant labelling between 45% and 33% for the 100 mM ^{13}C -sucrose solution and between 11% and 7% for the 20 mM ^{13}C -sucrose solution

(Figure 24a). This supported the afore-mentioned even distribution of labelling solution in the rosette, which leads to a uniform labelling.

3.1.4.2 Testing the influence of hypocotyl feeding on the plant metabolism

For the purpose of method validation a control feeding experiment was performed to test how the hypocotyl feeding assay influences the metabolite pool sizes. A population of 5-week-old *Arabidopsis* plants in a 7-9 leaf stage was split into three groups. Two groups were fed either with a 100 mM (100 mM) or a 20 mM (20 mM) ^{12}C -sucrose solution and one group neither cut nor fed was used as a control (control). After 4 hours single leaves were harvested from the plants for a GC-MS analysis of primary metabolites. Nine to ten replicates were harvested from each leaf position and each condition for a precise investigation of the feeding method.

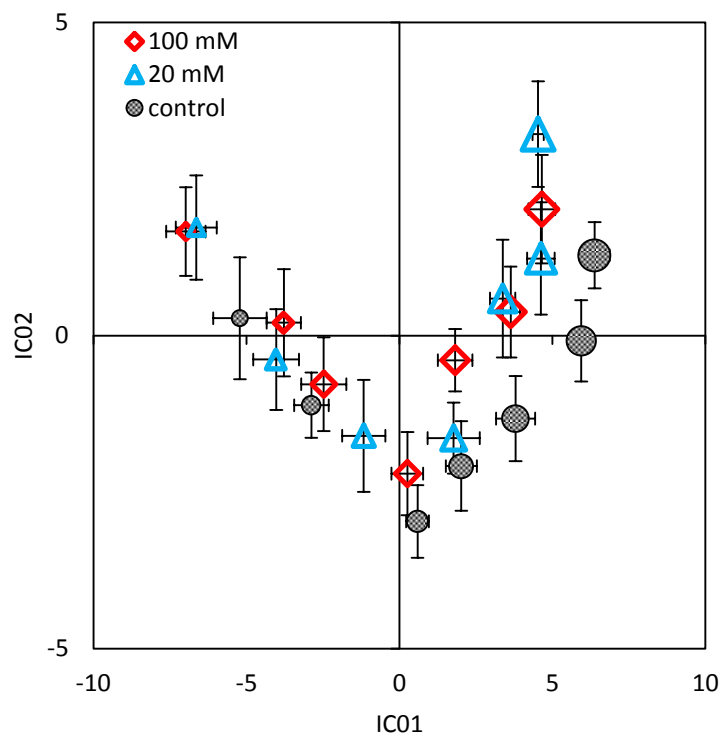


Figure 25: Global view on primary metabolites of plants fed by a hypocotyl feeding assay and control plants. ICA is calculated based on GC-MS profile data of the primary metabolism that was subjected to a PCA. ICA is based on 3 PCs covering 61% of the total variance. Displayed are the average values of each leaf position (small = young leaves; big = mature leaves). Error bars represent the standard error. Control = not fed; 20 mM = fed with a 20 mM ^{12}C -sucrose solution; 100 mM = fed with a 100 mM ^{12}C -sucrose solution. Averages are calculated out of 9-10 biological replicates.

Around 120 analytes were annotated in the GC-MS analysis of the methanol extract of single leaves. In order to get a first insight into the global metabolic difference between the hypocotyl feeding and the control, an ICA was calculated on the basis of 3 PCs covering 61% of the total variance. The ICA revealed again a separation between the developmental stages

of the different leaf positions and also a small separation between the feedings and the control (Figure 25), which was to be expected.

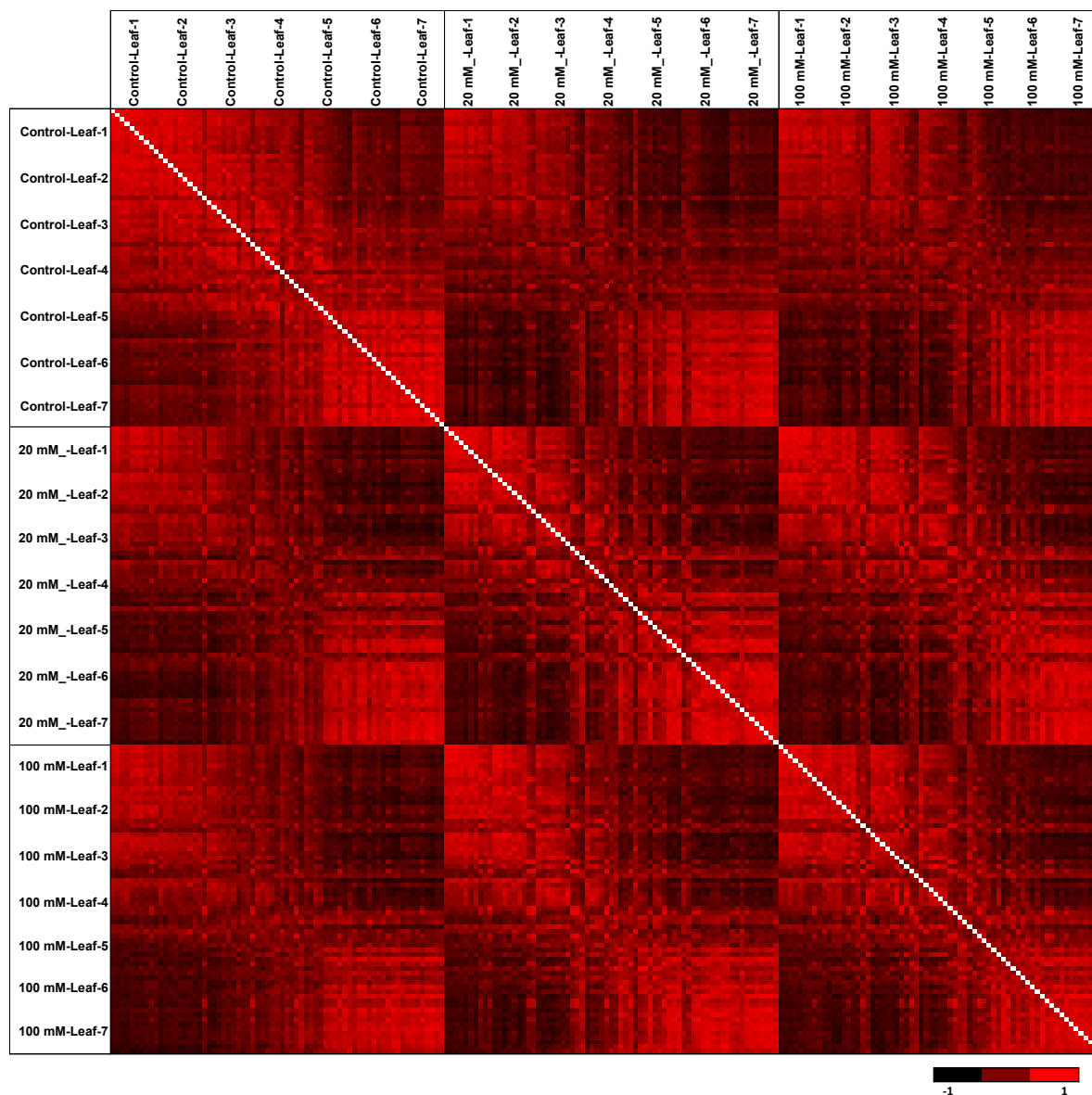


Figure 26: Clustering of samples of single leaf positions of control and ^{12}C -sucrose-fed plants of a hypocotyl feeding. Sample distance matrix is based on annotated analytes. Calculations are based on a Pearson correlation with an average linkage. Plants were fed with a 20 mM (20mM) and a 100 mM (100mM) ^{12}C -sucrose solution. Each column; row represents GC-MS primary metabolite data of annotated analytes.

The differences in metabolite profiles that were observed in the ICA were further examined. To find out which samples showed a similar metabolite profile, a correlation analysis was performed. To this end, each sample was correlated to all samples. The resulting correlation matrix based on a Pearson correlation with an average linkage validated the continuous change between leaf positions (Figure 26) that could already be observed in the ICA (Figure 25). The matrix shows in addition that same leaf positions correlate strongly with each other

for the different feedings, the control and between all, pointing out that the hypocotyl feeding has no global effect on the single leaf primary metabolites (Figure 26).

	Control-Leaf-1	Control-Leaf-2	Control-Leaf-3	Control-Leaf-4	Control-Leaf-5	Control-Leaf-6	Control-Leaf-7	20 mM_-Leaf-1	20 mM_-Leaf-2	20 mM_-Leaf-3	20 mM_-Leaf-4	20 mM_-Leaf-5	20 mM_-Leaf-6	20 mM_-Leaf-7	100 mM_-Leaf-1	100 mM_-Leaf-2	100 mM_-Leaf-3	100 mM_-Leaf-4	100 mM_-Leaf-5	100 mM_-Leaf-6	100 mM_-Leaf-7	Cluster
A115001-101	0.07	0.01	-0.08	-0.01	0.03	0.01	0.08	0.03	0.01	-0.09	-0.09	0.01	0.00	0.05	0.00	0.03	0.02	-0.03	0.08	0.08	0.09	1
A311002-101	0.07	-0.20	-0.30	-0.14	-0.01	0.09	0.18	0.09	-0.29	-0.34	-0.19	0.02	0.16	0.34	0.12	-0.12	-0.24	-0.20	0.02	0.09	0.17	
Octadecenoic acid, 9-	0.01	0.00	-0.06	0.05	0.01	0.01	-0.02	0.00	-0.07	-0.10	-0.06	0.07	0.08	0.12	0.02	-0.03	-0.02	-0.05	0.06	0.01	0.00	
Octadecadienoic acid, 9,12-	-0.18	-0.14	-0.11	0.04	0.01	0.02	-0.02	-0.24	-0.19	-0.12	-0.02	0.11	0.11	0.12	-0.14	-0.09	-0.06	-0.02	0.12	0.09	0.08	
Octadecatrienoic acid, 9,12,15-	-0.18	-0.23	-0.16	0.00	0.02	0.05	0.04	-0.22	-0.26	-0.16	-0.03	0.11	0.14	0.20	-0.11	-0.14	-0.12	-0.07	0.11	0.11	0.12	
Glycerol	-0.19	-0.16	-0.12	0.00	0.05	0.08	0.08	-0.15	-0.19	-0.04	0.01	0.17	0.17	0.18	-0.18	-0.14	-0.13	-0.06	0.09	0.14	0.19	
Phytol	-0.27	-0.23	-0.12	-0.02	0.06	0.05	0.00	-0.15	-0.17	0.00	0.08	0.19	0.18	0.12	-0.20	-0.16	-0.10	0.03	0.14	0.16	0.17	
A339002-101	-0.24	-0.28	-0.29	-0.18	-0.03	0.00	0.15	0.09	0.38	0.06	0.12	0.26	0.21	0.37	-0.14	0.11	0.04	0.05	0.26	0.26	0.26	
Serine	-0.07	-0.07	-0.15	-0.04	-0.04	-0.01	-0.04	0.10	0.04	0.04	0.02	0.09	0.11	0.16	0.07	0.06	0.04	-0.05	0.07	0.16	0.11	
similar to Glycerolaldopyranosid	-0.23	-0.28	-0.29	-0.18	-0.09	-0.09	-0.04	0.03	-0.04	0.03	0.02	0.07	0.08	0.18	0.05	0.00	0.00	-0.03	0.08	0.11	0.11	
A145015-101	-0.07	-0.13	-0.24	-0.20	-0.04	0.10	0.15	0.03	-0.02	-0.04	-0.02	0.29	0.28	0.28	0.04	-0.06	-0.10	-0.15	-0.03	0.12	0.25	
A145016-101	-0.07	-0.16	-0.27	-0.24	-0.07	0.05	0.10	0.05	-0.02	-0.06	-0.06	0.22	0.24	0.23	0.07	-0.06	-0.10	-0.21	-0.08	0.07	0.19	
A217004-101	-0.15	-0.12	-0.18	-0.13	-0.02	0.01	0.16	0.01	-0.06	-0.04	-0.04	0.12	0.18	0.33	-0.03	-0.03	-0.01	-0.05	0.02	0.12	0.27	
A214003-101	-0.26	-0.22	-0.18	-0.12	-0.01	0.03	0.15	-0.06	-0.03	0.01	0.07	0.22	0.25	0.22	-0.11	-0.05	-0.01	0.02	0.07	0.18	0.28	
A243001-101	-0.13	-0.11	-0.13	-0.09	-0.03	0.04	0.01	-0.01	-0.03	-0.02	-0.01	0.07	0.11	0.14	-0.02	-0.04	0.00	-0.01	0.05	0.07	0.12	
A174001-101	-0.14	-0.14	-0.15	-0.09	0.00	0.01	0.08	-0.01	-0.03	-0.02	0.01	0.12	0.15	0.21	-0.03	-0.04	-0.01	-0.01	0.08	0.12	0.19	
Unknown n-ketose II	-0.17	-0.14	-0.14	-0.08	0.00	-0.01	0.06	-0.03	-0.03	0.03	0.02	0.12	0.15	0.18	-0.04	-0.03	-0.03	0.02	0.07	0.12	0.16	
Caffeic acid, trans-	0.43	-0.08	0.05	0.12	-0.13	-0.15	-0.10	0.09	-0.30	0.54				0.11	0.00	0.04	0.00	-0.15	-0.19	0.00	0.15	
Glucose, 1,6-anhydro-, beta-	0.14	0.05	0.00	0.05	0.04	-0.09	-0.12	0.05	-0.05	-0.03	-0.04	-0.03	-0.06	0.02	0.05	0.01	0.03	-0.04	0.00	0.02	-0.08	
A213001-101	-0.16	0.14	-0.28					0.03	-0.02	-0.20	-0.27				0.15	-0.23	-0.19	-0.44		-0.16		
Asparagine	0.16	1.16	0.26	-0.41				0.80		-0.61			-0.66		0.36	-0.14		-0.21				
Glucose	-0.06	0.01	0.04	0.20	0.23	-0.02	-0.03	0.26	-0.02	-0.22	-0.30	-0.25	-0.08	-0.07	0.40	0.10	-0.06	-0.13	-0.11	-0.15	0.18	
Glyceric acid	0.02	-0.03	0.04	0.09	0.07	0.03	-0.09	0.17	0.01	0.00	-0.01	0.00	-0.03	-0.12	0.20	-0.01	-0.05	-0.01	-0.02	-0.01	-0.08	
Alanine	-0.03	0.13	0.06	0.09	0.05	0.04	-0.02	-0.02	-0.06	-0.02	-0.03	-0.09	-0.08	-0.10	-0.08	-0.09	-0.09	0.06	-0.03	-0.11	-0.06	
A211001-101	0.16	0.17	0.12	0.14	0.09	-0.04	-0.13	0.01	-0.06	-0.08	-0.09	-0.04	-0.04	-0.16	0.13	-0.01	0.00	0.02	0.02	-0.06	-0.05	
A254002-101	0.13	0.18	0.12	0.17	0.13	-0.03	-0.10	-0.03	-0.09	-0.07	-0.08	-0.03	-0.02	-0.15	0.09	-0.03	-0.02	0.03	0.05	-0.02	-0.02	
A116014-101	0.38	0.48	0.40	0.11	0.05	-0.25	-0.33	0.11	0.02	0.01	-0.06	-0.19	-0.18	-0.35	0.08	-0.13	-0.13	-0.15	-0.33	-0.43		
A203005-101	0.02	0.04	-0.04	-0.09	-0.10	-0.11	-0.14	-0.07	-0.20	-0.20	-0.26	-0.28	-0.28	-0.27	-0.08	-0.18	-0.18	-0.19	-0.19	-0.25	-0.22	
Glycine	0.26	0.39	0.32	0.26	0.25	-0.05	-0.09	0.01	-0.07	-0.01	-0.17	-0.26	-0.32	-0.33	0.12	-0.07	-0.05	-0.07	-0.13	-0.24	-0.26	
A251003-101	-0.20	-0.01	-0.03	-0.12	0.01	-0.07	-0.12	-0.08	0.04	-0.12	-0.18	-0.19	-0.18	-0.12	-0.16	-0.11	-0.01	-0.08	0.01	-0.07	-0.09	
Fructose	-0.30	-0.33	-0.25	-0.10	0.03	-0.09	0.05	0.34	0.12	-0.11	-0.17	-0.13	0.13	0.15	0.44	0.24	0.15	-0.02	0.06	0.01	0.44	
A182004-101	0.09	-0.08	-0.09	-0.21	-0.11	-0.06	0.10	0.06	0.05	-0.05	-0.07	0.00	-0.01	0.20	0.14	-0.02	0.02	-0.06	-0.06	-0.01	0.05	
Boric-acid_3TMS	0.14	0.11	-0.06	-0.06	-0.06	-0.09	0.07	0.21	0.08	0.08	0.03	0.02	0.04	0.12	0.12	0.12	0.05	-0.01	0.02	-0.04	-0.02	
Lactic acid	0.13	0.02	-0.11	-0.02	-0.09	-0.02	0.01	0.18	0.06	0.02	-0.06	0.03	0.00	0.10	0.12	0.07	-0.04	-0.05	-0.06	-0.02	-0.02	
Diethyleneglycol	0.13	0.09	-0.03	-0.02	-0.07	-0.05	0.00	0.10	0.01	-0.01	-0.05	-0.01	-0.05	0.04	0.07	0.03	0.01	-0.06	-0.01	0.00	-0.01	
A221004-101	0.13	0.11	-0.04	-0.05	-0.08	-0.04	0.00	0.13	0.05	0.01	-0.05	0.01	-0.02	0.09	0.10	0.08	0.03	-0.05	-0.03	-0.03	-0.02	
Hexanoic acid, 2-ethyl-	0.13	0.10	-0.02	-0.03	-0.08	-0.01	0.00	0.10	-0.01	-0.02	-0.06	-0.03	-0.02	0.08	0.08	0.07	0.02	-0.04	0.01	-0.02	-0.04	
Hexadecanoic acid	0.17	0.11	-0.03	-0.03	-0.07	-0.08	-0.05	0.16	0.05	-0.03	-0.08	-0.03	-0.03	0.05	0.17	0.10	0.05	-0.05	0.01	0.00	-0.01	
A165011-101	0.13	0.10	-0.03	-0.04	-0.08	-0.06	-0.04	0.13	0.03	0.01	-0.03	-0.03	-0.04	0.03	0.11	0.10	0.07	-0.02	0.00	-0.01	-0.03	
A260006-101	0.14	0.11	-0.03	-0.06	-0.09	-0.08	-0.06	0.15	0.05	0.02	-0.03	-0.02	-0.04	0.02	0.13	0.11	0.08	-0.02	0.01	-0.01	-0.04	
Dodecanoic acid	0.16	0.08	-0.05	-0.04	-0.11	-0.12	-0.10	0.19	0.07	0.01	-0.07	-0.03	-0.06	0.01	0.20	0.12	0.05	-0.02	-0.01	-0.04	-0.05	
Octadecanoic acid	0.17	0.11	-0.02	-0.03	-0.08	-0.08	-0.08	0.18	0.06	0.00	-0.05	-0.03	-0.06	0.01	0.17	0.12	0.06	-0.03	0.00	-0.01	-0.04	
Tetradecanoic acid	0.14	0.13	-0.02	-0.05	-0.09	-0.12	-0.10	0.17	0.06	0.02	-0.03	-0.05	-0.08	-0.02	0.16	0.11	0.07	0.00	-0.01	-0.04	-0.08	
A174005-101	0.12	0.00		-0.21	-0.14	-0.05	-0.08	0.30	0.19	0.10	-0.25	-0.07	-0.02	0.08	0.39	0.10	0.02	-0.11	-0.15	-0.06	-0.03	
A164017-101	0.17	0.03	-0.10	-0.16	-0.20		-0.12	0.24	0.13	-0.03	-0.16	-0.25	-0.17	0.04	0.26	0.11	0.04	-0.08	-0.15	-0.14	-0.13	
A313001-101	0.03	0.03	-0.15	-0.20	-0.14		-0.25	0.11	0.05	0.02	-0.23		-0.22	-0.04	0.17	0.03	-0.08	-0.13	-0.20	-0.19	-0.21	
A170001-101	0.16	0.02	-0.03	-0.04	-0.01	-0.10	-0.11	0.22	0.10	0.01	-0.04	-0.04	-0.05	-0.06	0.30	0.08	0.03	-0.03	-0.01	-0.03	-0.07	
A199004-101	0.16	0.10	-0.03	-0.09	-0.11	-0.12	-0.13	0.38	0.19	0.03	-0.05	-0.01	0.04	-0.04	0.56	0.19	0.09	-0.04	0.01	-0.03	-0.03	
A228001-101	0.27	-0.04	-0.18	-0.15				0.27	0.06	-0.03	-0.18				0.34	-0.09	-0.04	-0.06	-0.22			
Citric acid	0.48	0.09	-0.21	-0.35	-0.24	-0.24	-0.05	0.60	0.19	-0.17	-0.30	-0.28	-0.39	-0.01	0.61	0.17	0.04	-0.31	-0.24	-0.25	-0.24	
Erythronic acid	0.82	0.30	-0.04	-0.11	-0.04	-0.07	0.04	0.73	0.22	-0.10	-0.13	-0.11	-0.08	0.05	0.75	0.35	0.08	-0.06	-0.15	-0.10	-0.10	
A264005-101	0.61	0.13	-0.09	-0.27	-0.15	-0.19	-0.13	0.80	0.33	0.00	-0.16	-0.06	0.00	-0.03	0.84	0.32	0.11	-0.08	-0.15	-0.15	-0.09	
Threonic acid	0.85	0.37	0.06	-0.04	-0.06	-0.18	-0.15	0.88	0.39	0.04	-0.09	-0.14	-0.11	-0.								

across the different leaf positions comparing the feeding and the control, indicating a low influence of the hypocotyl feeding on single leaf metabolites.

To support these observed different responses, metabolites were further investigated by an analysis of variances (ANOVA). A parametric and a non-parametric test were used to select only for robustly changed metabolites. For a deeper insight a 2-way-ANOVA and a Mack-Skillings test were performed with a critical p-value of $p \leq 0.001$ to find metabolites that were significantly changed due to the hypocotyl feeding and the developmental differences between leaf positions. In addition changes in the interaction of these two categories were examined. Furthermore, analytes were sorted by F-ratios top-down and the top ten are shown in a heat map (Figure 28). Interactions showed generally higher p-values and therefore all analytes with a p-value of less than 0.05 are shown. In addition significance was tested with a Student's *t*-test between feedings and control for single leaf positions with a p-value of 0.05 before Bonferroni correction (n=120).

	NAME ANALYTE	Adj. P-value (ANOVA)	F-ratio (ANOVA)	Orig. P-value (M-S)	Hypocotyl feeding							Inter													
					Leaf_1 (control)	Leaf_2 (control)	Leaf_3 (control)	Leaf_4 (control)	Leaf_5 (control)	Leaf_6 (control)	Leaf_7 (control)	Leaf_1 (20mM)	Leaf_2 (20mM)	Leaf_3 (20mM)	Leaf_4 (20mM)	Leaf_5 (20mM)	Leaf_6 (20mM)	Leaf_7 (20mM)	Leaf_1 (100mM)	Leaf_2 (100mM)	Leaf_3 (100mM)	Leaf_4 (100mM)	Leaf_5 (100mM)	Leaf_6 (100mM)	Leaf_7 (100mM)
Hypocotyl feeding	Galactinol	<1E-16	488.3	<1E-16	0.01	0.01	0.01	0.01	0.02	0.01	0.01	0.24	0.16	0.11	0.08	0.08	0.06	0.04	0.24	0.13	0.10	0.08	0.07	0.07	0.05
	β-Alanine	<1E-16	482.7	<1E-16	0.04	0.03	0.03	0.03	0.03	0.02	0.01	0.17	0.15	0.15	0.12	0.10	0.08	0.05	0.17	0.14	0.14	0.12	0.11	0.08	0.05
	Raffinose	<1E-16	112.5	8.88E-16	0.01	0.01	0.01	0.01	0.03	0.03	0.02	0.13	0.11	0.10	0.08	0.10	0.07	0.06	0.15	0.10	0.08	0.08	0.08	0.08	0.06
	A231002-101	<1E-16	68.0	<1E-16	0.05	0.05	0.05	0.06	0.08	0.08	0.08	0.10	0.09	0.10	0.10	0.11	0.11	0.14	0.10	0.09	0.09	0.08	0.11	0.12	0.12
	γ-Butanoic acid (GABA)	<1E-16	61.1	<1E-16	0.01	0.00	0.00	0.00	0.00	0.00	0.00	0.01	0.01	0.01	0.01	0.01	0.01	0.00	0.01	0.01	0.01	0.01	0.01	0.01	0.00
	Unknown-Ketose III	<1E-16	55.0	<1E-16	0.10	0.09	0.08	0.09	0.09	0.07	0.07	0.14	0.12	0.11	0.10	0.10	0.09	0.09	0.15	0.13	0.12	0.12	0.11	0.10	0.10
	A211001-101-xxx	<1E-16	53.6	<1E-16	0.08	0.08	0.08	0.09	0.11	0.11	0.13	0.10	0.10	0.10	0.11	0.14	0.15	0.18	0.10	0.10	0.10	0.11	0.13	0.15	0.17
	Unknown-Ketose II	<1E-16	53.0	<1E-16	0.07	0.08	0.08	0.09	0.11	0.10	0.12	0.10	0.10	0.11	0.11	0.14	0.15	0.16	0.10	0.10	0.10	0.11	0.12	0.14	0.15
	Putrescine	<1E-16	49.5	1.17E-13	0.04	0.04	0.04	0.03	0.02	0.02	0.02	0.04	0.06	0.08	0.07	0.07	0.06	0.06	0.05	0.06	0.07	0.09	0.08	0.07	0.05
	Arabinose	<1E-16	48.3	2.32E-14	0.15	0.14	0.12	0.12	0.12	0.08	0.08	0.20	0.19	0.16	0.14	0.13	0.12	0.11	0.20	0.17	0.16	0.14	0.13	0.12	0.12
Inter	Fructose	9.63E-04	2.9	-	0.02	0.02	0.02	0.03	0.04	0.03	0.05	0.07	0.05	0.03	0.03	0.02	0.06	0.07	0.10	0.07	0.06	0.03	0.05	0.05	0.11
	A214003-101	0.01069	2.3	-	0.11	0.12	0.11	0.12	0.12	0.08	0.07	0.08	0.07	0.07	0.07	0.08	0.08	0.06	0.10	0.08	0.08	0.09	0.09	0.08	0.08
	A213001-101	0.03068	2.0	-	0.13	0.13	0.12	0.13	0.12	0.08	0.07	0.09	0.08	0.08	0.08	0.08	0.09	0.06	0.13	0.09	0.09	0.10	0.10	0.08	0.08

Figure 28: Heat map of significantly changed metabolites due to hypocotyl feeding. Shown are the top ten analytes that change significantly in the different categories. Significance was tested with a 2-way-ANOVA (ANOVA) and a Mack-Skillings test (M-S). The different feedings (Hypocotyl feeding) were tested as well as the interaction (Inter) between hypocotyl feeding and the different leaf positions. Analytes were sorted by F-ratio top-down and a p-value of $p \leq 0.05$. Values shown are averages of normalised responses of 9-10 replicates.

The strongest increases were found for galactinol and raffinose (Figure 28, Figure 29), indicating an activation of the stachyose pathway. These increases were observed especially in young leaves with an up to 23-fold increase, but less in mature leaves, resulting in a decreasing curve from young to mature leaves and a strong change of the isomolar pattern found in the control plants. The heat map of Figure 28 also shows that three more sugars

increase in the hypocotyl feeding category: unknown-ketoses I, II and III. Likewise increased were β -alanine, putrescine and γ -aminobutyric acid (GABA) (Figure 28, Figure 29).

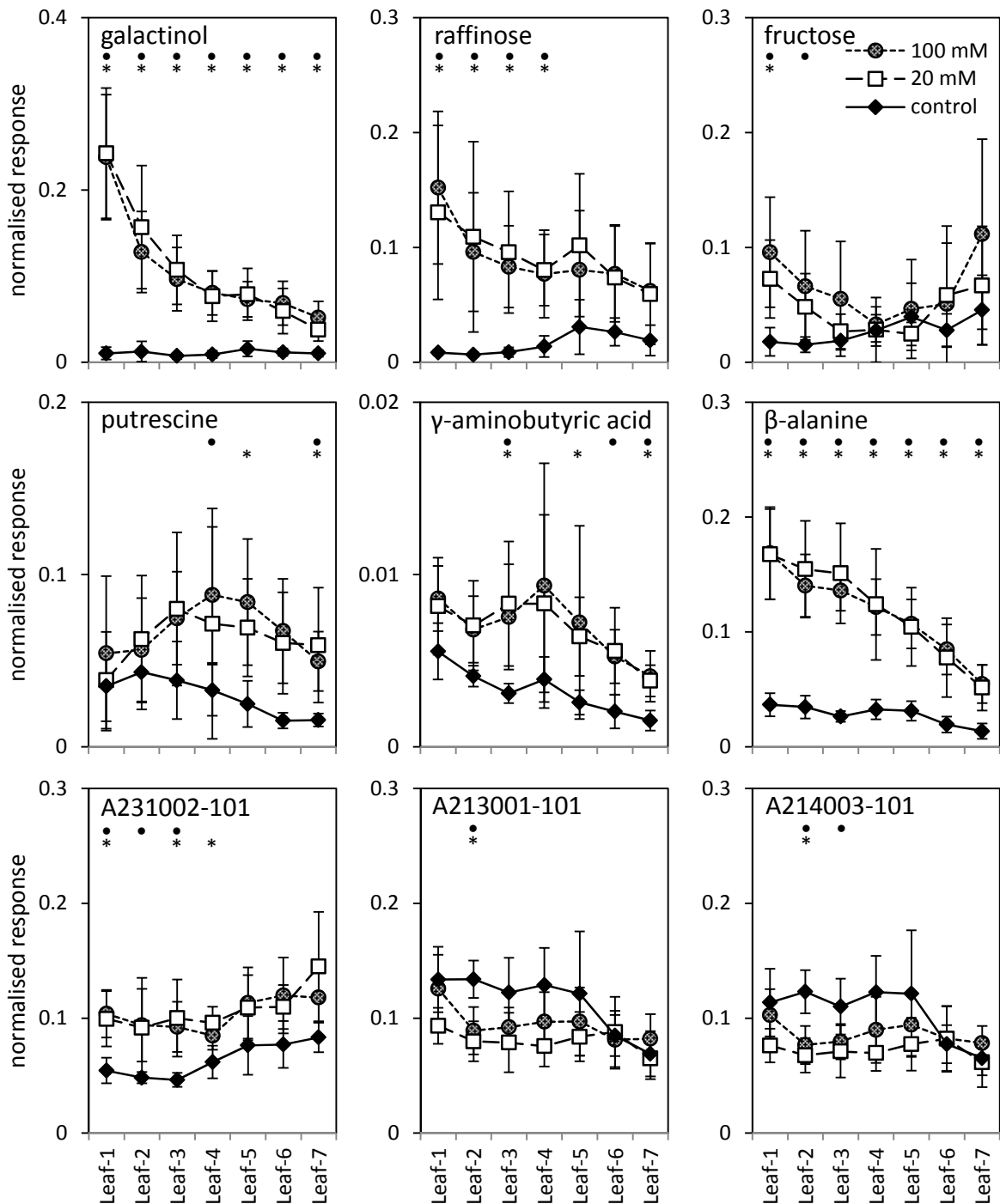


Figure 29: Analytes changed significant due to the hypocotyl feeding assay. Shown are the top six analytes that changed significantly for the interaction and the top five analytes that changed significantly for the feeding (see heat map (Figure 28)). Differences in single leaf positions were tested with a Student's *t*-test with a Bonferroni corrected *p*-value of 0.05. Significance between 100 mM and control is indicated as (*), for 20 mM and control as (*). Data points are averages of 9-10 replicates and error bars represent the standard error.

Moreover, three unknown analytes were significantly changed (Figure 28, Figure 29). A231002-101 showed an increase due to the hypocotyl feeding. But the two unknowns A213001-101 and A214003-101 showed a decrease in leaf positions 1-4 (Figure 29). More precisely a significant decrease for the two in leaf position 2 and only for A214003-101 in leaf position 3 when feeding a 100 mM ^{13}C -sucrose solution, making these analytes interesting for further studies. Only galactinol and putrescine were found to be changed also in the validation experiment for the petiole feeding but with higher p-values. Comparing the mean differences between control and 20 mM in both experiments, galactinol was found to increase in leaf position 1 1.6 times more in the hypocotyl feeding than in the petiole feeding. The two analytes showed a very similar behaviour in both experiments (Figure 29, Figure 21).

3.2 The single leaf metabolism of sequential developmental stages in an *Arabidopsis* rosette

3.2.1 Metabolic pool size differences between single leaf positions in *Arabidopsis* rosettes

The single leaves of a plant are usually in different developmental stages. Leaves can be grouped in three categories: young, still expanding net sink leaves, old, mature net source leaves and intermediate leaves in between. In the experiments mentioned above it was shown that single leaves of an *Arabidopsis* rosette are metabolically different. To find out more about these different stages, single leaves of *Arabidopsis* rosettes were examined.

Measuring the growth of each leaf position in an *Arabidopsis* rosette led to growing curves shown in Figure 30. The data of absolute leaf growth showed that young and mature leaves had a low growth rate and intermediate leaves had a high growth rate (Figure 30a). Intermediate leaves thus grow with the highest velocity. The data of relative growth, however, showed that the young leaves increase the most compared to their initial length (Figure 30b). The older the leaves were, the smaller the relative gain of length became. Based on the observation of these two graphs, leaves were grouped into three categories: leaf 1 and leaf 2 as “young leaves”, leaf 3 and leaf 4 as “intermediate leaves” and leaf 5 to leaf 7 as “mature leaves”.

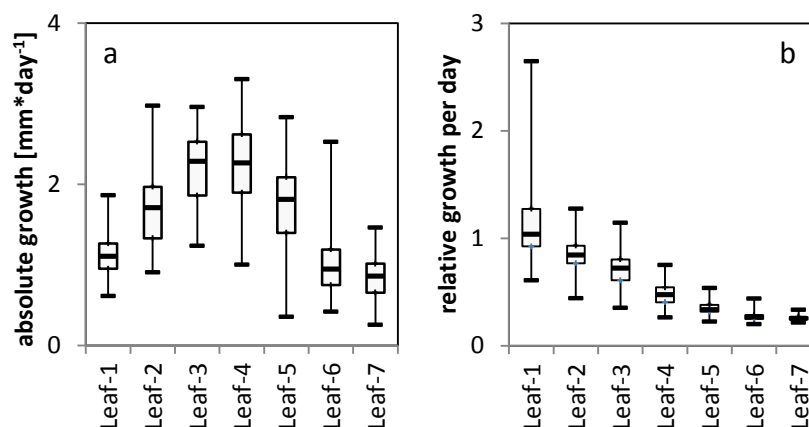


Figure 30: Leaf growth. Absolute leaf growth of single leaf positions per day (a) and relative leaf growth of single leaf positions per day (b). Measurements were done with Image J. Diagrammed are boxplots of 42-49 replicates.

After classifying the leaves by growth, a GC-MS profiling of primary metabolites was performed on single leaf methanol extracts of two independent experiments. As shown in

Figure 31a, 122 analytes could be annotated in experiment one and 206 analytes in experiment two. In total both datasets had 93 analytes in common.

To get a first global view of the metabolite profile, the data was subjected to an ICA based on two PCs covering 57% of the total variance (Figure 31b). The ICA showed a clear separation between old and young leaves in both components. The data resulted in a curve-like structure in the plot, revealing a continuous change in metabolite profile from young to mature leaves. To find the analytes that cause these differences between the leaf positions, an analysis of variances was performed on the 93 common analytes. For both sets a one-way-ANOVA and a Kruskal-Wallis test were used with a critical p-value of $p \leq 0.05$ for all four tests. In addition a slope and a correlation were calculated to select analytes that showed a similar behaviour. The results for all 93 analytes are shown in a heat map (Figure 32).

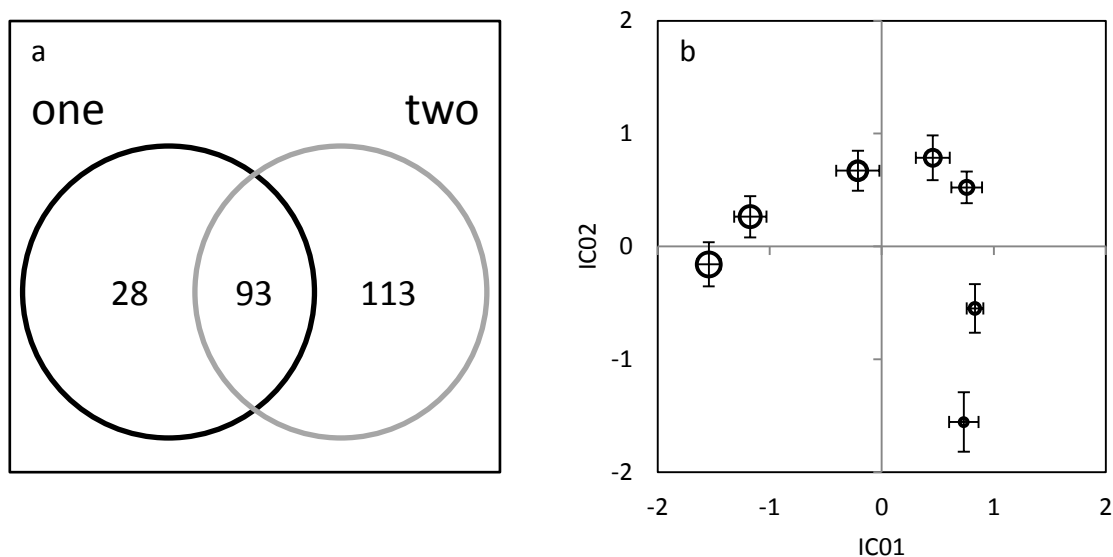


Figure 31: Global view of single leaf GC-MS primary metabolite analysis of *Arabidopsis* rosettes. A Venn diagram of the two independent biological replicate measurements (one, two) shows the numbers of annotated analytes (a). Diagrammed are the results of an ICA calculated on the base of 2 PCs covering 57% of total variance. Small circles represent young leaves, increasing to large circles that represent mature leaves. Shown are average values of 9-10 replicates; error bars represent the standard error (b).

The analysis revealed 30 significantly changed analytes for the different leaf positions. To find out if metabolite pool sizes and growth are related to each other, a correlation analysis was performed. Therefore averages for each analyte and each leaf position were calculated out of the transformed data (see 2.7) and subjected to a hierarchical clustering based on a Pearson correlation with an average linkage. The growth data was transformed in the same way and added to the hierarchical cluster analysis. With a distance threshold of 0.4 the data

could be divided into five clusters: four clusters that correlate and anti-correlate to relative and absolute growth and one cluster that does not correlate to growth (Figure 33). The largest group of 10 analytes could be annotated to known unknowns. The second largest group were amino acids that all showed a decrease in pool size from young to mature leaves and thus a correlation to relative leaf growth (Figure 32, Figure 33e), namely aspartic acid, β -alanine, γ -aminobutyric acid, glutamic acid, pyroglutamic acid, threonine, and the amine putrescine. Further correlated to this cluster were lipid related compounds, i.e. cholesterol, tetracosanoic acid and sinapic acid a precursor of phenylpropanoids. Metabolites containing phosphates were also correlated to this cluster, namely phosphoric acid and glycerophosphoglycerol. In addition to this, a group of unknowns were found in this cluster including the unknown-ketose-I. Another big cluster consists of metabolites anti-correlating to the relative leaf growth like glycerol and galactoglycerol (Figure 33b). Further sugars like raffinose and the unknown-ketoses-II were found in this cluster as well as octadecanoic acid (all-cis-9, 12, 15) and three unknown analytes. Another cluster consist of inositol-phosphate and two unknown analytes (Figure 33c) that were correlated less than 0.4 to the relative leaf growth and clustered therefore in a separate cluster, as were the absolute leaf growth (Figure 33a) and the anti-absolute leaf growth (Figure 33d).

Metabolite	Metabolite	Experiment ONE							Experiment TWO														
		Class	Name	Leaf 1	Leaf 2	Leaf 3	Leaf 4	Leaf 5	Leaf 6	Leaf 7	slope	F-ratio (ANOVA)	raw p-value (ANOVA)	p-value (K-W)	Leaf 1	Leaf 2	Leaf 3	Leaf 4	Leaf 5	Leaf 6	slope	F-ratio (ANOVA)	raw p-value (ANOVA)
Amino Acids	Threonine	0.29	0.26	0.28	0.10	0.02	-0.46	-0.53	-0.13	9.5	2.31E-07	6.69E-06	0.10	0.14	0.12	0.06	-0.11	-0.20	-0.07	4.4	2.04E-03	3.02E-04	0.93
Amino Acids	Alanine, beta-	0.11	0.18	-0.03	0.05	0.04	-0.19	-0.36	-0.05	10.3	7.16E-08	6.26E-06	0.03	0.02	0.09	0.14	-0.13	-0.20	-0.05	3.4	1.04E-02	6.43E-03	0.56
Amino Acids	Aspartic acid	0.89	0.63	0.39	-0.05	-0.41	-0.81	-0.89	-0.35	46.8	0.00E+00	5.54E-10	0.18	0.25	0.08	0.02	-0.14	-0.40	-0.12	3.5	8.70E-03	3.34E-02	0.95
Amino Acids	Pyroglutamic acid	0.53	0.42	0.18	0.00	-0.44	-1.03	-1.19	-0.30	28.7	1.22E-15	2.88E-08	0.32	0.39	0.07	-0.16	-0.42	-0.56	-0.20	25.2	1.04E-12	8.21E-08	0.95
Amino Acids	Butyric acid, 4-amino-	0.28	0.17	0.05	0.14	-0.04	-0.17	-0.29	-0.08	9.8	8.63E-07	9.46E-05	0.21	0.17	0.06	-0.06	-0.21	-0.11	-0.08	2.6	3.76E-02	1.61E-02	0.80
Amino Acids	Glutamic acid	0.80	0.49	0.19	-0.03	-0.39	-0.80	-0.89	-0.31	51.9	0.00E+00	1.88E-10	0.45	0.36	0.04	-0.08	-0.21	-0.14	-0.14	10.0	9.94E-07	1.14E-05	0.90
Fatty Acids**	Octadecatrienoic acid, 9,12,15 (Z)	-0.13	-0.18	-0.11	0.05	0.06	0.10	0.09	0.06	4.7	5.61E-04	2.55E-04	-0.32	0.01	0.02	0.09	-0.08	0.02	0.04	3.8	5.55E-03	1.43E-03	0.33
Fatty Acids**	Tetracosanoic acid	0.36	0.26	0.09	0.01	-0.08	-0.18	-0.29	-0.11	43.8	0.00E+00	2.16E-10	0.10	0.25	0.08	-0.05	-0.17	-0.19	-0.08	6.4	1.14E-04	2.23E-04	0.89
Fatty Acids**	Hexacosanoic acid	0.26	0.19	0.07	0.08	-0.17	-0.33	-0.53	-0.12	27.3	1.11E-15	4.18E-10	0.05	0.25	0.02	-0.05	-0.16	-0.26	-0.08	4.6	1.43E-03	1.60E-03	0.88
Lipids	Cholesterol	0.26	0.27	0.03	0.01	-0.10	-0.20	-0.26	-0.10	15.6	1.95E-10	3.42E-08	0.19	0.11	0.11	-0.07	-0.11	-0.15	-0.07	3.9	5.25E-03	1.48E-03	0.89
N-Compounds	Putrescine	0.11	0.22	0.14	0.11	-0.04	-0.12	-0.20	-0.05	3.3	7.17E-03	6.13E-04	0.49	0.28	0.20	-0.09	-0.13	-0.13	-0.13	8.7	5.21E-06	7.64E-05	0.67
Phenylpropanoids	Sinapic acid, cis-	0.26	0.19	0.10	0.01	-0.15	-0.41	-0.61	-0.13	46.7	0.00E+00	1.16E-09	0.06	0.08	0.18	-0.02	-0.22	-0.36	-0.09	8.3	8.16E-06	5.52E-05	0.91
Phosphates	Phosphoric acid	0.40	0.31	0.08	0.00	-0.19	-0.33	-0.43	-0.15	25.1	7.22E-15	2.30E-09	0.39	0.23	0.11	-0.07	-0.25	-0.41	-0.16	19.4	9.24E-11	8.65E-08	0.99
Phosphates	Glycerophosphoglycerol	0.42	0.28	0.11	-0.05	-0.08	-0.45	-0.67	-0.16	27.1	3.77E-15	3.21E-09	0.30	0.26	0.15	-0.11	-0.40	-0.57	-0.19	25.3	9.98E-13	5.29E-08	0.95
Phosphates	Inositol 1-phosphate	0.59	0.43	0.05	-0.09	-0.25	-0.34	-0.12	-0.19	33.1	3.33E-16	6.03E-08	0.43	0.28	0.12	-0.19	-0.31	-0.48	-0.19	13.2	3.61E-08	1.67E-06	0.97
Polyols	Glycerol	-0.15	-0.12	-0.08	0.04	0.10	0.12	0.12	0.06	8.4	1.11E-06	2.12E-05	-0.19	-0.06	0.14	0.05	0.02	0.03	0.04	4.4	2.14E-03	2.05E-04	0.50
Sugars	Unknown-Ketose I	0.12	0.15	0.15	-0.06	-0.15	-0.21	-0.20	-0.08	7.9	3.30E-06	1.43E-05	0.14	0.21	0.18	0.00	-0.32	-0.51	-0.14	18.5	2.28E-10	1.84E-06	0.96
Sugars	Unknown-Ketose II	-0.08	-0.06	-0.05	0.01	0.09	0.08	0.14	0.04	11.0	2.77E-08	1.96E-07	-0.20	0.02	0.00	0.04	0.06	0.10	0.05	2.9	2.17E-02	7.80E-05	0.75
Sugars	Raffinose	-0.18	-0.28	-0.19	-0.05	0.33	0.25	0.07	0.12	4.5	1.22E-03	7.62E-04	-0.77	-0.49	-0.15	0.24	0.39	0.42	0.26	13.1	5.23E-08	1.66E-05	0.83
MSTs	A170001-101	0.13	0.06	0.02	0.09	-0.05	-0.15	-0.33	-0.05	10.5	5.37E-08	5.21E-08	-0.01	0.07	0.06	0.02	-0.01	-0.25	-0.04	4.4	2.18E-03	2.27E-05	0.77
MSTs	A177004-101	0.16	0.11	0.04	0.13	-0.04	-0.24	-0.35	-0.07	15.0	1.67E-10	1.60E-08	0.20	0.18	0.24	-0.03	-0.17	-0.22	-0.10	5.2	6.53E-04	2.50E-03	0.75
MSTs	A211001-101	-0.06	-0.06	-0.07	-0.01	0.08	0.09	0.16	0.04	13.7	8.12E-10	3.66E-08	-0.22	-0.09	-0.02	0.05	0.17	0.14	0.08	7.0	4.51E-05	1.33E-07	0.87
MSTs	A221004-101	0.17	0.22	0.15	0.03	-0.04	-0.40	-0.59	-0.11	18.6	4.46E-12	4.28E-08	0.31	0.28	0.12	0.08	-0.26	-0.38	-0.15	11.8	1.38E-07	2.14E-06	0.91
MSTs	Galactosylglycerol	-0.03	-0.08	-0.10	0.02	0.21	0.11	0.16	0.05	6.9	1.30E-05	1.07E-06	-0.35	-0.18	-0.01	0.18	0.08	0.18	0.10	8.8	4.28E-06	2.04E-05	0.56
MSTs	A237002-101	-0.05	-0.03	-0.05	-0.01	0.16	0.05	0.10	0.03	3.0	1.19E-02	9.04E-04	-0.17	-0.06	0.10	0.06	0.05	0.11	0.05	3.3	1.09E-02	1.38E-03	0.38
MSTs	A250001-101	-0.05	-0.02	-0.08	0.07	0.08	0.10	0.25	0.04	4.4	9.71E-04	6.78E-05	-0.11	-0.13	0.00	0.05	0.08	0.25	0.07	4.1	3.44E-03	6.96E-06	0.78
MSTs	A300001-101	0.36	0.26	0.07	-0.02	-0.04	-0.29	-0.49	-0.12	18.7	2.77E-12	3.66E-09	0.29	0.14	0.04	-0.05	-0.17	-0.30	-0.11	17.5	4.79E-10	7.61E-08	0.98
MSTs	A304001-101	-0.01	0.04	0.01	0.00	-0.13	-0.10	-0.66	-0.03	6.2	4.44E-05	3.31E-03	0.22	0.28	0.10	-0.02	-0.19	-0.63	-0.17	8.2	9.43E-06	2.08E-04	0.81
MSTs	A203009-101	0.11	-0.16	-0.26	-0.10	0.03	0.13	0.22	0.02	6.8	1.54E-05	3.42E-05	-0.19	-0.22	-0.04	0.11	-0.03	0.16	0.07	4.9	9.97E-04	2.03E-03	0.20
MSTs	A207003-101	0.23	0.16	0.03	-0.03	-0.05	0.07	-0.07	-0.04	2.4	4.07E-02	1.17E-03	0.64	0.35	0.05	-0.13	-0.25	-0.03	-0.15	16.7	9.72E-10	7.98E-07	0.97

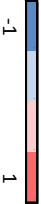


Figure 32: Heat map of metabolites that change significantly across leaf positions. Averages of relative response ratios (log10) are shown for these metabolites. Significance was tested in experiments one and two with a one-way-ANOVA (ANOVA) and a Kruskal-Wallis test (K-W) and a critical p-value of $p \leq 0.05$ for all four tests. In addition slopes, F-ratios and p-values are shown for both experiments as well as a Pearson correlation between experiments one and two. Slopes are calculated from leaf 1 to leaf 6.

The largest group correlates to the relative growth and consists of amino acids and phosphates, indicating that these compounds are important for growing leaves.

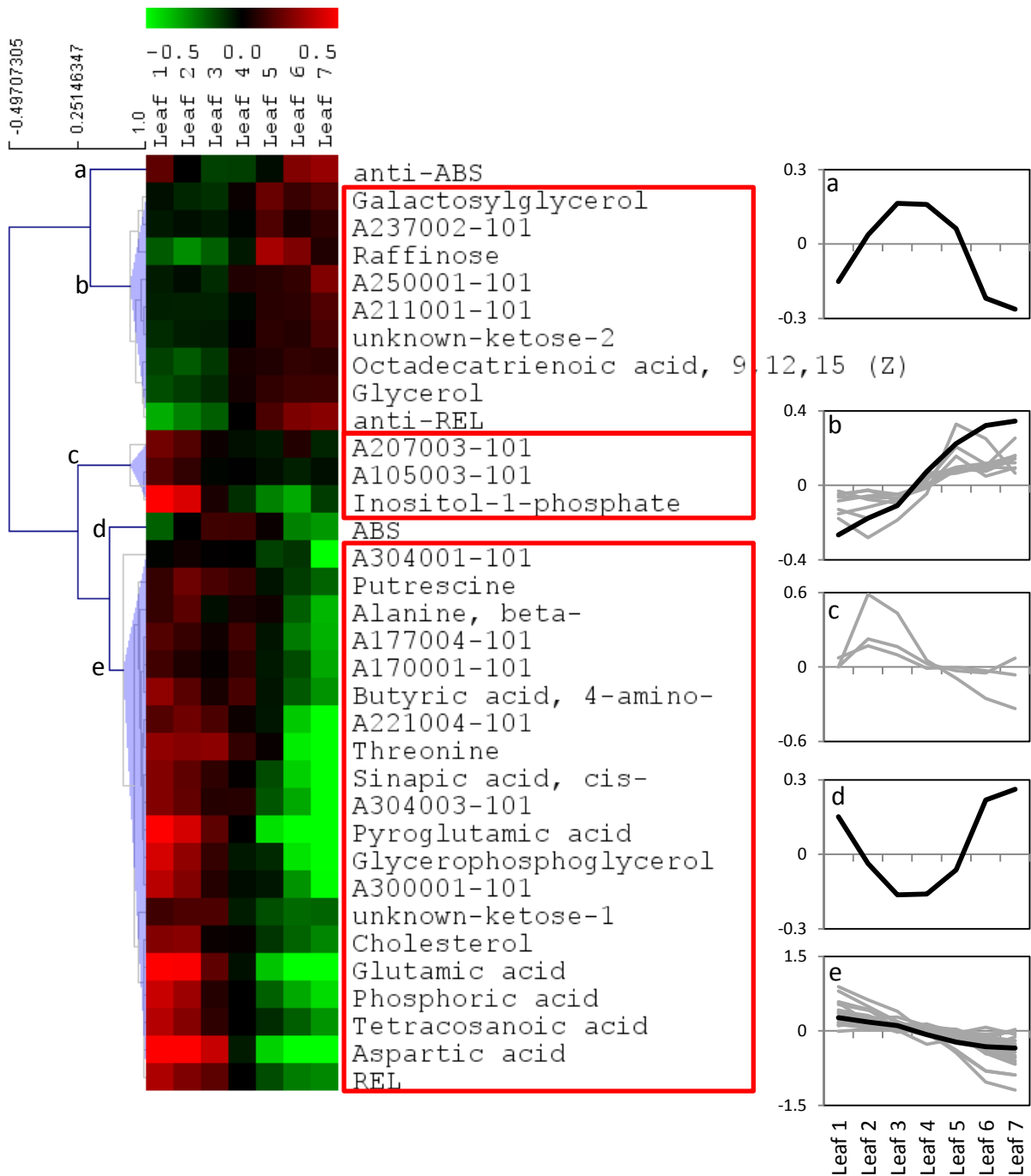


Figure 33: Clustering metabolites to leaf growth. Significantly changed metabolites are hierarchically clustered with a Pearson correlation and an average linkage. The distance threshold was set to 0.4. Shown is log median centred data in 5 clusters, anti-correlated to absolute leaf growth (a), anti-correlated to relative leaf growth (b), no correlation to growth (c), correlated to absolute leaf growth (d) and correlated to relative leaf growth (e).

3.2.2 Metabolic differences of single leaves between cold and warm development

It has been reported that temperature has an influence on growth (Pantin *et al.* 2011). The examination of single leaf primary metabolites in plants grown under normal temperatures revealed that metabolite pool sizes were associated with growth. The following experiment was designed to find out whether single leaf primary metabolism is altered in plants grown in the cold.

To analyse the primary metabolites of *Arabidopsis* single leaves in cold, a batch of plants was germinated and grown in a phytotron with standard long day (16h/8h, light/dark) conditions at 10 °C for a total of 10 weeks. Methanol extracts of single leaves were analysed by GC-MS and compared to the two afore-mentioned single leaf experiments grown under normal temperatures (control one and two) (see 3.2.1). The data set of the cold experiment was fused with the data sets of control experiments one and two and reduced to the common analytes. This led to a reduction of annotated analytes to a total of 66 (Figure 34).

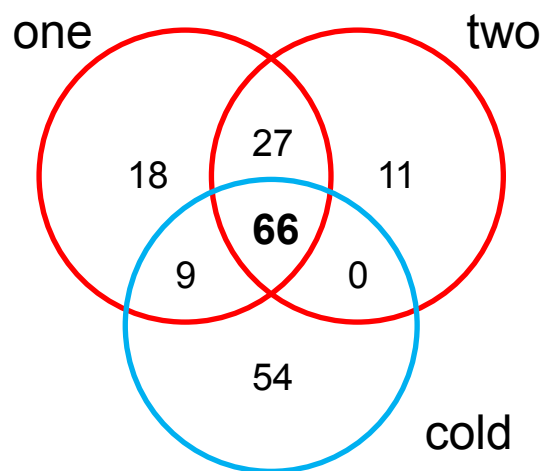


Figure 34: Overview of annotated analytes in one cold experiment and two control experiments.

For the statistical analysis, the reduced data sets of each experiment were transformed to relative response ratios (\log_{10}). The data sets were analysed pairwise cold to one and cold to two. Both new datasets were subjected to a two-way-ANOVA regarding the developmental aspects of the different leaf positions and the cold treatment. Since leaf position 7 is missing in experiment two, only leaf positions 1 to 6 were regarded in the statistics. To find the specific analytes that show a change in the relative response of the different leaf positions, the interaction of treatment and development was examined. In addition to a positive correlation between the control experiments, a critical p-value of $p \leq 0.05$ for each joined dataset was

chosen. For only four analytes a change of trend across the leaf positions could be found (Figure 35).

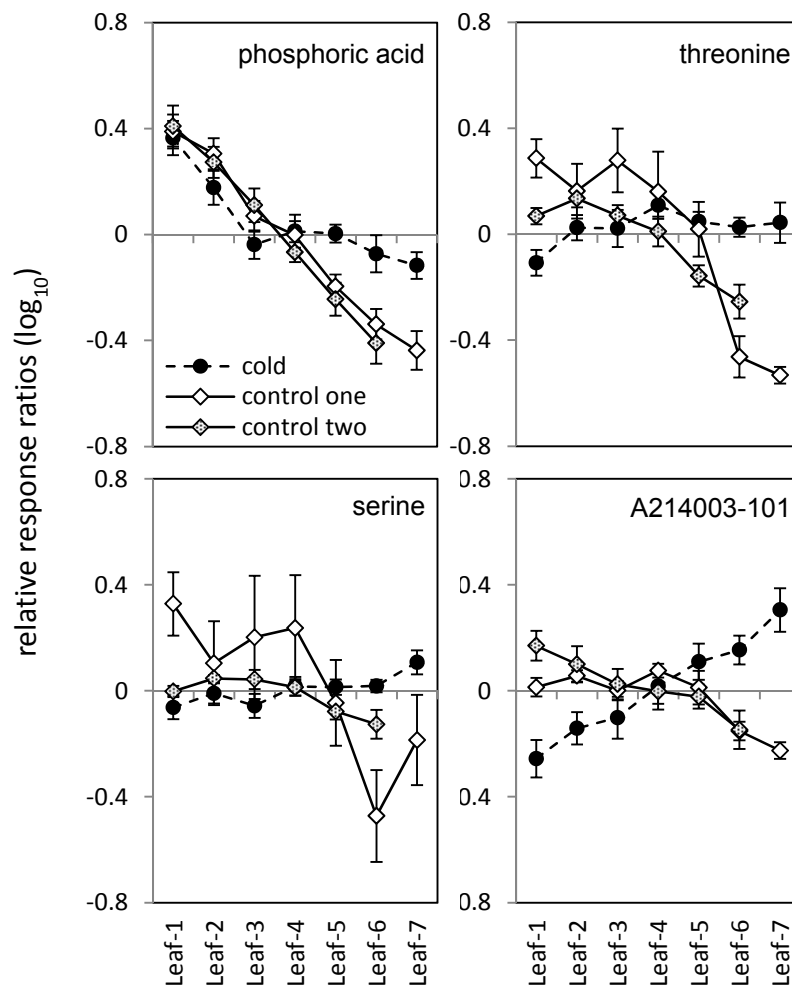


Figure 35: Change in relative trend over leaf positions due to cold growth. Shown are averages of relative response ratios (\log_{10}) of significantly changed analytes of 9-11 replicates. Significance was tested with a two-way-ANOVA with a critical p-value of 0.05 between cold and control one and cold and control two. Error bars represent the standard error.

The analytes phosphoric acid, threonine, serine and A214003-101 showed a decrease from leaf 1 to leaf 7 that changed due to cold growth. Threonine and serine showed a constant response across the different leaves. Phosphoric acid showed a decrease in relative response from leaf 1 to leaf 3 and then a constant response. The unknown A214003-101 showed an opposite trend (trend = relative pool size changes of leaf position 1 to leaf position 7) in cold, i.e. an increase from leaf 1 to leaf 7.

3.2.3 Hypocotyl feeding of ^{13}C -sucrose and stable isotope tracing in single leaves of plants grown under control conditions

The different pool sizes across leaf positions in WT plants already showed some interesting trends for groups of metabolites (Figure 33). Leaves with a high growth rate are described to be net sink, which get carbohydrates and energy from the mature net source leaves. The major transport carbohydrate is sucrose. To find out how carbon from externally fed ^{13}C -sucrose is allocated in the different leaves, the following experiment was designed.

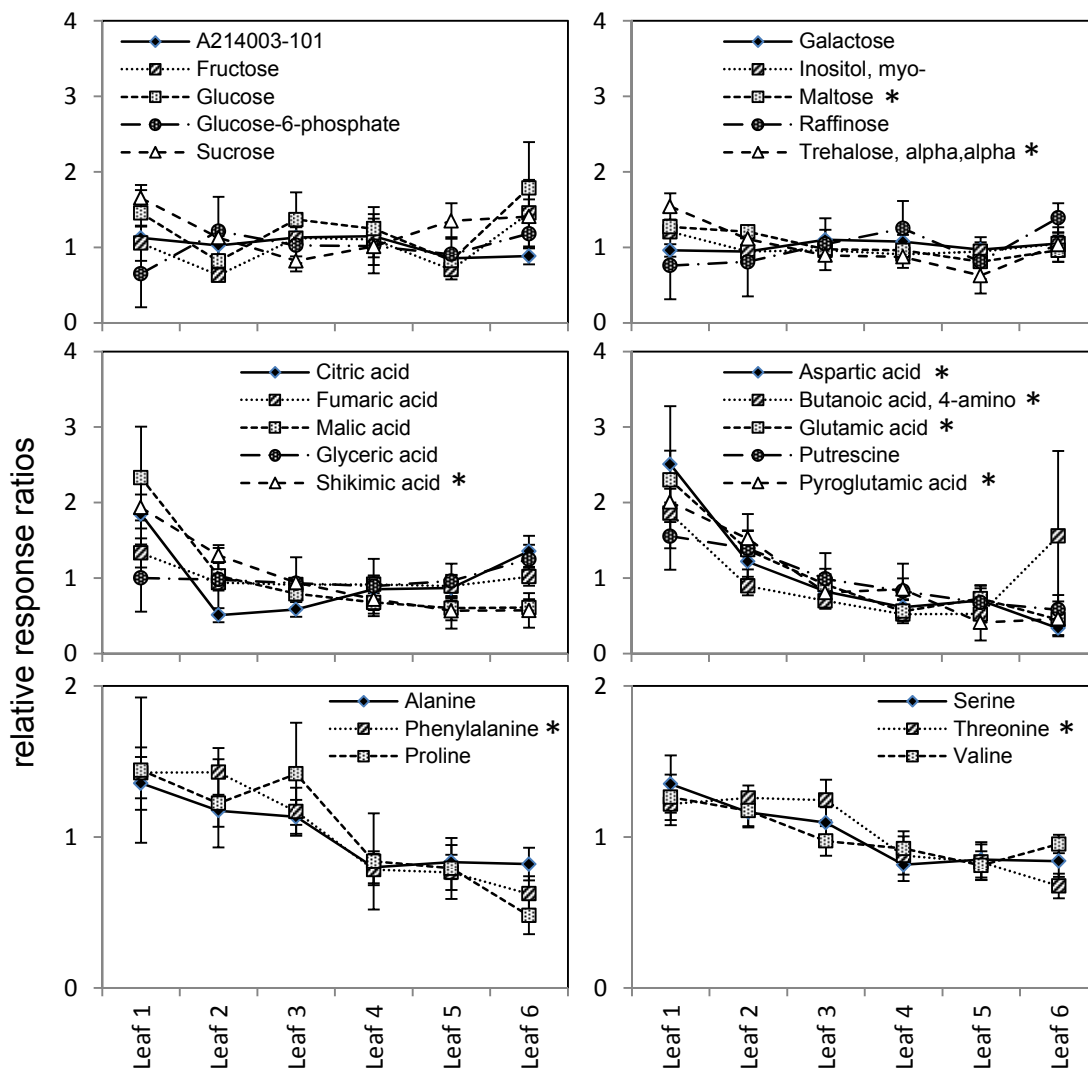


Figure 36: Conventional pool size data of primary metabolites after a hypocotyl feeding with 20 mM ^{13}C -sucrose solution. Shown are averages of median centred normalised responses to diagram the differences in leaf position. Calculation based on 9-11 replicates, error bars represent the standard error. Significance was tested by a one-way-ANOVA and a Kruskal-Wallis test with a critical p-value of $p \leq 0.05$. Significance was in addition tested in a hypocotyl feeding with a 100 mM ^{13}C -sucrose solution. Metabolites that showed significance in all four tests are marked (*).

For a deeper investigation of carbon allocation from sucrose into the single leaf metabolism of *Arabidopsis* plants, a hypocotyl feeding experiment with ^{13}C -sucrose was performed.

Three batches of plants were grown under control conditions. In a 7-9 leaf stage plants of two batches were fed with a 20 mM and a 100 mM ^{13}C -sucrose solution via the hypocotyl for 4 hours. Afterwards single leaves were harvested and methanol extracts analysed by GC-MS.

In the first part only conventional pool size data are shown and in the second part the additional information of the stable isotope tracing calculations are included.

As shown before, the hypocotyl feeding itself had an influence on the metabolism; the data can therefore not be compared directly to the conventional pool size data of unfed plants. The examination of the conventional pool size data is repeated for this experiment as the conditions have changed in comparison to the data presented above (see 3.2.1). For the investigation 26 known metabolites could be annotated in the data set. To find metabolites that showed an association of pool sizes to single leaf positions and to confirm the previous results of pool size changes correlating to growth (see 3.2.1), a one-way-ANOVA and a Kruskal-Wallis test were performed with a critical p-value of $p \leq 0.05$. As observed in the experiment above (see 3.2.1) some metabolites showed a very similar behaviour regarding the pool sizes across different leaf positions. Metabolites that showed a significant pool size change across leaf positions before and in this experiment are glutamic acid, pyroglutamic acid, aspartic acid, γ -aminobutyric acid and threonine. Maltose pool size did not change significantly. Trehalose showed significant change only for the Kruskal-Wallis test, but not for the ANOVA. Although the metabolites phenylalanine and shikimic acid showed very low p-values they could only be annotated in one of the two experiments and therefore were not listed in the results.

The integration of the stable isotope data is the comparison of conventional pool size and the ^{13}C -pool. The ^{13}C -pool represents the labelled part of the metabolite pool of sucrose origin, assuming a 100% labelled sucrose pool (see 2.6). The analysis provides a snapshot of carbon allocation of sucrose origin at a given point in time. The data was further selected for a significant change in conventional pool size or in the ^{13}C -pool. The ^{13}C -pool data was also tested with a one-way-ANOVA and a Kruskal-Wallis test with a critical p-value of $p \leq 0.05$.

The data reveals that pool sizes do not change significantly between the hypocotyl feeding with a 20 mM and a 100 mM ^{13}C -sucrose solution, except for glucose and fructose. For these metabolites, pool sizes on average increase 9-fold and 4-fold, respectively, between the 20 mM and 100 mM ^{13}C -sucrose feeding. For the other metabolites, the trends that can be observed across the single leaf positions are similar between both feedings.

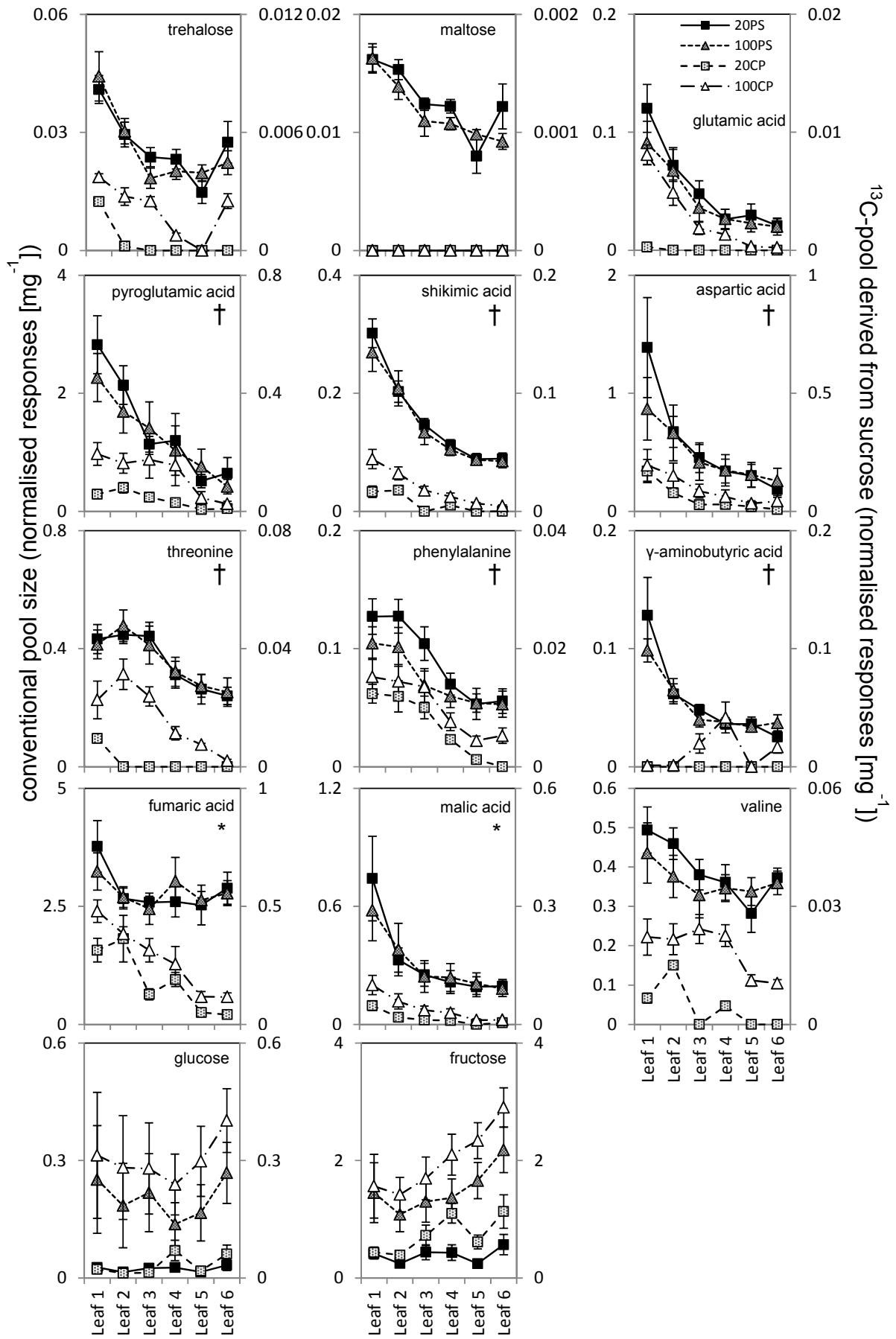


Figure 37: Pool sizes and carbon allocation of significantly changed metabolites in different leaf positions. Data derived from a hypocotyl feeding. The left Y-axis shows the conventional pool size for a feeding with a 100 mM (100PS) and a 20 mM (20PS) ¹³C-sucrose solution. The right Y-axis shows the ¹³C part of the pool derived from ¹³C-sucrose for a 20 mM (20CP) and a 100 mM (100CP) ¹³C-sucrose solution. Significance was tested with a one-way-ANOVA and a Kruskal-Wallis test with a critical p-value of $p \leq 0.05$. Metabolites that are significant for all four tests either for the conventional pool size data (†) or the ¹³C-pool (*) derived from sucrose are shown. Diagrammed are averages of 9-11 replicates. Error bars represent the standard error.

Regarding the ¹³C-pools, metabolites with no or almost no labelling could be seen, such as maltose or γ -aminobutyric acid (Figure 37), indicating a very low amount of carbon from sucrose in these pools at the given point in time. On the other hand, there is a group of metabolites that showed the same size of ¹³C-pool for both ¹³C-sucrose concentrations, namely aspartic acid, phenylalanine, fumaric acid and malic acid. These metabolites also showed a generally higher degree of labelling relative to the conventional pool size in comparison to other metabolites, indicating that these pools had received more carbon from sucrose than other metabolites at the given point in time. In between, there are metabolites that had integrated ¹³C from the 100 mM ¹³C-sucrose solution, but less or none from the 20 mM ¹³C-sucrose solution, such as trehalose, glutamic acid, threonine and valine and borderline cases like pyroglutamic acid and shikimic acid.

3.2.4 Relative ¹³C composition under cold development

In addition to the experiments presented above, plants grown in the cold were fed with ¹³C-sucrose to trace the stable isotope in the single leaf metabolism. Plants were grown under cold conditions (10 °C), and in a 7-9 leaf stage, a hypocotyl feeding with a 20 mM ¹³C-sucrose solution was performed for 4 hours. Afterwards, single leaves were harvested and methanol extracts analysed by GC-MS. The data was compared with the data of the control plants grown under normal temperature regime and fed with a 20 mM and a 100 mM ¹³C-sucrose solution (see 3.2.3). For comparison the data of the two experiments was transformed to relative response ratios (\log_{10}), fused and submitted to a two-way-ANOVA and a Mack-Skilling test with a critical p-value of $p \leq 0.05$. Of a total of 24 annotated known analytes, the trends of 4 analytes differed significantly from the control across the different leaf positions (Figure 38).

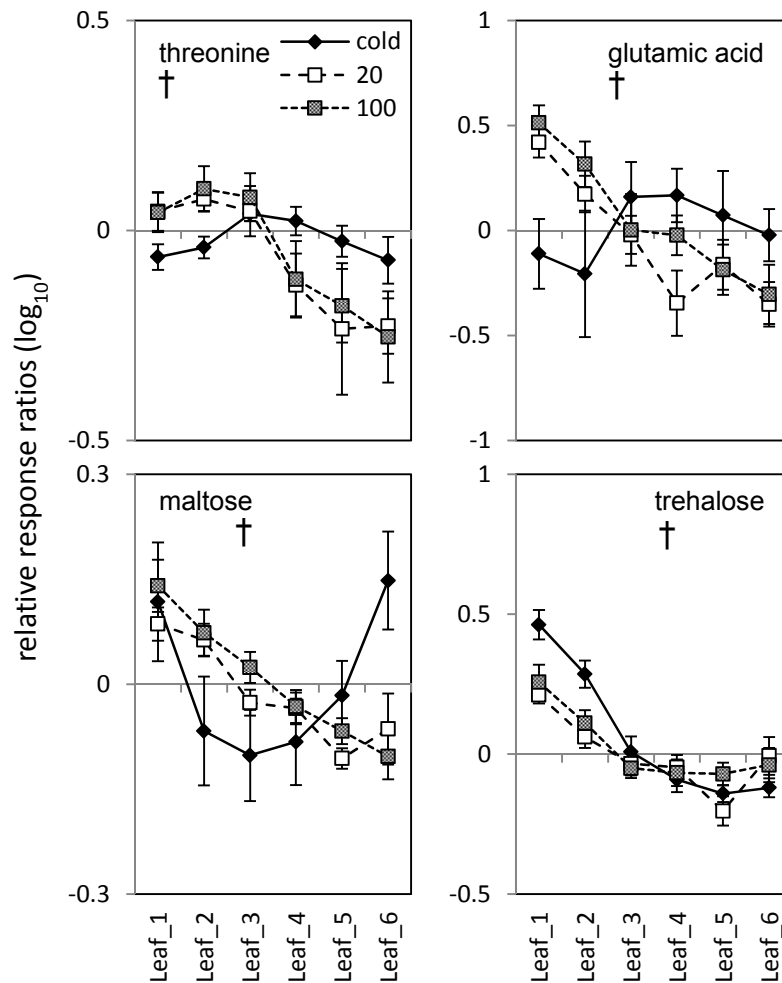


Figure 38: Pool size of primary metabolites after a hypocotyl feeding with 20 mM ¹³C-sucrose solution of control plants and plants grown in the cold. Shown are averages of relative response ratios to diagram the different trends in leaf position. Calculation based on 9-11 replicates, error bars represent the standard error. Significance was tested by a two-way-ANOVA and a Mack-Skillings test with a critical p-value of $p \leq 0.05$. Significance was in addition tested in a hypocotyl feeding with a 100 mM ¹³C-sucrose solution. Metabolites showing significance in all four tests are marked (†).

The pool size trend of threonine changed from a decrease from young (leaf 1-2) to mature leaves (leaf 5-6) in the controls into a more or less constant pool across the different leaf positions in the cold. As compared to a more or less constant decrease from young to mature leaves in the controls, glutamic acid showed low pool sizes in young leaves, high pool sizes in intermediate leaves (leaf 3-4) and intermediate pool sizes in mature leaves in the cold. Trehalose showed only minor changes. The decrease in pool size from young to mature leaves in the cold was more pronounced than in the controls. For maltose, the trend changed from a constant decrease in pool size from young to mature leaves in the controls to a more curve-like shape in the cold, where highest pool sizes were found in leaf 1 and leaf 6, and leaves 2 to 5 showed low pool sizes.

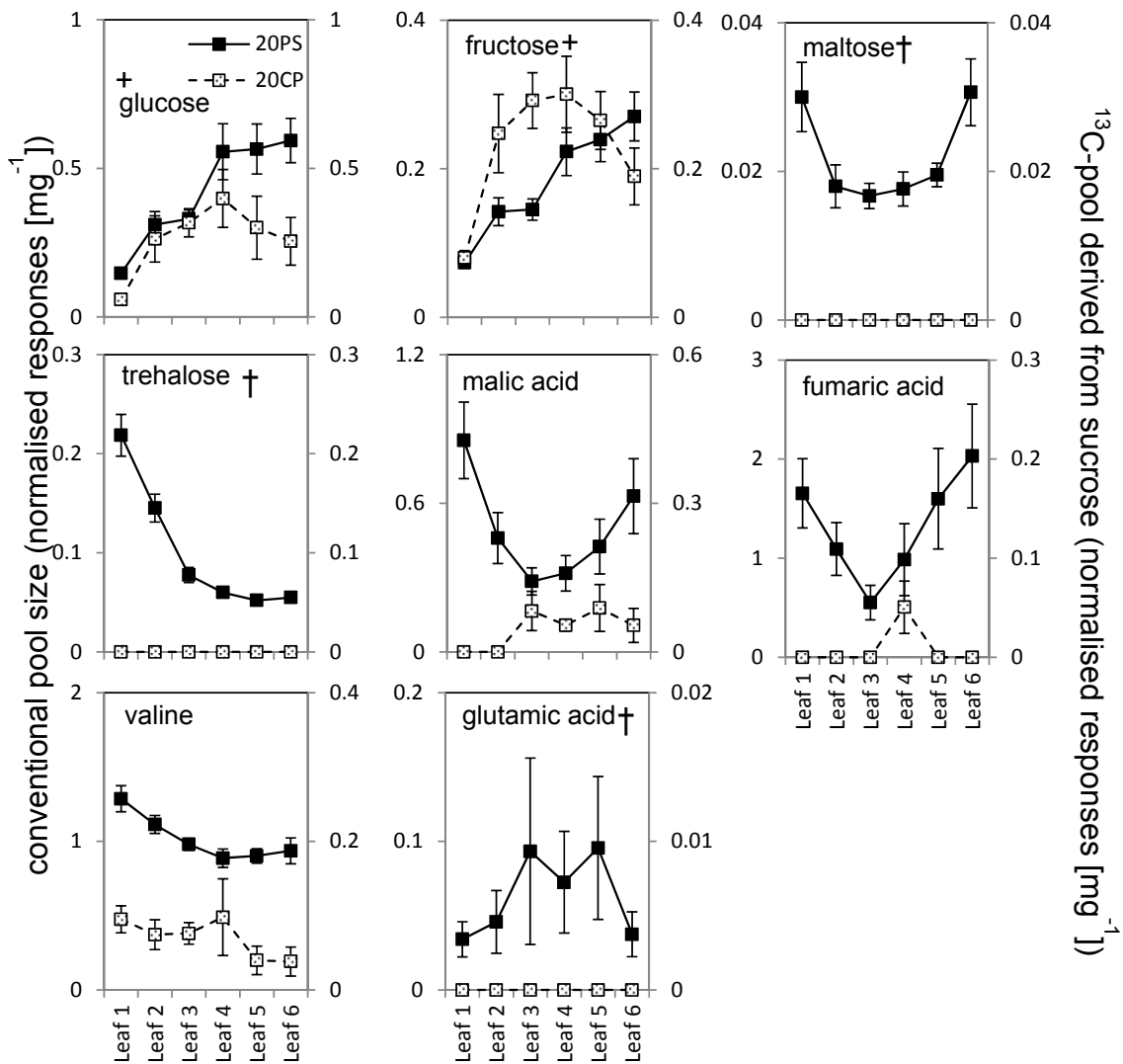


Figure 39: Metabolite pool sizes and carbon allocation of hypocotyl-fed plants grown in the cold. The left Y-axis shows the conventional pool size for a feeding with a 20 mM (20PS) ^{13}C -sucrose solution. The right Y-axis shows the ^{13}C part of the pool derived from ^{13}C -sucrose for a feeding with a 20 mM (20CP) ^{13}C -sucrose solution. Trends of pool sizes were compared between control plants and plants grown in the cold with a two-way-ANOVA and a Mack-Skillings test with a critical p-value of $p \leq 0.05$. Metabolites that are significant for conventional pool size data are marked (†). Significance of ^{13}C -pools for different leaf positions is marked (+). Diagrammed are averages of 9-11 replicates. Error bars represent the standard error.

For a further characterisation, ^{13}C -pools were analysed and compared to the ones of the controls. The ^{13}C -pools of only five metabolites could be determined, indicating that the carbon from sucrose did not reach all the metabolites that it reached in the control plants. The five metabolites were the cleavage products of sucrose, fructose and glucose, further fumaric acid, malic acid and valine (Figure 39). The second observation was that the pool sizes describe different trends from the ones observed in the controls (Figure 37). Malic acid and fumaric acid showed a very similar trend as maltose: high pool size in young and mature leaves and low in intermediate leaves of plants grown in the cold (Figure 39). For plants grown under normal conditions, malic acid showed a constant decrease in pool size. Pool

sizes for fumaric acid were nearly constant except for leaf 1 with a higher value. Maltose showed a decrease of pool size to leaf 3 and stayed on a constant plateau in leaf 4 to leaf 6. Pool sizes of fructose and glucose did not show a significant trend in the control experiments; both exhibited only minor changes across leaf positions (Figure 37). However, in the plants grown in cold, both described significant increase in pool size from leaf 1 to leaf 6 (Figure 39). Valine, interestingly, is the only metabolite in the cold for which the ^{13}C -pool confirms the pool size trend. This is in contrast with the controls, where ^{13}C -pools confirmed the pool size trends more often (Figure 37).

The ^{13}C -pools of glucose, fructose and malic acid showed a different trend from the conventional pool size. Glucose ^{13}C -pools described an increase to leaf 4 and a decrease to mature leaves. Fructose showed low ^{13}C -pools in young and mature leaves and high ^{13}C -pools in intermediate leaves. Malic acid ^{13}C -pools showed only a constant level in leaf 3 to leaf 6 but no label in young leaves. For fumaric acid there was only a detectable labelling in leaf 4 for two replicates, suggesting a borderline case of labelling for this metabolite.

The different trends for conventional pool size and ^{13}C -pool could already be observed in the control experiments for 2 metabolites, namely pyroglutamic acid and fumaric acid (Figure 37). ^{13}C -pool of pyroglutamic acid showed a plateau for young leaves and intermediate leaves and a decrease for mature leaves, whereas conventional pool size describes a constant decrease from leaf 1. Fumaric acid showed a similar behaviour; pool sizes decreased from leaf 1 to a constant plateau for intermediate and mature leaves, whereas ^{13}C -pool decreased constantly from leaf 1.

3.3 First analysis of *REIL1* and *REIL2*

3.3.1 Promoter-GUS studies for *in situ* expression analysis

For the analysis of the *in situ* expression of both genes, promoter-GUS plants were produced by transformation with *Agrobacterium tumefaciens* containing different constructs. For a visualisation of gene expression, promoter regions of *REIL1* and *REIL2* and the promoter regions of *DREB1A* and *DREB2A*, each 1000bp upstream of the gene, were fused with a GUS-eGFP construct and cloned in *Arabidopsis* plants (Supplemental_3-3-1).

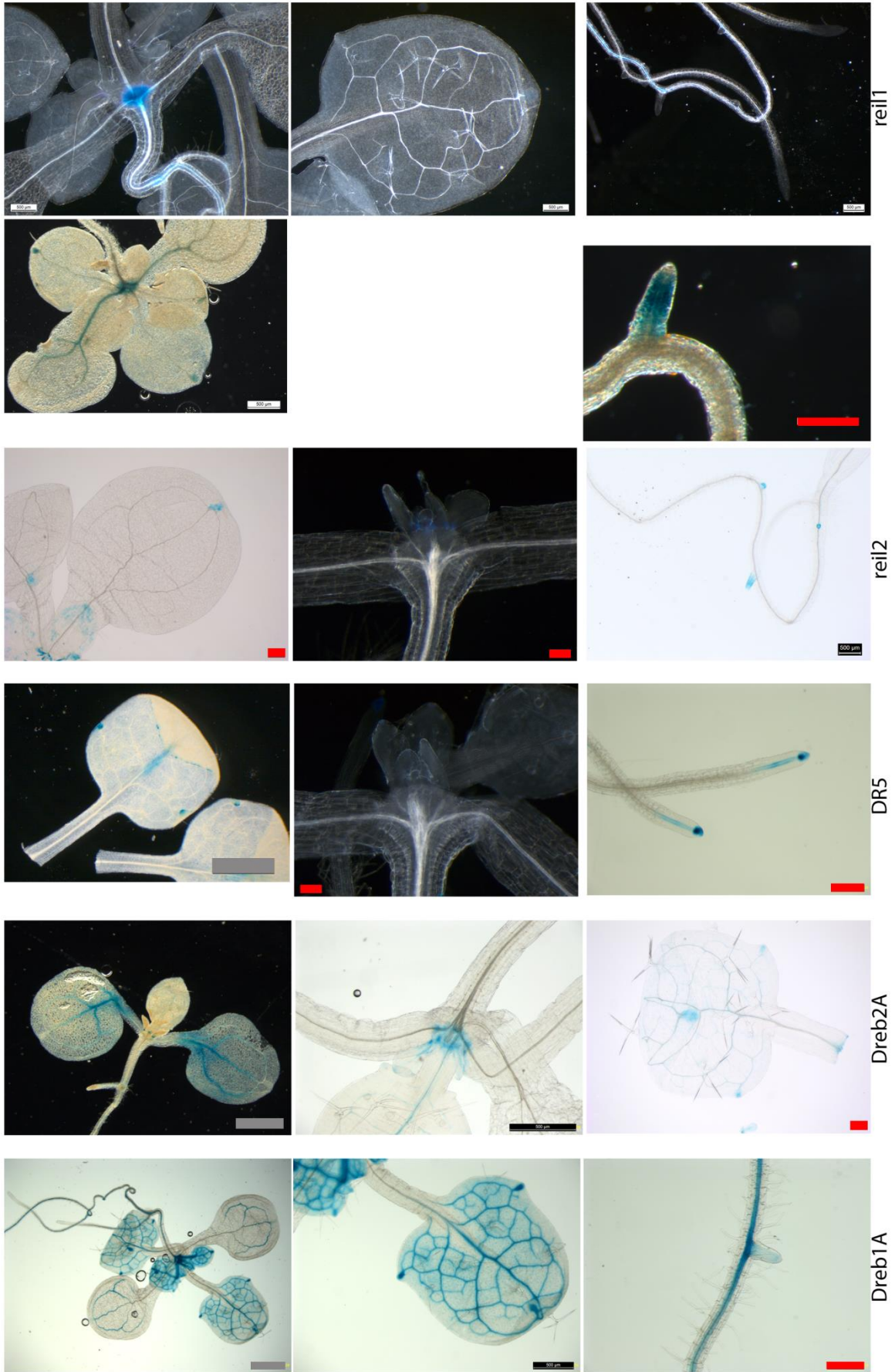


Figure 40: Promoter-GUS studies of 2-4-week-old plants grown in the cold. Plants were treated with the same staining solution and concentrations. Grey size bars represent a size of 1 mm; black and white bars represent a size of 500 µm; red bars represent a size of 200 µm.

After the construct-containing plants were selected, the expression was microscopically analysed by a GUS staining. *REIL2* has been reported to increase expression under cold stress (Schmidt *et al.* 2013).

Further, the analysis of the promoter region by a multi-alignment of *Arabidopsis* with *Eutrema parvulum*, *Brassica rapa*, *Eutrema salsugineum*, *Arabidopsis lyrata* and *Camelina sativa* revealed that the promoter region is highly conserved (personally communicated by Korkuc and Kopka). In this conserved promoter region a DREB-element and an auxin-responsive element could be found besides other cis-elements (personally communicated by Korkuc and Kopka). Therefore the *DREB1A* and *DREB2A* promoters were included in the analysis. The auxin reporter DR5-GUS, which was kindly provided by Dr Jens Schwachtje (van Dongen group), was also included in the study.

Table 7: Promoter-GUS plants that showed a GUS expression in the listed tissues; x represents a weak expression and xx a strong expression.

Type	central cylinder	root tip	hydathode	shoot centre	stipules
<i>REIL1</i>	x		x	xx	
<i>REIL2</i>		xx	x		x
<i>DREB1A</i>	xx		xx	xx	xx
<i>DREB2A</i>			x		x
DR5		xx	x		x

It has been reported that *reil1* and *reil2* did not show a phenotype under normal growth conditions (Schmidt *et al.* 2013). For the *reil1* no phenotype could be found up to now, but two independent *reil2* developed a morphological phenotype when grown under cold conditions (Schmidt *et al.* 2013). Therefore the GUS expression was tested on seedlings grown on plates for 2 to 6 weeks in normal temperatures and in the cold. For normal temperatures no expression could be seen for the promoter of *REIL1* and *REIL2*. The cultivation at 10 °C showed a specific expression pattern for both promoter-GUS plants (Table 7). The analysis of the GUS expression revealed that the promoters of *REIL1* and *REIL2* showed different expression patterns. *REIL1* showed promoter activity in the central cylinder of the root but not in the root tip, very similar to the expression found for *DREB1A*, but less active (Figure 40). *REIL2* showed promoter activity in the root tip, more precisely in

the zone of cell division, similar to the auxin reporter DR5 that also showed activity in the root tip, but only in the meristem and in the developing vascular tissue (Figure 40). Both *REIL* genes showed promoter activity in the hydathode of the leaf tip, a similar activity could be shown for the DR5 reporter (Figure 40). Much stronger and more focused to the vascular system was the expression observed for *DREB1A* and *DREB2A* in the leaf (Figure 40). In the shoot centre a very strong staining for *REIL1* could be found that was very similar to the expression seen in the *DREB1A* plants (Figure 40). This staining is in the centre of the shoot, but appears not to be in the apical meristem (Schmidt 2013). For *REIL2* an expression was found in the stipules (Figure 40), which was also found for the *DREB2A* and *DREB1A* plants and has been reported for the DR5 plants (Aloni *et al.* 2003).

3.3.2 Single leaf metabolic analysis of *reil2* grown in the cold

The phenotype of the *reil2* that has been reported before (Schmidt 2013; Schmidt *et al.* 2013) showed a change in the leaf morphology of plants grown in the cold. It has also been reported that plants shifted to a cold environment kept the morphology of the previously developed leaves but changed the morphology of newly developed leaves. Further it has been reported that leaf morphology changed again when the inflorescence emerged or plants were shifted back to normal temperatures. This led to the hypothesis that the *reil2* gene takes part in the process of leaf development in the cold. Metabolic examinations resulted in the hypothesis that the metabolism of *reil2* stayed in a vegetative state, although the inflorescence had already emerged (Schmidt 2013). WT plants in contrast changed their metabolic profile due to the transition from vegetative to generative state. The same had been found for global transcript levels. Secondary metabolites and lipids of *reil2* in a generative state had been found between the vegetative and generative state of the WT, indicating changes in the same direction, but less strong than in the WT. This result had been interpreted to the effect that *reil2* plants stay in a physiologically vegetative state, i.e. they stay young (Schmidt 2013). The comparison of primary, secondary and lipid metabolites and transcripts between *reil2* and the WT in the vegetative state did not show any changes on a global level.

To find out if the metabolism of young leaves is altered and changes could not be found earlier because only whole rosettes were analysed, a single leaf analysis of both *reil2* lines was performed. To this end, plants were germinated and grown for 10 weeks in a phytotron with cold conditions (10 °C), then single leaves were harvested and primary metabolites

analysed with a GC-MS-based method as described before. To visualise the global changes in single leaf metabolism, profile data was subjected to a PCA. The results of 3 PCs for *reil2.1* and WT covering 69% of the total variance were subjected to an ICA (Figure 41), as were the results of 4 PCs for *reil2.2* and WT covering 73% of the total variance (Figure 41).

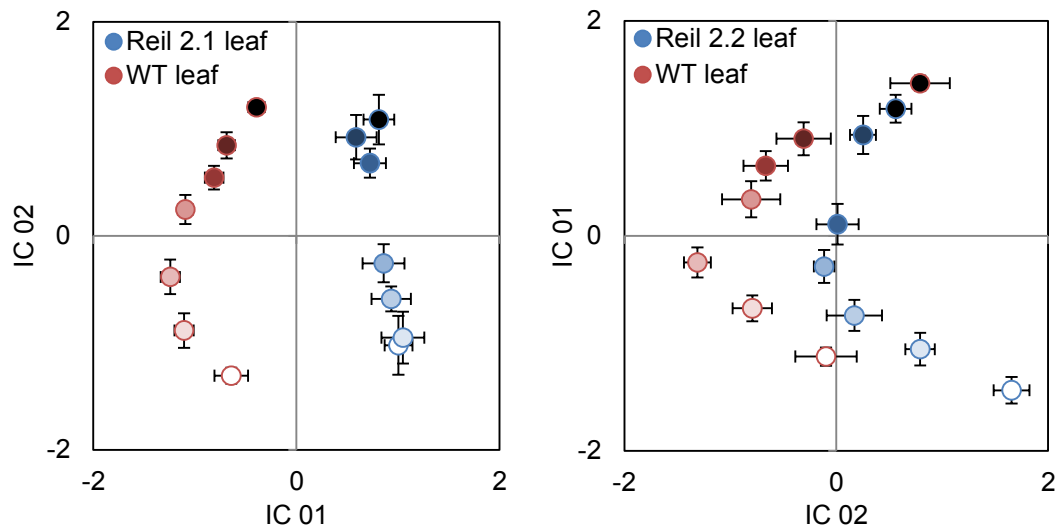


Figure 41: Global single leaf primary metabolism differences between WT and *reil2.1* (a) and *reil2.2* (b). The ICA shows the metabolite profile data of leaves in different developmental stages. WT data is shown in comparison to MT data. Dots represent the leaf positions which decrease in brightness from the youngest (leaf 1) to the oldest leaf (leaf 7). Diagrammed are the averages of each leaf position; error bars represent the standard error. Error bars are not shown for values that are smaller than the size of the dot.

Figure 41 shows that single leaves of WT plants clearly separate from each other in the ICA. The data points describe a curve similar to the ones found in earlier analyses (Figure 17, Figure 25 and Figure 31). The distribution of single leaves of the *reil2.2* was similar to the one of the WT, but with a shift that seems to be stronger in young leaves than in old leaves. The data points of the *reil2.1* do not describe a curve, like it could be seen for WT and *reil2.2*, but are more linear. In addition the leaf positions were not distinguished from each other as strongly as in the other plants. But the ICA separated the leaves in two groups of leaf positions 1-4 and leaf positions 5-7, i.e. young and intermediate leaves are distinct from mature leaves.

4 Discussion

In this work a classical approach of isotope tracing, using a non-photosynthetic labelling, was combined with a metabolite profiling, so as to gain information not only on a metabolic phenotype, but also on carbon distribution from a specific precursor. Therefore the feeding of a labelled precursor, its measurements and calculations were examined to find a method which comprises a fast and efficient labelling for screening pool size changes and altered carbon distribution in single leaves.

4.1 Metabolic inactivation harvest of multiple single leaves from a whole rosette

For metabolite analysis an inactivation of the plant enzymes is necessary because the metabolism responds very quickly to environmental changes. This has a high impact on the reproducibility of metabolite pool size measurements and can also cause artefacts (Kopka *et al.* 2004). Metabolism must therefore be rapidly quenched. Different methods for inactivation of *Arabidopsis* plant metabolism are known. A quick harvest and immediate snap-freezing in liquid nitrogen for normal leaf tissue is a commonly used option (Kopka *et al.* 2004). Further a freeze-clamp can be used, especially for thick tissue, in the centre of which the metabolism would not be inactivated fast enough: two metal blocks that are pre-cooled in liquid nitrogen simultaneously squash and freeze the tissue very rapidly (Ap Rees *et al.* 1977).

To allow a single leaf metabolite profiling analysis of one *Arabidopsis* rosette a special harvesting method had to be designed. Single leaves were classified by their specific developmental stage to allow paired analyses of the leaves. For a fast quenching of the metabolism the freeze-clamp method had to be rejected, because squashing the plant would render a distinction of single leaf material impossible. Snap-freezing full rosettes by dousing with liquid nitrogen and cutting off single leaves afterwards had to be rejected, too, because due to their brittleness in a frozen state leaves and often complete rosettes broke into tiny pieces that could not be reconstructed. The only feasible option was to cut leaves off the rosette sequentially and to immediately snap-freeze them in liquid nitrogen. Using this method, 2 to 10 seconds were needed for one leaf but far less than 1 minute for all leaves of a whole rosette. Still, the harvesting time and the sequential cutting of leaves will have an impact on the plant metabolism. An attempt to harvest randomly and thereby randomize artefacts caused by the fixed harvesting order had to be rejected because of a substantial increase of harvesting time up to more than 5 minutes. As a consequence pool sizes of

metabolites with a fast turnover rate, like intermediates of the Calvin-Benson cycle (Stitt *et al.* 2003), may possibly not be determined without artefacts.

4.2 Determination of sample amount

For relative and absolute quantification of metabolites one basic requirement is the exact determination of the sample size or amount for a normalisation (Dethloff *et al.* submitted). Depending on the analysis a specific measure is appropriate, for example leaf surface for the analysis of waxes or dry weight for the analysis of cell wall. Most suitable for the analysis of soluble leaf metabolites is to measure the fresh (Dethloff *et al.* submitted) or the dry weight (Kueger *et al.* 2012). To avoid weighing, the volume of the sample can be determined if tissues have the same density.

The task was to determine a suitable measurement without affecting the metabolism, i.e. to keep the metabolism inactive. The determination of leaf volume was rejected because leaf area and thickness could not be determined easily, fast and precisely without perturbation of the plant. By snap-freezing full rosettes in liquid nitrogen and subsequently freeze-drying them (Kueger *et al.* 2012) dry material can be achieved. Afterwards single leaves can be harvested and weighed. However, this method was also rejected due to limitations of gravimetric determination (see 3.1.2; and below). Finally, the fresh weight was chosen as a measure for relative and absolute metabolite quantification. For the purpose of preciseness a lower weight limit of 2 mg was determined for measuring small leaves in a frozen state, because measurements of smaller weights led to a relative error of more than 50%. If this error was carried on to the metabolite quantification it would lead to an artificially induced variation that would possibly be beyond the biological. Samples with a smaller weight can therefore only be interpreted for their metabolic composition.

4.3 Fast extraction of metabolites

For a precise analysis of primary metabolites with a GC-MS, the metabolites need to be extracted from the sample. The extraction process is necessary to gain an enriched fraction of primary metabolites (Kopka *et al.* 2004), otherwise other fractions like cell wall or membrane components will interfere with the analysis. For the extraction and ¹³C-enrichment of primary metabolites different methods are known. Samples can be extracted with a phase separation into a hydrophilic and a hydrophobic solvent fraction, or without a phase separation. A commonly used solvent mixture to create a phase separation is methanol/chloroform/water (Dethloff *et al.* submitted), where a ¹³C-enrichment of primary metabolites is found in the

upper phase and a ^{13}C -enrichment of lipids is found in the lower phase. An extraction without phase separation can be done with a mix of methanol and water (Roessner *et al.* 2000; Dethloff *et al.* submitted). A range of different other extraction methods are also known, all based on the principle of extracting fractions enriched with compounds of interest without activating the metabolism. As the extraction methods differ in their solving properties, the recovery of metabolites needs to be controlled. For this purpose precise amounts of internal standards are added to the extraction to control the recovery of specific compound classes.

In this work the extraction with a methanol/water mix was reduced to a pure methanol extraction to cope with the quantity of samples on the one hand and with the wide range of sample weights on the other hand. Due to the analysis of single leaves, the quantity of samples increased 6-7 times compared to the analysis of full rosettes. The sample weight ranged from 2 mg to > 50 mg and the solvent volume was adapted in order to keep the solvent-to-sample ratio in a small range, because solving properties are dependent on this ratio. Although very hydrophilic compounds like sugars and amino acids are more soluble in a mix of water and methanol, all major primary metabolites could be found in the analysis of the extracts. To take the recovery of these compound groups into account, ^{13}C -sorbitol was added to the samples as an internal standard.

4.4 Feeding methods

4.4.1 Feeding solution distribution in the rosette is dependent on connectivity of the vascular tissue in the shoot

By cutting a leaf lamina and feeding a solution into the plant via the petiole, the solution can be distributed via the xylem, phloem, apoplast or symplast. This aspect was investigated by using two different dyes that can act as phloem (CFDA) or xylem markers (Calcofluor White). The phloem marker was used to simulate the behaviour of externally fed sucrose, which is known to accumulate in the phloem (Turgeon *et al.* 1988). The co-feeding of these two dyes as a mix resulted in a differential stain in both tissues, indicating a distribution via all transportation systems (Figure 13). The same was proposed by Lin *et al.* (2010). However, they finally assumed a major translocation via the phloem and the apoplast. A compound that is actively taken up into the phloem along its transport route will end up accumulating in the phloem and thus will in majority be distributed into the tissue on its natural way. Therefore

the uptake and translocation of sucrose could not be confirmed finally. Regarding the results from Lin and co-authors and the results presented here, it seems likely to be a mixed translocation, where sucrose is taken up into the phloem over time.

The petiole feeding assay of dyes showed a systemic distribution in the plant, thus an accumulation in young leaves as well as in mature and intermediate leaves in one half of the rosette (Figure 12). A very similar dye distribution pattern has also been reported for other dicot plants fed with dyes in a petiole feeding approach by Lin *et al.* (2010, 2011). This typical distribution could be caused by the connection of the vascular tissue in the shoot, which favours a distribution to orthostichous leaves (Orians *et al.* 2005).

This leads to the question: If sucrose is taken up into the phloem along the transport route, does the method still allow a feeding of the systemic leaves? The ^{13}C -sucrose distribution was very similar to the results of the dye feeding, which indeed showed a systemic distribution of the label (Figure 14). The petiole feeding assay showed a high variation of labelling between plants and between leaves, which made an analysis difficult. The variation between the leaves is determined by the systemic distribution and difficult to change. As an approach to reduce the variation of feeding efficiencies between plants, leaf lamina were cut under tap water to avoid cavitation of the xylem and under EDTA to avoid callose formation in the phloem (King *et al.* 1974). Both had no obvious effect on the feeding variations for the dye (data not shown) and were therefore not continued. To reduce the variation between leaves of a rosette the hypocotyl feeding assay was developed. In the studies of Lin *et al.* a hypocotyl feeding had not been done because nodulation in the root was investigated (Lin *et al.* 2010). With the hypocotyl feeding a more homogeneous and more efficient method was found. The hypocotyl feeding showed a more equal distribution of dye (Figure 23) and ^{13}C -sucrose (Figure 24) in the rosette, possibly because all vessels had access to the feeding solution and their connectivity did not affect the distribution any longer. In young leaves a slightly higher ^{13}C -enrichment was measured, which could be caused by either a larger ratio between transport rate and total sucrose pool or an increased metabolisation of sucrose compared to the older leaves.

A further investigation and optimisation were not done because feeding of ^{13}C -sucrose resulted in a sufficiently reproducible distribution and a sufficient amount of label in the plant metabolism.

It could be tested if an optimisation of the feeding solution can be achieved by using a buffer system to keep pH and osmotic potential constant for different precursors and different concentrations as it has been used for disc assays (Roessner-Tunali *et al.* 2004; Timm *et al.* 2008). An adjustment of the feeding solution was not followed up in this work because it was shown that additional compounds can influence the feeding and uptake of the fed precursor (see 3.1.3.2).

4.4.2 Metabolic changes caused by the feeding

The aim of this work was to investigate the carbon allocation of a specific precursor in plant metabolism. How the feeding assays influence the plant metabolism is therefore an essential aspect. To investigate the isotope allocation of non-photosynthetic precursors in the plant, classically leaf disc assays are performed (Roessner-Tunali *et al.* 2004; Timm *et al.* 2008). The controls for these assays are usually performed using the same conditions and only changing from a labelled to an ambient precursor. Not much has been published about the metabolic differences between an intact, non-fed leaf, and a punched-out leaf disc in a solution. It is known that cutting or any other damage of a leaf induces wound stress responses in the plant. Recently, it has been reported that the jasmonic acid level, a hormone that activates wound response in the plant, is dependent on the degree of damage caused by the wounding (Heil *et al.* 2012).

To investigate which metabolites were influenced by the feeding methods presented here, metabolite pool sizes were investigated in single leaves of plants fed with different ¹²C-sucrose solutions and compared to the pool sizes measured in single leaves of unfed control plants. The study revealed that the major part of the metabolites was not affected by the feeding either via the petiole (Figure 17) or via the hypocotyl (Figure 25).

Nevertheless some metabolites are affected. In the hypocotyl feeding galactinol and raffinose were increased, indicating an activation of the stachyose pathway (tetrasaccharides). These metabolites are known to increase in *Arabidopsis* during drought, salt and cold stress (Taji *et al.* 2002; Zuther *et al.* 2004). Furthermore, putrescine, β -alanine and GABA were increased. It has been reported that these metabolites increase after heat shock (Kaplan *et al.* 2004), and in addition for putrescine it has been shown that pool size increases during cold (Guy *et al.* 2008). These three metabolites are connected to each other. Putrescine can act as a precursor for GABA and for β -alanine biosynthesis (Fait *et al.* 2008). Fructose also showed an increase and its accumulation is known for drought and heat stress (Guy *et al.* 2008).

The increase of these metabolites indicates that the plants were in a stress situation. The common ground of the mentioned stresses is a water deficit in the cell caused by absence, unavailability or deprivation of water. Metabolites accumulate and act as protectant molecules to stabilise proteins or to prevent water loss by increasing the osmotic potential in the plant. This could be caused by the detachment of the root system, which should lead to an immediate drop of turgor pressure and loss of natural water flow. In addition it could be caused by the feeding of sucrose solution or water that will change the osmotic potential of xylem and phloem and perturb the natural water flow between tissues.

In the petiole feeding, out of the above-mentioned metabolites only putrescine and galactinol increased significantly, indicating a reduced response of the plant to a water stress. In contrast to the hypocotyl feeding an increase of glycine and glyceric acid was found, which has also been reported for plants under salt stress (Brosche *et al.* 2005), indicating again a water stress in the plants. Further shikimic acid showed an increase, suggesting an activation of the phenylpropanoid pathway, which is activated in response to various stresses including wounding (Solecka 1997). This increase could be a mild response to the detachment of the leaf.

All increases were stronger in young leaves than in mature leaves except for the putrescine increase that was stronger in mature leaves, indicating that young developing tissue might be better protected against damage caused by water stress. It further shows that stress responses differ between the developmental states of the leaves and already shows the importance of single leaf analysis.

The feeding methods presented here show that the metabolism is slightly affected by the feeding. Still, it seems that the plants show a response especially to a water deficit, which should be taken into account when using this method.

4.5 ^{13}C -quantification for net isotope flow calculations

To determine the net carbon flow into a specific metabolite pool the determination of the total ^{13}C in the sample is necessary. As shown above for the dye (Figure 12) and the ^{13}C -sucrose (Figure 14) feeding, the distribution within the rosette varies between single leaves especially when using the petiole feeding assay. To determine the amount of ^{13}C the sum of all ^{13}C -pools could be used. Therefore metabolite pools must be quantified exactly, including the specific determination of recovery (see 2.5.3) (Dethloff *et al.* submitted). In addition all metabolite pools with a ^{13}C -enrichment must be known and be measurable (see 2.6). This

approach had to be rejected, as a lot of measured metabolites were unknowns. Additionally, the large carbon-containing fractions like starch and cell wall components could not be measured in parallel to the primary metabolites. Their separate measurement would have been time-consuming and would thus have contradicted the concept of developing a fast and easy screening method for carbon allocation. Another way of determining the exact amount of ^{13}C is to measure the isotope ratio between ^{12}C and ^{13}C , which can be done by a stable isotope ratio mass spectrometry measurement. However, the use of a stable isotope ratio measurement had to be rejected, too, because of the low amount of sample material.

To still determine the total ^{13}C in each sample a non-metabolisable standard was co-fed to ^{13}C -sucrose to estimate its total amount in the leaf (see 3.1.3.2). A correlation analysis of the co-fed compounds (Figure 15) in the study showed that the global distribution is similar, suggesting that such an estimation is possible. The amount of ^{13}C -sorbitol was higher than the amount of lactulose and ^{13}C -sucrose (Figure 15), indicating that the uptake rate is dependent on the chemical properties of the compound. Further the ^{13}C -enrichments of sucrose, glucose and fructose (Figure 16) illustrate that the co-feeding had an impact on the incorporation of ^{13}C -sucrose. Lactulose presumably inhibits invertases by binding and blocking the catalytic centre of the enzyme, which resulted in an accumulation of ^{13}C -sucrose and reduction of fructose and glucose (Figure 16), shown as the ^{13}C -enrichment compared to the control. ^{13}C -sorbitol presumably inhibits the uptake of sucrose into the plant, which was supported by the low ^{13}C -enrichments for sucrose, fructose and glucose (Figure 16). Both hypotheses were not further investigated. The co-feeding of a non-metabolisable standard was rejected because of its influence on sucrose feeding.

Without an internal standard another approach was needed to normalise the high variation of feeding. As consequence the ^{13}C -enrichment of sucrose was used for standardisation because the up and down stream metabolite ^{13}C -enrichments are dependent on the provided amount of ^{13}C -sucrose. By using this normalisation the variation between different plants could be drastically reduced and the feeding assay became feasible.

4.6 Metabolic differences between single leaves of an *Arabidopsis* rosette

4.6.1 Metabolite pool sizes mark developmental stages

Like all plants, an *Arabidopsis* rosette has leaves in different developmental stages. These stages range from leaf primordia on the meristem to young sink leaves that are in the beginning of growth, to intermediate leaves in a phase of strong expansion and structural growth, to mature, full source leaves, to old leaves where senescence is already in progress. The present study focuses on leaves in a developmental stage between young sink leaves and mature source leaves. These leaves that are in the process of expansion growth (Figure 30) also undergo a transition from sink to source (Turgeon 1989). This conversion in development is accompanied by a major change in the carbohydrate metabolism (Pantin *et al.* 2012). Mature source leaves that are photosynthetically highly active (Figure 1) provide the supply for the photosynthetically less active developing leaves of the rosette (Figure 1). In addition to energy supply, growth in young leaves depends on an increasing turgor for the expansion and on the supply of cell wall building blocks (Somerville *et al.* 2004) to stabilise the expanded cell. A recent study presenting transcript profiles and quantitative proteomics revealed that one leaf harvested at different ages, i.e. different developmental stages, had altered transcript as well as altered protein compositions (Baerenfaller *et al.* 2012).

The aim of this experiment was to examine single leaf metabolite profiles of different developmental stages which were classified by their growth. Metabolite pool sizes revealed a robust association to relative leaf growth (Figure 33). A cluster of metabolites containing mainly amino acids, some phosphates and lipid-related compounds correlates to relative leaf growth. The demand for amino acids could have different reasons: amino acids could be used to increase the osmotic potential of the vacuole for expansion growth (Hummel *et al.* 2010) and/or a supply of amino acids could be needed for an increased protein biosynthesis in young leaves (Pantin *et al.* 2012). Further the unknown-ketose-1 is the only carbohydrate that correlates to relative leaf growth. It would therefore be an interesting candidate for an identification attempt. In addition to this, a range of unknown metabolites were found to be correlated to growth, which indicates their association to the *Arabidopsis* metabolome and their relevance for growth. They are therefore candidates for identification and further investigation. A pronounced decrease, i.e. an association to relative leaf growth, was shown for phosphoric acid pool sizes. Phosphoric acid is assumed to be a breakdown product of

phosphorylated compounds (personally communicated by Erban A.), which would indicate a generally higher level of phosphorylated compounds in young leaves.

Together with the mentioned amino acids these metabolites are good marker candidates for the relative developmental state of a single leaf.

The analysis revealed a second cluster of metabolites that were negatively correlated to the relative leaf growth. Some metabolites in this cluster, especially glycerol, unknown-ketose-II and other unknown metabolites, seem to be markers of a late developmental stage. Metabolites associated to lipid metabolism were not further investigated, but seem to be associated to growth. To reach a high photosynthesis rate in mature leaves, chloroplast number and size increase (Pantin *et al.* 2012) and this process is accompanied by an increasing demand for thylakoid membrane components. Therefore, the investigation of lipid metabolism in a specific lipid analysis would be of interest.

Carbohydrates and TCA cycle intermediates did not show a significant difference related to leaf developmental stages. Although most of them revealed a specific pattern, it was either not significant or not reproducible in independent experiments. It has been reported that pool sizes of sucrose and starch are markers for growth of whole plants (Sulpice *et al.* 2009). However, to monitor growth of single leaves in a rosette they do not seem to be markers, as pool size of sucrose stayed constant across the different leaf positions. The information provided by the publication of Baerenfaller *et al.* 2012 indicates that transcripts and protein levels are also correlated to growth. However, a detailed comparison of transcript, protein and metabolite data could not be done due to time limitations.

The observation of very clear trends of most measured metabolite pool sizes indicates a fine regulation of metabolism between different leaf positions of one plant.

4.6.2 Carbon allocation from ^{13}C -sucrose in primary metabolites between different developmental leaf stages reveals pronounced differences

Metabolite profiling measurements only provide information on changes in pool size. If the specific metabolic pathway is tightly regulated and stays in a homeostasis, possible changes in carbon flow will not be detected. To overcome this lack of information, an easy method for carbon allocation from a specific precursor was developed. This method which is based on a metabolite profiling provides estimations on relative carbon allocation. This data can be

interpreted analogically to the conventional pool size data collected from the same single leaf measurement.

Source leaves maintain the supply of carbohydrates to sink leaves in an *Arabidopsis* rosette. The developing sink leaves perform a transition to become source leaves (Turgeon 1989). This transition is accompanied by various changes in central carbon metabolism, enzymatic machinery, phloem structure and other anatomical changes to favour CO₂ assimilation and carbohydrate export (Pantin *et al.* 2012). It has been shown that in young leaves carbon from photosynthesis is incorporated in proteins while imported carbon from sucrose is mainly used to build up cell wall (Turgeon 1989).

Still, little is known about the relative carbon allocation from sucrose in single leaves of different developmental stages. The results presented here provide a first insight.

The fructose and glucose ¹³C-pools were higher than their actual pool sizes (Figure 37). In theory this should not happen when sucrose is the only source of ¹³C, because this means glucose and fructose ¹³C-enrichments exceed the ¹³C-enrichment of sucrose. It is assumed that a part of the fed ¹³C-sucrose was already cleaved by invertases before it was translocated into the cell, so that not only sucrose but also glucose and fructose were sources of ¹³C. The multiple ¹³C sources led to the assumption that the ¹³C-pools were constantly overestimated, but this should not influence the interpretation of relative carbon allocation. Another reason for the increased ¹³C-pools could be that the ¹³C-enrichment of the sucrose pool had a peak within 4 hours and was decreasing afterwards because more photosynthetically fixed carbon than ¹³C was transported to the tissue after a specific feeding time. This seems to be unlikely, however, as ¹³C-sucrose was constantly provided to the plant. To finally clarify this, the uptake-rate of solution in the rosette could be measured over 4 to 5 hours with small time frames.

¹³C-pools were generally higher in young leaves except for fructose ¹³C-pools. This shows that the integration of carbon into these pools happens at a higher rate. For some metabolites ¹³C-pools were almost equal for the 20 mM and for the 100 mM feeding, which indicates that these pools are fed faster from sucrose than pools where only the 100 mM feeding leads to a ¹³C-enrichment.

For nearly all measured metabolites the ¹³C-pools supported the observed pool size trends across the different leaf positions. Fumaric acid and pyroglutamic acid made an exception.

They showed a divergent behaviour of pool size and ^{13}C -pool. Fumaric acid is of special interest, as the downstream ^{13}C -pool of malic acid reflects the normal pool size trend again. This indicates that the fumaric acid pool may have been fed with carbon from a source that was not sucrose and/or that the fumaric acid pool was split into one pool that feeds the TCA cycle and one inert pool that accumulates with leaf age and is not fed by sucrose anymore.

The ^{13}C -pool of GABA showed nearly no label and an unexpected pattern. If metabolites are of low abundance and close to the detection limit isotopomers of fragments are not easy to detect. If these fragments cannot be detected, the intensity measured is zero. This fact results in a non-labelling although metabolites are enriched. This illustrates the limit of the method and shows that low abundant metabolites have to be treated with caution.

4.7 Metabolic differences between single leaves of an *Arabidopsis* rosette in cold-grown plants

4.7.1 Single leaves adjust metabolites differently during cold growth

Metabolite pools of a range of metabolites increase in cold treated plants (Guy *et al.* 2008). Very similar metabolites seem also to be increased in cold grown plants (Gray *et al.* 2005). Single leaves show a different metabolic pattern that is associated with the developmental stage and the relative growth of these leaves in normal temperatures (see above 4.6). Are these patterns different for plants grown in the cold?

In the following some metabolic adaptations to growth in the cold will be shown. It has been reported that the ratio of starch and sucrose changes in favour of sucrose (Strand *et al.* 1999) and that both pool sizes are elevated (Gorsuch *et al.* 2010). The central carbohydrate metabolism is most prominently changed. Pool sizes have been reported to be elevated for xylose, glucose, fructose, sucrose, galactose and raffinose (Guy *et al.* 2008). Furthermore intermediates of the TCA cycle are increased (Cook *et al.* 2004) as well as amino-related compounds like proline, aspartate, ornithine and putrescine (Cook *et al.* 2004; Guy *et al.* 2008). However, much less is known about the relative changes across different developmental stages of leaves grown in the cold.

To find metabolites with differential responses in the different leaf stages, single leaf metabolite profiles of plants grown under normal temperatures and grown in the cold (10 °C) were compared regarding their relative pool size changes. The analysis revealed robust pool size differences for four metabolites (Figure 35). The two amino acids threonine and serine

(Supplemental Fig. 6) are known to increase in cold stress (Kaplan 2004; Schmidt 2013). The similar pool size changes of both between normal and cold conditions across the different leaves are very interesting in that these metabolites are distinct in their pathways but seem to be regulated in a similar manner (Figure 35). This fact makes these two metabolites quite interesting targets for further studies. Another very interesting target is the unknown A214003-101. This metabolite nearly inverts its trend from normal to cold temperatures. The analysis of the mass spectrum reveals similarities to glucose as a first hint for identification (Supplemental Fig. 4; Supplemental Fig. 5).

The global metabolic pattern that was found in single leaves of both plants grown in the cold and plants grown under normal conditions revealed that the relative behaviour of metabolites stayed the same, indicating a regulation of metabolism between leaves in different developmental stages.

4.7.2 Carbon allocation from ^{13}C -sucrose differs in primary metabolites of different developmental leaf stages in cold-grown plants

As only some metabolites showed a different behaviour across different leaf positions, an investigation of carbon allocation was quite interesting. It has already been reported for *Arabidopsis* that growth is a temperature-dependent process. It is assumed to be reduced by 50% at 10 °C compared to standard temperatures (Pantin *et al.* 2011).

The first approach of labelling plants grown in the cold revealed that carbon was allocated much more slowly in the plants and in their metabolism, as only five metabolites showed a detectable ^{13}C -enrichment (Figure 39). Further the turn-over of fructose seemed to be very high in intermediate leaves as these ^{13}C -pools were higher than the conventional pool sizes. Glucose ^{13}C -pools showed a similar trend, but at the same level as their pool sizes. The metabolite pools that showed an interesting behaviour in the conventional metabolite profiling as well as the pools of fumaric acid and malic acid could not be labelled properly. For further studies adapted experiments with higher concentrations of a ^{13}C -sucrose solution should be more informative.

4.8 Expression of *REIL* genes and single leaf metabolism of *reil2* in the cold

The knock-out of the *REIL2* gene leads to a severe morphological phenotype in the cold, but nearly no changes in the metabolite pool sizes or expression of transcripts have been found on a rosette level (Schmidt 2013). Up to now no phenotype of the *reil1* could be found,

although the double knock-out of both genes leads to a growth arrest in the cold. The morphological phenotype of the *reil2* indicates that the gene is involved in leaf development in the cold (Schmidt *et al.* 2013). For a more detailed analysis of the gene function it is important to know in which tissues these genes are active. To increase the resolution for a metabolic characterisation a single leaf analysis of different developmental leaf stages can be done. In combination with a stable isotope tracing this analysis should show which metabolites and pathways are affected and might give a hint how metabolism and morphology are connected.

In the cold the *reil2* shows a reduced growth and forms small spoon-shaped leaves (Schmidt 2013; Schmidt *et al.* 2013). The metabolic and transcriptomic analysis of full rosettes in a vegetative state shows that *reil2* does not globally differ from the WT. The metabolome and the transcriptome of *reil2* stay in a vegetative state and do not shift to a generative state, as opposed to the WT.

The promoter-GUS studies of the *REIL1* gene revealed an activity in the shoot centre, vascular tissue and hydathodes, as well as in the vascular tissue of the root (Figure 40). This indicates an involvement of the gene in the development of vascular tissue. The expression of the *REIL2* gene is similar to the expression of DR5. Both were found to be expressed in stipules, hydathodes and in the differential zone of the root tip (Figure 40). This indicates that the gene could be connected to an auxin regulation pathway, which is also supported by the promoter study that revealed an auxin-responsive element. Admittedly, an *in silico* expression analysis did not show a response to auxin, which should be re-examined using an *in vitro* plat essay with auxin. Still, the very similar expression locations of *reil2* and DR5 and the fact that leaf morphology of the mutant was altered indicate that *REIL2* is involved in a developing process.

The first insight into the analysis of single leaf metabolism already revealed strong differences between *reil2* and WT (Figure 41). The continuous change in single leaf metabolism across sequential leaves that was demonstrated in the ICA for the WT was not found for the *reil2*, where single leaves showed a discontinuous change of metabolism, basically two metabolic states, separating young and mature leaves (Figure 41). This indicates that the single leaves do not have such a clear metabolic state as the WT, which leads to the assumption that metabolite pool sizes may be less correlated to the different developmental stages of the single leaves. Changes may be less continuous and more

pronounced between young and mature leaves. Observed changes were stronger for the *reil2.1* than for the *reil2.2*, which reflects the strength of the respective morphological phenotype.

A deeper investigation of the metabolite analysis should show which metabolite pool sizes are changed in particular. Further a stable isotope tracing with labelled sucrose should reveal whether a change in the development of leaves causes a differential usage of sucrose. Assuming that only the metabolism of young leaves is changed, a single leaf analysis might reveal an altered metabolism which remains hidden in a full rosette analysis. In addition the examination of sucrose carbon allocation might generate further insights into the function of the *REIL2* gene. Some stable isotope tracing measurements examining carbon allocation of sucrose in single leaf metabolites have already been done, but could not be analysed in the given time.

5 **Outlook**

The petiole and hypocotyl feeding methods as well as the measurements and calculations to determine carbon distribution from a specific precursor described in this work are completed and are currently being used to investigate carbon allocation from ^{13}C -sucrose fed into single leaves of *reil* mutants.

The investigation of single leaf metabolites in leaves of different developmental stages yielded very interesting results that will be further investigated. In addition to the experiments done on single leaves in this work, experiments with a higher number of pooled samples have already been performed to support the previous results and further investigate low abundant metabolites. In addition to this experiment the behaviour of cold-grown plants will be examined. A transcript profiling has already been done on pooled leaf samples of cold-grown plants and needs to be evaluated. Further these samples have also been used to create metabolite profiles of primary metabolites, of secondary metabolites and of lipids. With this systemic approach a more detailed analysis of the processes in leaves of different developmental stages becomes possible. With the data provided by Baerenfaller and co-authors a comparison of transcript, protein level, metabolite level and carbon allocation data will be done to describe the different developmental leaf stages in detail. The data presented in this work and the additional data mentioned above will lead to a detailed description of leaves in different developmental stages.

Both examined *reil2* showed strong growth reduction in the cold, but metabolites of full rosettes seemed to be affected only on a minor level. The examinations of single leaf metabolism (pool sizes and carbon allocation of sucrose) of the *reil2* will hopefully provide new insights into the primary and secondary effects caused by the knock-out of the gene.

6 Abbreviations

<i>Arabidopsis</i>	<i>Arabidopsis thaliana</i> accession Columbia-0
ANOVA	Analysis of Variance
BSTAF	N,O-Bis(trimethylsilyl)trifluoroacetamide
CFDA	carboxyfluorescein diacetate
CHCl ₃	chloroform
DMF	dimethylformamide
DMSO	dimethyl sulfoxide
DNA	deoxyribonucleic acid
DREB1A	<u>D</u> ehydration <u>R</u> esponse <u>E</u> lement B1A
DREB2A	<u>D</u> ehydration <u>R</u> esponse <u>E</u> lement B2A
EtOH	ethanol
GABA	γ-aminobutyric acid
GC-EI-TOF-MS/ GC-MS	gas chromatography with electron ionisation and time of flight mass spectrometry detector
GFP	green fluorescence protein
HCL	hierarchical clustering
ICA	Independent Component Analysis
IS	internal standard
MeOH	methanol
PCA	Principle Component Analysis
PCR	polymerase chain reaction
REI	<u>R</u> Equired for <u>I</u> sotropic bud growth
REIL	<u>R</u> EI- <u>L</u> ike
RNA	ribonucleic acid
TCA cycle	tricarboxylic acid cycle; citric acid cycle
X-Gluc	5-Bromo-4-chloro-3-indolyl-β-D-glucuronide

7 List of figures and tables

Figure 1: Carbon flow into the leaf at relative final leaf sizes.	3
Figure 2: Visualisation of the sink to source border in <i>Arabidopsis</i> leaves.	4
Figure 3: Determination of leaf positions and harvesting scheme.	20
Figure 4: Molecular ion, fragment ion, and respective isotopomers of trimethylsilylated succinic acid.	23
Figure 5: Partial mass spectrum of glucose.	25
Figure 6: Correlation analysis of isotopomer sum.	26
Figure 7: ^{13}C enrichment of all samples for the selected mass fragments.	27
Figure 8: Determination of leaf position in <i>Arabidopsis</i> rosettes.	30
Figure 9: Determining the quality of normalisation by fresh weight.	32
Figure 10: Attempt of Stomata feeding.	34
Figure 11: Scheme of the petiole feeding assay.	35
Figure 12: Distribution of dye in <i>Arabidopsis</i> rosettes after petiole feeding.	36
Figure 13 Longitudinal section of a feeding petiole after feeding with a mix of Calcofluor White and CFDA.	37
Figure 14: Distribution of ^{13}C -sucrose in <i>Arabidopsis</i> rosettes after a petiole feeding assay.	38
Figure 15: Testing distribution of internal standards in a co-feeding.	39
Figure 16: ^{13}C -enrichment measurements in co-fed plants.	40
Figure 17: Global differences in primary metabolites of a petiole feeding test and control plants.	42
Figure 18: Correlation of the single leaf position samples of control and ^{12}C -sucrose (12C) fed plants.	43
Figure 19: Heat map of annotated analytes of petiole feeding and control data.	44

Figure 20: Heat map of significantly changed analytes after petiole feeding with 20 mM ¹² C-sucrose solution.	46
Figure 21: Selection of analytes changed due to petiole feeding.	47
Figure 22: Scheme of the hypocotyl feeding assay.	48
Figure 23: Testing the distribution of a dye by a hypocotyl feeding assay.	48
Figure 24: Distribution of ¹³ C-sucrose in Arabidopsis rosettes fed by a hypocotyl feeding.	49
Figure 25: Global view on primary metabolites of plants fed by a hypocotyl feeding assay and control plants.	50
Figure 26: Clustering of samples of single leaf positions of control and ¹² C-sucrose-fed plants of a hypocotyl feeding.	51
Figure 27: Heat map of annotated analytes between hypocotyl-fed and control plants.	52
Figure 28: Heat map of significantly changed metabolites due to hypocotyl feeding.	54
Figure 29: Analytes changed significant due to the hypocotyl feeding assay.	55
Figure 30: Leaf growth.	57
Figure 31: Global view of single leaf GC-MS primary metabolite analysis of <i>Arabidopsis</i> rosettes.	58
Figure 32: Heat map of metabolites that change significantly across leaf positions.	60
Figure 33: Clustering metabolites to leaf growth.	61
Figure 34: Overview of annotated analytes in one cold experiment and two control experiments.	62
Figure 35: Change in relative trend over leaf positions due to cold growth.	63
Figure 36: Conventional pool size data of primary metabolites after a hypocotyl feeding with 20 mM ¹³ C-sucrose solution.	64

Figure 37: Pool sizes and carbon allocation of significantly changed metabolites in different leaf positions.	66
Figure 38: Pool size of primary metabolites after a hypocotyl feeding with 20 mM ¹³ C-sucrose solution of control plants and plants grown in the cold.	68
Figure 39: Metabolite pool sizes and carbon allocation of hypocotyl-fed plants grown in the cold.	69
Figure 40: Promoter-GUS studies of 2-4 week old plants grown in the cold.	71

List of tables:

Table 1: Partial results of transcript profiling of <i>reil1</i> and <i>reil2</i> rosettes in a vegetative state compared to WT.	9
Table 2: Table of promotor-GUS constructs and plants.	12
Table 3: Components to generate a GUS staining solution.	16
Table 4: the different dyes that were used for plant labelling.	18
Table 5: The extraction volume of methanol is adapted to the fresh weight.	20
Table 6: Labelling test solutions for ¹³ C-sucrose quantification with internal standards	.39
Table 7: Promoter-GUS plants that showed a GUS expression in the listed tissues.	72

8 Supplemental

Supplemental on CD:

Raw data for the result chapters can be found in the corresponding supplemental files.

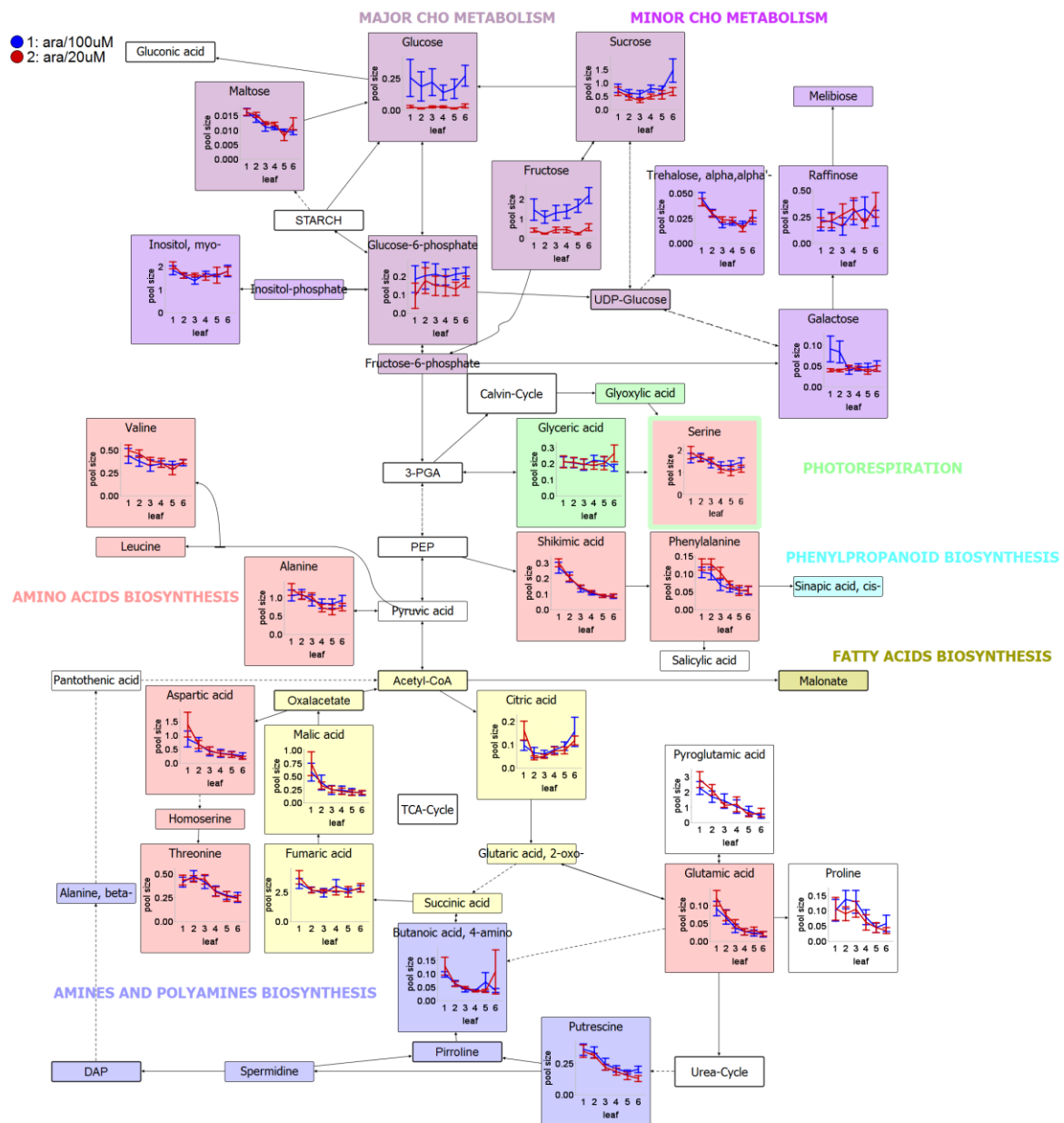
For example the supplemental table containing raw data and calculations for 3.2.1 “Metabolic pool size differences between single leaf positions in *Arabidopsis* rosettes can be found in “Supplemental_3-2-1.xlsx”

Additionally:

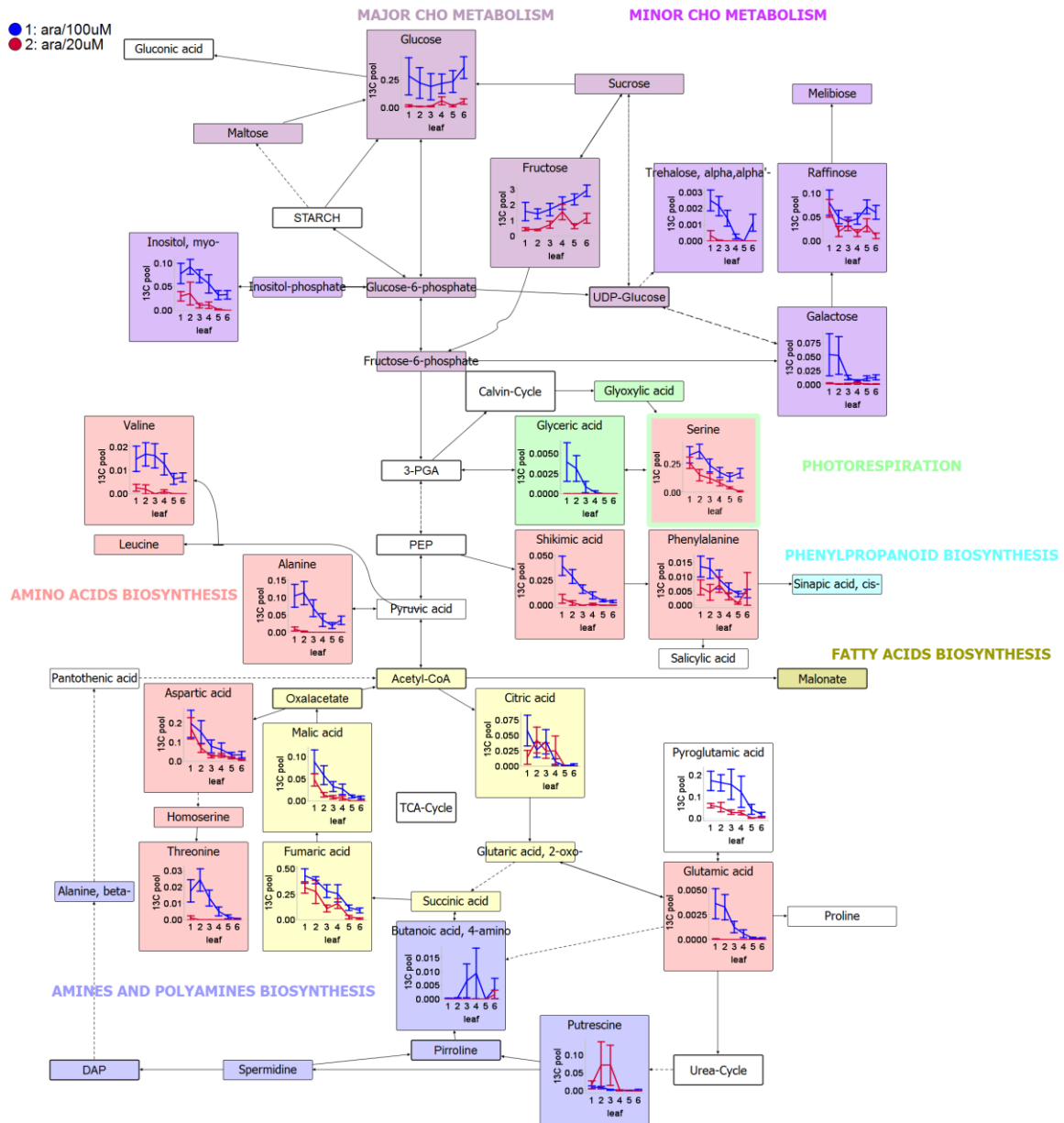
Analytes-description.xlsx contains a description of the analytes annotated in the GC-MS data with information about derivate, CAS-No., metabolite, etc.

PhD-Thesis-Frederik-Dethloff.pdf contains this thesis as a pdf-file.

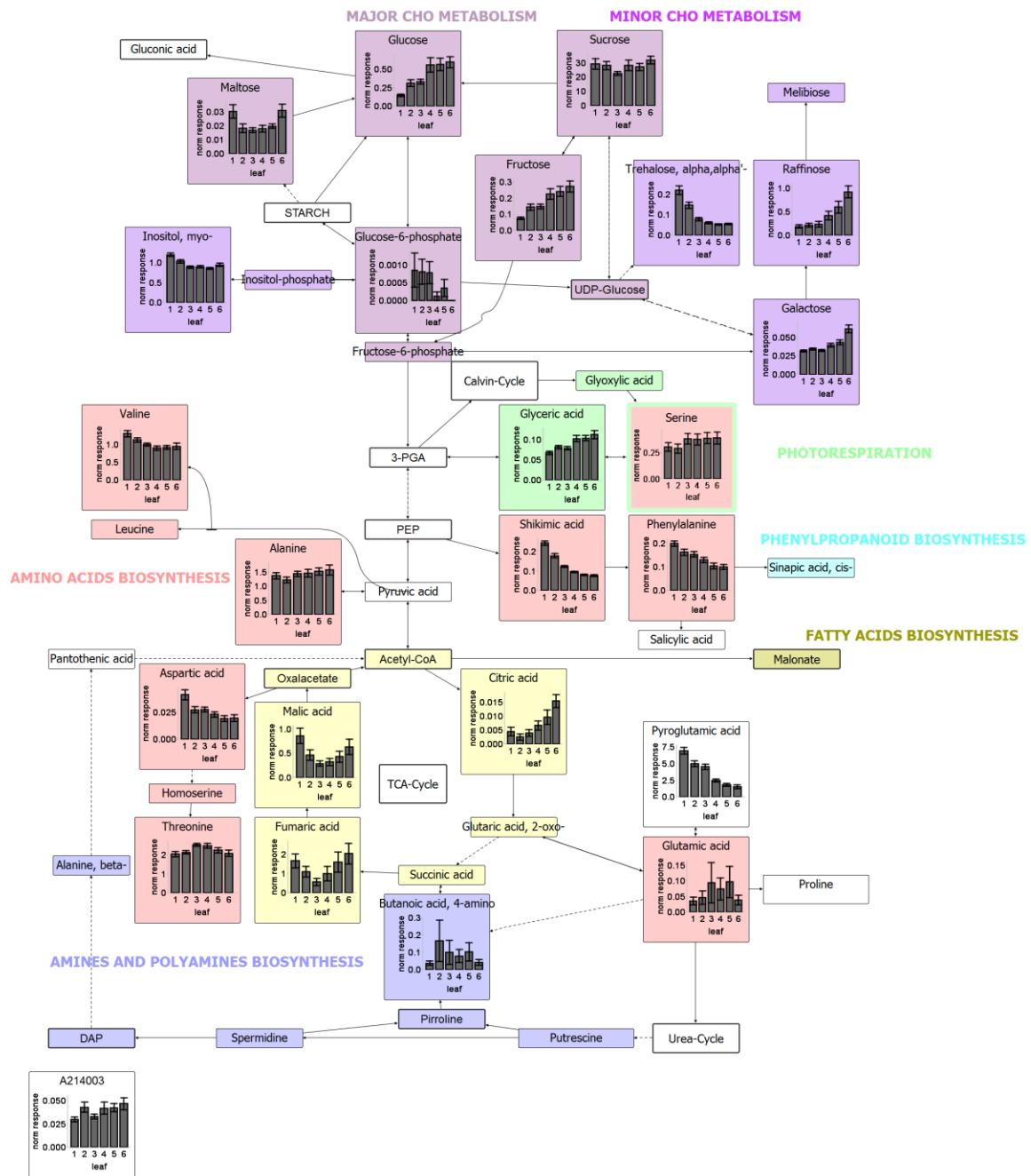
8.1 Supplemental figures



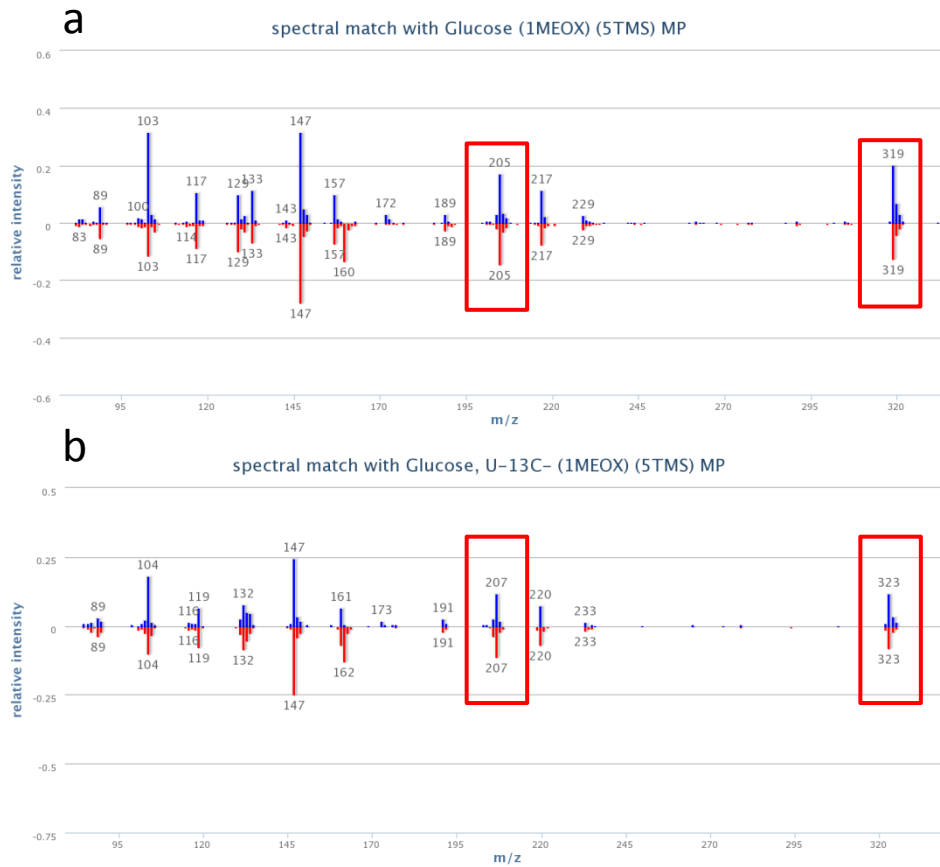
Supplemental Fig. 1: Metabolite pool sizes derived from hypocotyl feeding with a 20 mM and a 100 mM ^{13}C -sucrose solution mapped on a reduced pathway of primary metabolism. Diagrammed are averages of normalised responses; error bars represent the standard error.



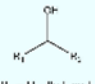
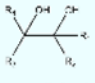
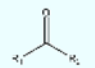
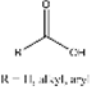
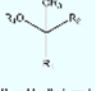
Supplemental Fig. 2: Metabolite ^{13}C -pools derived from hypocotyl feeding with a 20 mM and a 100 mM ^{13}C -sucrose solution mapped on a reduced pathway of primary metabolism. Diagrammed are averages of ^{13}C -pools; error bars represent the standard error.



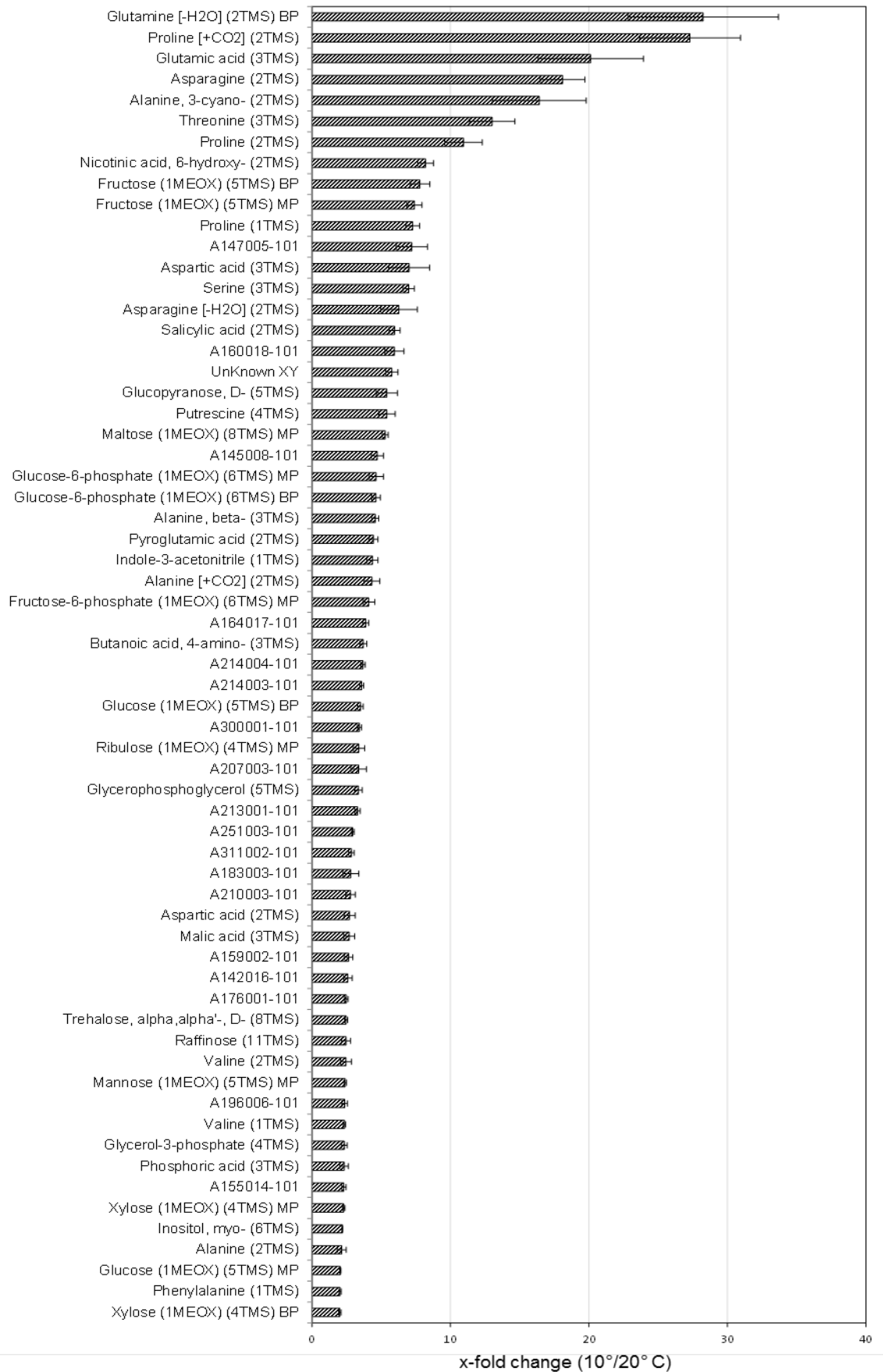
Supplemental Fig. 3: Metabolite pool sizes derived from hypocotyl feeding with a 20 mM ^{13}C -sucrose solution from plants grown in the cold. Single leaf data is mapped on a reduced pathway of primary metabolism. Diagrammed are averages of normalised responses; error bars represent the standard error.



Supplemental Fig. 4: Mass spectral of the unknown A214003 vs glucose (a) and A214003 fully ¹³C labelled vs U-¹³C-glucose. The mass fragments 205 and 319 show the same mass shift when labelled and were therefore used for the calculations of enrichments. Data was modified from the GMD.

Functional Group Prediction Results							(Show Details...)
functional group	image	prediction	probability	adjusted probability	support	description	contained in unknown, not annotated yet
Prim Alcohol	$\text{R}-\text{OH}$ $\text{R} = \text{alkyl}$	present ✓	100.00%	12.76%	284	intensity lq - 103 >= 2.5748872995 and intensity lq - 102 < 2.0401987791 and intensity ...	unknown ⚠
Sec Alcohol	 $\text{R}_1 = \text{H, alkyl, aryl}$ $\text{R}_2 = \text{H, alkyl, aryl}$	present ✓	99.85%	5.85%	688	intensity lq - 217 >= 2.3706843138 and intensity lq - 103 >= 2.067753911 and intensity ...	unknown ⚠
Alcohol	$\text{R}-\text{OH}$ $\text{R} = \text{H, alkyl, aryl}$	present ✓	99.85%	1.86%	698	intensity lq - 103 >= 2.5748872995 and intensity lq - 217 >= 1.1120529413	unknown ⚠
1,2 Diol	 $\text{R}_1 = \text{H, alkyl, aryl}$ $\text{R}_2 = \text{H, alkyl, aryl}$ $\text{R}_3 = \text{H, alkyl, aryl}$ $\text{R}_4 = \text{H, alkyl, aryl}$	present ✓	99.72%	8.24%	709	intensity lq - 217 >= 2.3706843138 and intensity lq - 103 >= 2.0688993216 and intensity ...	unknown ⚠
Hydroxy	$\text{R}-\text{OH}$ $\text{R} = \text{alkyl, aryl}$	present ✓	99.62%	1.19%	811	intensity lq - 103 >= 2.5338769555 and intensity lq - 217 >= 1.1120529413	unknown ⚠
Carbonyl	 $\text{R}_1 = \text{H, alkyl, aryl}$ $\text{R}_2 = \text{H, alkyl, aryl}$	present ✓	81.56%	21.75%	208	intensity lq - 89 >= 2.1427367687 and < 2.5713683844 and intensity lq - 172 >= 0.8238890648 ...	unknown ⚠
Carboxylic Acid	 $\text{R} = \text{H, alkyl, aryl}$	absent ✗	100.00%	1.71%	349	intensity lq - 217 >= 2.3706843138 and intensity lq - 292 < 2.3957662821 and intensity ...	unknown ⚠
Acetal	 $\text{R} = \text{H, alkyl, aryl}$ $\text{R}_2 = \text{H, alkyl, aryl}$ $\text{R}_1 = \text{alkyl, aryl}$ $\text{R}_4 = \text{alkyl, aryl}$	absent ✗	99.98%	0.00%	4,962	intensity lq - 361 < 0.5611459732 and intensity lq - 204 < 2.3971363306	unknown ⚠

Supplemental Fig. 5: Functional group prediction of A214003 with the decision tree algorithm of the GMD.



Supplemental Fig. 6: Metabolites increasing in plants grown in the cold. Diagrammed are significantly increased metabolites of full rosette GC-MS primary metabolite analysis. Significance was tested with a one-way-ANOVA and a Kruskal-Wallis test with a critical p-value of $p \leq 0.001$ for both tests. Shown are averages of x-fold changes between pool sizes measured in plants grown at 20 °C and 10 °C; only analytes with at least a 2-fold increase are shown; error bars represent the standard error. Data modified after Schmidt 2013.

9 Literature

Allen, D. K., I. G. L. Libourel and Y. Shachar-Hill (2009). "Metabolic flux analysis in plants: coping with complexity." Plant, Cell & Environment **32**(9): 1241-1257.

Allwood, J. W., A. Erban, S. de Koning, W. B. Dunn, A. Luedemann, A. Lommen, L. Kay, R. Loscher, J. Kopka and R. Goodacre (2009). "Inter-laboratory reproducibility of fast gas chromatography-electron impact-time of flight mass spectrometry (GC-EI-TOF/MS) based plant metabolomics." Metabolomics **5**(4): 479-496.

Aloni, R., K. Schwalm, M. Langhans and C. Ullrich (2003). "Gradual shifts in sites of free-auxin production during leaf-primordium development and their role in vascular differentiation and leaf morphogenesis in *Arabidopsis*." *Planta* **216**(5): 841-853.

Ap Rees, T., W. A. Fuller and B. W. Wright (1977). "Measurements of glycolytic intermediates during the onset of thermogenesis in the spadix of *Arum maculatum*." Biochimica et Biophysica Acta (BBA) - Bioenergetics **461**(2): 274-282.

Audi, G., O. Bersillon, J. Blachot and A. H. Wapstra (2003). "The Nubase evaluation of nuclear and decay properties." Nuclear Physics A **729**(1): 3-128.

Baerenfaller, K., C. Massonnet, S. Walsh, S. Baginsky, P. Buhlmann, L. Hennig, M. Hirsch-Hoffmann, K. A. Howell, S. Kahlau, A. Radziejwoski, D. Russenberger, D. Rutishauser, I. Small, D. Stekhoven, R. Sulpice, J. Svozil, N. Wuyts, M. Stitt, P. Hilson, C. Granier and W. Gruissem (2012). "Systems-based analysis of *Arabidopsis* leaf growth reveals adaptation to water deficit." Molecular systems biology **8**: 606.

Baxter, C. J., H. Redestig, N. Schauer, D. Reipsilber, K. R. Patil, J. Nielsen, J. Selbig, J. Liu, A. R. Fernie and L. J. Sweetlove (2007). "The Metabolic Response of Heterotrophic *Arabidopsis* Cells to Oxidative Stress." Plant Physiology **143**(1): 312-325.

Bouchabké, O., F. Tardieu and T. Simonneau (2006). "Leaf growth and turgor in growing cells of maize (*Zea mays* L.) respond to evaporative demand under moderate irrigation but not in water-saturated soil." Plant, Cell & Environment **29**(6): 1138-1148.

Brosche, M., B. Vinocur, E. Alatalo, A. Lamminmaki, T. Teichmann, E. Ottow, D. Djilianov, D. Afif, M.-B. Bogeat-Triboulot, A. Altman, A. Polle, E. Dreyer, S. Rudd, L. Paulin, P. Auvinen and J. Kangasjarvi (2005). "Gene expression and metabolite profiling of *Populus euphratica* growing in the Negev desert." Genome Biology **6**(12): R101.

- Bunce, J. A. (1977). "Leaf Elongation in Relation to Leaf Water Potential in Soybean." Journal of Experimental Botany **28**(1): 156-161.
- Callos, J. D. and J. I. Medford (1994). "Organ positions and pattern formation in the shoot apex." The Plant Journal **6**(1): 1-7.
- Calvin, M. (1956). "The photosynthetic carbon cycle." Journal of the Chemical Society (Resumed)(0): 1895-1915.
- Calvin, M. (1964). "The path of carbon in photosynthesis." Nobel Lectures Chemistry 1942–1962: pp. 618-644.
- Chinnusamy, V., J. Zhu and J.-K. Zhu (2007). "Cold stress regulation of gene expression in plants." Trends in Plant Science **12**(10): 444-451.
- Cho, H.-T. and D. J. Cosgrove (2000). "Altered expression of expansin modulates leaf growth and pedicel abscission in *Arabidopsis thaliana*." Proceedings of the National Academy of Sciences **97**(17): 9783-9788.
- Clough, S. J. and A. F. Bent (1998). "Floral dip: a simplified method for *Agrobacterium*-mediated transformation of *Arabidopsis thaliana*." The Plant Journal **16**(6): 735-743.
- Doyle, J. J. and E. E. Dickson (1987). "Preservation of Plant-Samples for DNA Restriction Endonuclease Analysis." Taxon **36**(4): 715-722.
- Cook, D., S. Fowler, O. Fiehn and M. F. Thomashow (2004). "A prominent role for the CBF cold response pathway in configuring the low-temperature metabolome of *Arabidopsis*." Proceedings of the National Academy of Sciences of the United States of America **101**(42): 15243-15248.
- Craig, H. (1953). "The geochemistry of the stable carbon isotopes." Geochimica et Cosmochimica Acta **3**(2–3): 53-92.
- Cross, J. M., M. von Korff, T. Altmann, L. Bartzetko, R. Sulpice, Y. Gibon, N. Palacios and M. Stitt (2006). "Variation of Enzyme Activities and Metabolite Levels in 24 *Arabidopsis* Accessions Growing in Carbon-Limited Conditions." Plant Physiology **142**(4): 1574-1588.
- Dale, J. E. (1988). "The Control of Leaf Expansion." Annual Review of Plant Physiology and Plant Molecular Biology **39**: 267-295.

Dawson, T. and P. Brooks (2001). Fundamentals of Stable Isotope Chemistry and Measurement. Stable Isotope Techniques in the Study of Biological Processes and Functioning of Ecosystems. M. Unkovich, J. Pate, A. McNeill and D. J. Gibbs, Springer Netherlands. **40**: 1-18.

Dawson, T. E., S. Mambelli, A. H. Plamboeck, P. H. Templer and K. P. Tu (2002). "Stable Isotopes in Plant Ecology." Annual Review of Ecology and Systematics **33**(ArticleType: research-article / Full publication date: 2002 / Copyright © 2002 Annual Reviews): 507-559.

Deeken, R., D. Geiger, J. Fromm, O. Koroleva, P. Ache, R. Langenfeld-Heyser, N. Sauer, S. May and R. Hedrich (2002). "Loss of the AKT2/3 potassium channel affects sugar loading into the phloem of *Arabidopsis*." Planta **216**(2): 334-344.

Delatte, T. L., P. Sedijani, Y. Kondou, M. Matsui, G. J. de Jong, G. W. Somsen, A. Wiese-Klinkenberg, L. F. Primavesi, M. J. Paul and H. Schluepmann (2011). "Growth Arrest by Trehalose-6-Phosphate: An Astonishing Case of Primary Metabolite Control over Growth by Way of the SnRK1 Signaling Pathway." Plant Physiology **157**(1): 160-174.

Dethloff, F., A. Erban, I. Orf, A. Jessica, F. Ines, Olga Beine-Golovchuk, S. Stefanie, S. Jens and K. Joachim (submitted). Profiling methods to identify cold regulated primary metabolites using gas chromatography coupled to mass spectrometry, Methods in Molecular Biology Humana Press Inc; NJ, USA.

Ehlert, C., C. Maurel, F. Tardieu and T. Simonneau (2009). "Aquaporin-Mediated Reduction in Maize Root Hydraulic Conductivity Impacts Cell Turgor and Leaf Elongation Even without Changing Transpiration." Plant Physiology **150**(2): 1093-1104.

Ehlert, C., C. Plassard, S. J. Cookson, F. Tardieu and T. Simonneau (2011). "Do pH changes in the leaf apoplast contribute to rapid inhibition of leaf elongation rate by water stress? Comparison of stress responses induced by polyethylene glycol and down-regulation of root hydraulic conductivity." Plant, Cell & Environment **34**(8): 1258-1266.

Erban, A., N. Schauer, A. R. Fernie and J. Kopka (2007). "Nonsupervised construction and application of mass spectral and retention time index libraries from time-of-flight gas chromatography-mass spectrometry metabolite profiles." Methods Mol Biol **358**: 19-38.

Fait, A., H. Fromm, D. Walter, G. Galili and A. R. Fernie (2008). "Highway or byway: the metabolic role of the GABA shunt in plants." Trends in Plant Science **13**(1): 14-19.

- Fambrini, M. and C. Pugliesi (2013). "Usual and unusual development of the dicot leaf: involvement of transcription factors and hormones." Plant Cell Reports **32**(6): 899-922.
- Fernie, A. R., P. Geigenberger and M. Stitt (2005). "Flux an important, but neglected, component of functional genomics." Current Opinion in Plant Biology **8**(2): 174-182.
- Fiehn, O., J. Kopka, P. Dormann, T. Altmann, R. N. Trethewey and L. Willmitzer (2000). "Metabolite profiling for plant functional genomics." Nat Biotechnol **18**(11): 1157-1161.
- Flury, M. and H. Fluhler (1994). "Brilliant Blue Fcf as a Dye Tracer for Solute Transport Studies - a Toxicological Overview." Journal of Environmental Quality **23**(5): 1108-1112.
- Fricke, W. (2002). "Biophysical Limitation of Cell Elongation in Cereal Leaves." Annals of Botany **90**(2): 157-167.
- Geigenberger, P. and M. Stitt (1991). "A "futile" cycle of sucrose synthesis and degradation is involved in regulating partitioning between sucrose, starch and respiration in cotyledons of germinating *Ricinus communis* L. seedlings when phloem transport is inhibited." Planta **185**(1): 81-90.
- Giersch, C., U. Heber, G. Kaiser, D. A. Walker and S. P. Robinson (1980). "INTRACELLULAR METABOLITE GRADIENTS AND FLOW OF CARBON DURING PHOTOSYNTHESIS OF LEAF PROTOPLASTS." Archives of Biochemistry and Biophysics **205**(1): 246-259.
- Gorsuch, P. A., S. Pandey and O. K. Atkin (2010). "Temporal heterogeneity of cold acclimation phenotypes in *Arabidopsis* leaves." Plant, Cell & Environment **33**(2): 244-258.
- Graham, D. and B. D. Patterson (1982). "Responses of Plants to Low, Nonfreezing Temperatures: Proteins, Metabolism, and Acclimation." Annual Review of Plant Physiology **33**(1): 347-372.
- Gray, G. R. and D. Heath (2005). "A global reorganization of the metabolome in *Arabidopsis* during cold acclimation is revealed by metabolic fingerprinting." Physiologia Plantarum **124**(2): 236-248.
- Guy, C., F. Kaplan, J. Kopka, J. Selbig and D. K. Hinch (2008). "Metabolomics of temperature stress." Physiologia Plantarum **132**(2): 220-235.

- Hannah, M. A., A. G. Heyer and D. K. Hinch (2005). "A Global Survey of Gene Regulation during Cold Acclimation in *Arabidopsis thaliana* ." PLoS Genet **1**(2): e26.
- Harb, A., A. Krishnan, M. M. R. Ambavaram and A. Pereira (2010). "Molecular and Physiological Analysis of Drought Stress in *Arabidopsis* Reveals Early Responses Leading to Acclimation in Plant Growth." Plant Physiology **154**(3): 1254-1271.
- Heidarvand, L. and R. Maali Amiri (2010). "What happens in plant molecular responses to cold stress?" Acta Physiologiae Plantarum **32**(3): 419-431.
- Heil, M., E. Ibarra-Laclette, R. M. Adame-Álvarez, O. Martínez, E. Ramirez-Chávez, J. Molina-Torres and L. Herrera-Estrella (2012). "How Plants Sense Wounds: Damaged-Self Recognition Is Based on Plant-Derived Elicitors and Induces Octadecanoid Signaling." PLoS ONE **7**(2): e30537.
- Huege, J., J. Goetze, D. Schwarz, H. Bauwe, M. Hagemann and J. Kopka (2011). "Modulation of the Major Paths of Carbon in Photorespiratory Mutants of *Synechocystis*." PLoS ONE **6**(1): e16278.
- Huege, J., Jan Goetze, Frederik Dethloff, Bjoern Junker and J. Kopka (2012). Quantification of Stable Isotope Label in Metabolites Via Mass Spectrometry. Plant Chemical Genomics, Humana Press Inc; NJ, USA. Methods in Molecular Biology.
- Huege, J., R. Sulpice, Y. Gibon, J. Lisec, K. Koehl and J. Kopka (2007). "GC-EI-TOF-MS analysis of in vivo carbon-partitioning into soluble metabolite pools of higher plants by monitoring isotope dilution after (CO₂)-C-13 labelling." Phytochemistry **68**(16-18): 2258-2272.
- Hummel, I., F. Pantin, R. Sulpice, M. Piques, G. Rolland, M. Dauzat, A. Christophe, M. Pervent, M. Bouteillé, M. Stitt, Y. Gibon and B. Muller (2010). "*Arabidopsis* Plants Acclimate to Water Deficit at Low Cost through Changes of Carbon Usage: An Integrated Perspective Using Growth, Metabolite, Enzyme, and Gene Expression Analysis." Plant Physiology **154**(1): 357-372.
- Hummel, J., N. Strehmel, J. Selbig, D. Walther and J. Kopka (2010). "Decision tree supported substructure prediction of metabolites from GC-MS profiles." Metabolomics **6**(2): 322-333.

- Imlau, A., E. Truernit and N. Sauer (1999). "Cell-to-Cell and Long-Distance Trafficking of the Green Fluorescent Protein in the Phloem and Symplastic Unloading of the Protein into Sink Tissues." The Plant Cell Online **11**(3): 309-322.
- Jamet, E., M. Kopp and B. Fritig (1985). "The Pathogenesis-Related Proteins of Tobacco - their Labeling from C-14 Amino-Acids in Leaves Reacting Hypersensitively to Infection by Tobacco Mosaic-Virus." Physiological Plant Pathology **27**(1): 29-41.
- Junker, B. H., J. Lonien, L. E. Heady, A. Rogers and J. Schwender (2007). "Parallel determination of enzyme activities and in vivo fluxes in Brassica napus embryos grown on organic or inorganic nitrogen source." Phytochemistry **68**(16-18): 2232-2242.
- Kaiser, G. and U. Heber (1984). "Sucrose Transport into Vacuoles Isolated from Barley Mesophyll Protoplasts." Planta **161**(6): 562-568.
- Kaiser, G., E. Martinoia and A. Wiemken (1982). "Rapid Appearance of Photosynthetic Products in the Vacuoles Isolated from Barley Mesophyll Protoplasts by a New Fast Method." Zeitschrift Fur Pflanzenphysiologie **107**(2): 103-113.
- Kaplan, F., J. Kopka, D. Haskell, W. Zhao, K. Schiller, N. Gatzke, D. Sung and C. Guy (2004). "Exploring the temperature-stress metabolome of *Arabidopsis*." Plant Physiol **136**: 4159 - 4168.
- Kaplan, F., J. Kopka, D. W. Haskell, W. Zhao, K. C. Schiller, N. Gatzke, D. Y. Sung and C. L. Guy (2004). "Exploring the temperature-stress metabolome of *Arabidopsis*." Plant Physiology **136**(4): 4159-4168.
- King, R. W. and J. A. D. Zeevaart (1974). "Enhancement of Phloem Exudation from Cut Petioles by Chelating Agents." Plant Physiology **53**(1): 96-103.
- Kohorn, B. D., M. Kobayashi, S. Johansen, J. Riese, L.-F. Huang, K. Koch, S. Fu, A. Dotson and N. Byers (2006). "An *Arabidopsis* cell wall-associated kinase required for invertase activity and cell growth." The Plant Journal **46**(2): 307-316.
- Kopka, J., A. Fernie, W. Weckwerth, Y. Gibon and M. Stitt (2004). "Metabolite profiling in plant biology: platforms and destinations." Genome Biology **5**(6): 109.

Kopka, J., N. Schauer, S. Krueger, C. Birkemeyer, B. Usadel, E. Bergmuller, P. Dormann, W. Weckwerth, Y. Gibon, M. Stitt, L. Willmitzer, A. R. Fernie and D. Steinhauser (2005). "GMD@CSB.DB: the Golm Metabolome Database." Bioinformatics **21**(8): 1635-1638.

Kriedemann, P. (1986). "Stomatal and Photosynthetic Limitations to Leaf Growth." Functional Plant Biology **13**(1): 15-31.

Kueger, S., D. Steinhauser, L. Willmitzer and P. Giavalisco (2012). "High-resolution plant metabolomics: from mass spectral features to metabolites and from whole-cell analysis to subcellular metabolite distributions." The Plant Journal **70**(1): 39-50.

Lebreton, A., C. Saveanu, L. Decourty, J. C. Rain, A. Jacquier and M. Fromont-Racine (2006). "A functional network involved in the recycling of nucleocytoplasmic pre-60S factors." Journal of Cell Biology **173**(3): 349-360.

Lee, Y. P., A. J. Fleming, C. Körner and F. Meins Jr (2009). "Differential expression of the CBF pathway and cell cycle-related genes in *Arabidopsis* accessions in response to chronic low-temperature exposure." Plant Biology **11**(3): 273-283.

Lin, Y.-H., M.-H. Lin, P. M. Gresshoff and B. J. Ferguson (2011). "An efficient petiole-feeding bioassay for introducing aqueous solutions into dicotyledonous plants." Nat. Protocols **6**(1): 36-45.

Lin, Y. H., B. J. Ferguson, A. Kereszt and P. M. Gresshoff (2010). "Suppression of hypernodulation in soybean by a leaf-extracted, NARK- and Nod factor-dependent, low molecular mass fraction." New Phytologist **185**(4): 1074-1086.

Lisec, J., N. Schauer, J. Kopka, L. Willmitzer and A. R. Fernie (2006). "Gas chromatography mass spectrometry-based metabolite profiling in plants." Nat Protoc **1**(1): 387-396.

Lockhart, J. A. (1965). "An analysis of irreversible plant cell elongation." Journal of Theoretical Biology **8**(2): 264-275.

Luedemann, A., K. Strassburg, A. Erban and J. Kopka (2008). TagFinder for the quantitative analysis of gas chromatography-mass spectrometry (GC-MS)-based metabolite profiling experiments. **24**: 732-737.

Ma, J., M. Hanssen, K. Lundgren, L. Hernández, T. Delatte, A. Ehlert, C.-M. Liu, H. Schluepmann, W. Dröge-Laser, T. Moritz, S. Smeekens and J. Hanson (2011). "The sucrose-

regulated *Arabidopsis* transcription factor bZIP11 reprograms metabolism and regulates trehalose metabolism." New Phytologist **191**(3): 733-745.

Masakapalli, S. K., P. Le Lay, J. E. Huddleston, N. L. Pollock, N. J. Kruger and R. G. Ratcliffe (2010). "Subcellular Flux Analysis of Central Metabolism in a Heterotrophic *Arabidopsis* Cell Suspension Using Steady-State Stable Isotope Labeling." Plant Physiology **152**(2): 602-619.

Mizukami, Y. (2001). "A matter of size: developmental control of organ size in plants." Current Opinion in Plant Biology **4**(6): 533-539.

Mordacq, L., M. Mousseau and E. Deleens (1986). "A ¹³C method of estimation of carbon allocation to roots in a young chestnut coppice." Plant, Cell & Environment **9**(9): 735-739.

Morris, C. J., J. F. Thompson and C. M. Johnson (1969). "Metabolism of Glutamic Acid and N-Acetylglutamic Acid in Leaf Discs and Cell-free Extracts of Higher Plants." Plant Physiology **44**(7): 1023-1026.

Morris, D. A. and G. Kadir (1972). "Pathways of auxin transport in the intact pea seedling (*Pisum sativum* L.)." Planta **107**(2): 171-182.

Muller, B., G. Bourdais, B. Reidy, C. Bencivenni, A. Massonneau, P. Condamine, G. Rolland, G. Conéjéro, P. Rogowsky and F. Tardieu (2007). "Association of Specific Expansins with Growth in Maize Leaves Is Maintained under Environmental, Genetic, and Developmental Sources of Variation." Plant Physiology **143**(1): 278-290.

Murashige, T. and F. Skoog (1962). "A Revised Medium for Rapid Growth and Bio Assays with Tobacco Tissue Cultures." Physiologia Plantarum **15**(3): 473-497.

Nargund, S. and G. Sriram (2013). "Designer labels for plant metabolism: statistical design of isotope labeling experiments for improved quantification of flux in complex plant metabolic networks." Molecular Biosystems **9**(1): 99-112.

Oparka, C. M. D., O.A.M. Prior, D.B. Fisher (1994). "Real-time imaging of phloem unloading in the root tip of *Arabidopsis*." The Plant Journal **6**(5): 8.

Oparka, K. J., D. A. M. Prior and K. M. Wright (1995). Symplastic communication between primary and developing lateral roots of *Arabidopsis thaliana*. **46**: 187-197.

Orians, C. M., S. D. P. Smith and L. Sack (2005). "How are leaves plumbed inside a branch? Differences in leaf-to-leaf hydraulic sectoriality among six temperate tree species." Journal of Experimental Botany **56**(418): 2267-2273.

Pantin, F., T. Simonneau and B. Muller (2012). "Coming of leaf age: control of growth by hydraulics and metabolics during leaf ontogeny." New Phytologist **196**(2): 349-366.

Pantin, F., T. Simonneau, G. Rolland, M. Dauzat and B. Muller (2011). "Control of Leaf Expansion: A Developmental Switch from Metabolics to Hydraulics." Plant Physiology **156**(2): 803-815.

Parent, B. and F. Tardieu (2012). "Temperature responses of developmental processes have not been affected by breeding in different ecological areas for 17 crop species." New Phytologist **194**(3): 760-774.

Paul, M. J. and C. H. Foyer (2001). "Sink regulation of photosynthesis." Journal of Experimental Botany **52**(360): 1383-1400.

Peterson, B. J. and B. Fry (1987). "Stable Isotopes in Ecosystem Studies." Annual Review of Ecology and Systematics **18**(ArticleType: research-article / Full publication date: 1987 / Copyright © 1987 Annual Reviews): 293-320.

Roessner-Tunali, U., J. Liu, A. Leisse, I. Balbo, A. Perez-Melis, L. Willmitzer and A. R. Fernie (2004). "Kinetics of labelling of organic and amino acids in potato tubers by gas chromatography-mass spectrometry following incubation in ¹³C labelled isotopes." The Plant Journal **39**(4): 668-679.

Roessner, U., C. Wagner, J. Kopka, R. N. Trethewey and L. Willmitzer (2000). "Simultaneous analysis of metabolites in potato tuber by gas chromatography-mass spectrometry." The Plant Journal **23**(1): 131-142.

Rolland, F., E. Baena-Gonzalez and J. Sheen (2006). "Sugar Sensing and Signaling in Plants: Conserved and Novel Mechanisms." Annual Review of Plant Biology **57**(1): 675-709.

Roscher, A., N. J. Kruger and R. G. Ratcliffe (2000). "Strategies for metabolic flux analysis in plants using isotope labelling." Journal of Biotechnology **77**(1): 81-102.

Schaefer, J., L. D. Kier and E. O. Stejskal (1980). "Characterization of Photorespiration in Intact Leaves Using ¹³Carbon Dioxide Labeling." Plant Physiology **65**(2): 254-259.

Schaefer, J., E. O. Stejskal and C. F. Beard (1975). "Carbon-13 Nuclear Magnetic Resonance Analysis of Metabolism in Soybean Labeled by $^{13}\text{CO}_2$." Plant Physiology **55**(6): 1048-1053.

Schauer, N., D. Steinhauser, S. Strelkov, D. Schomburg, G. Allison, T. Moritz, K. Lundgren, U. Roessner-Tunali, M. G. Forbes, L. Willmitzer, A. R. Fernie and J. Kopka (2005). "GC-MS libraries for the rapid identification of metabolites in complex biological samples." FEBS Lett **579**(6): 1332-1337.

Schmidt, S. (2013). Untersuchung des Einflusses der stressregulierten reil homologen Gene auf die Physiologie und den Metabolismus von *Arabidopsis thaliana*. Max Planck Institut für Molekulare Pflanzenphysiologie; Applied Metabolome Analysis, Universität Potsdam.

Schmidt, S., F. Dethloff, O. Beine-Golovchuk and J. Kopka (2013). "The REIL1 and REIL2 Proteins of *Arabidopsis thaliana* are required for Leaf Growth in the Cold." Plant Physiology.

Shindo, C., G. Bernasconi and C. S. Hardtke (2007). "Natural Genetic Variation in *Arabidopsis*: Tools, Traits and Prospects for Evolutionary Ecology." Annals of Botany **99**(6): 1043-1054.

Simard, S., D. Durall and M. Jones (1997). "Carbon allocation and carbon transfer between *Betula papyrifera* and *Pseudotsuga menziesii* seedlings using a ^{13}C pulse-labeling method." Plant and Soil **191**(1): 41-55.

Solecka, D. (1997). "Role of phenylpropanoid compounds in plant responses to different stress factors." Acta Physiologiae Plantarum **19**(3): 257-268.

Somerville, C., S. Bauer, G. Brininstool, M. Facette, T. Hamann, J. Milne, E. Osborne, A. Paredez, S. Persson, T. Raab, S. Vorwerk and H. Youngs (2004). "Toward a systems approach to understanding plant-cell walls." Science **306**(5705): 2206-2211.

Sovonick, S. A., D. R. Geiger and R. J. Fellows (1974). "Evidence for Active Phloem Loading in the Minor Veins of Sugar Beet." Plant Physiology **54**(6): 886-891.

Stitt, M. and A. R. Fernie (2003). "From measurements of metabolites to metabolomics: an 'on the fly' perspective illustrated by recent studies of carbon–nitrogen interactions." Current Opinion in Biotechnology **14**(2): 136-144.

Stitt, M. and S. C. Zeeman (2012). "Starch turnover: pathways, regulation and role in growth." Current Opinion in Plant Biology **15**(3): 282-292.

Strand, A., V. Hurry, S. Henkes, N. Huner, P. Gustafsson, P. Gardestrom and M. Stitt (1999). "Acclimation of *Arabidopsis* leaves developing at low temperatures. Increasing cytoplasmic volume accompanies increased activities of enzymes in the Calvin cycle and in the sucrose-biosynthesis pathway." Plant Physiology **119**(4): 1387-1397.

Strassburg, K., D. Walther, H. Takahashi, S. Kanaya and J. Kopka (2010). "Dynamic Transcriptional and Metabolic Responses in Yeast Adapting to Temperature Stress." Omics-a Journal of Integrative Biology **14**(3): 249-259.

Strehmel, N., J. Hummel, A. Erban, K. Strassburg and J. Kopka (2008). "Retention index thresholds for compound matching in GC-MS metabolite profiling." J Chromatogr B Analyt Technol Biomed Life Sci **871**(2): 182-190.

Sulpice, R., E. T. Pyl, H. Ishihara, S. Trenkamp, M. Steinfath, H. Witucka-Wall, Y. Gibon, B. Usadel, F. Poree, M. C. Piques, M. Von Korff, M. C. Steinhauser, J. J. B. Keurentjes, M. Guenther, M. Hoehne, J. Selbig, A. R. Fernie, T. Altmann and M. Stitt (2009). "Starch as a major integrator in the regulation of plant growth." Proceedings of the National Academy of Sciences of the United States of America **106**(25): 10348-10353.

Sulpice, R., S. Trenkamp, M. Steinfath, B. Usadel, Y. Gibon, H. Witucka-Wall, E.-T. Pyl, H. Tschoep, M. C. Steinhauser, M. Guenther, M. Hoehne, J. M. Rohwer, T. Altmann, A. R. Fernie and M. Stitt (2010). "Network Analysis of Enzyme Activities and Metabolite Levels and Their Relationship to Biomass in a Large Panel of *Arabidopsis* Accessions." The Plant Cell Online **22**(8): 2872-2893.

Szeczowka, M., R. Heise, T. Tohge, A. Nunes-Nesi, D. Vosloh, J. Huege, R. Feil, J. Lunn, Z. Nikoloski, M. Stitt, A. R. Fernie and S. Arrivault (2013). "Metabolic Fluxes in an Illuminated *Arabidopsis* Rosette." Plant Cell **25**(2): 694-714.

Taji, T., C. Ohsumi, S. Iuchi, M. Seki, M. Kasuga, M. Kobayashi, K. Yamaguchi-Shinozaki and K. Shinozaki (2002). "Important roles of drought- and cold-inducible genes for galactinol synthase in stress tolerance in *Arabidopsis thaliana*." Plant J **29**(4): 417-426.

Timm, S., A. Nunes-Nesi, T. Pamik, K. Morgenthal, S. Wienkoop, O. Keerberg, W. Weckwerth, L. A. Kleczkowski, A. R. Fernie and H. Bauwe (2008). "A Cytosolic Pathway for the Conversion of Hydroxypyruvate to Glycerate during Photorespiration in *Arabidopsis*." Plant Cell **20**(10): 2848-2859.

- Turgeon, R. (1989). "The Sink-Source Transition in Leaves." Annual Review of Plant Physiology and Plant Molecular Biology **40**: 119-138.
- Turgeon, R. and L. E. Wimmers (1988). "Different Patterns of Vein Loading of Exogenous [¹⁴C]Sucrose in Leaves of *Pisum sativum* and *Coleus blumei*." Plant Physiology **87**(1): 179-182.
- Van Winden, W. A., C. Wittmann, E. Heinzle and J. J. Heijnen (2002). "Correcting mass isotopomer distributions for naturally occurring isotopes." Biotechnology and Bioengineering **80**(4): 477-479.
- Wagner, C., M. Sefkow and J. Kopka (2003). "Construction and application of a mass spectral and retention time index database generated from plant GC/EI-TOF-MS metabolite profiles." Phytochemistry **62**(6): 887-900.
- Walter, A., W. K. Silk and U. Schurr (2009). Environmental Effects on Spatial and Temporal Patterns of Leaf and Root Growth. Annual Review of Plant Biology. **60**: 279-304.
- Wang, H., Q. Qi, P. Schorr, Adrian J. Cutler, W. L. Crosby and L. C. Fowke (1998). "ICK1, a cyclin-dependent protein kinase inhibitor from *Arabidopsis thaliana* interacts with both Cdc2a and CycD3, and its expression is induced by abscisic acid." The Plant Journal **15**(4): 501-510.
- Watanabe, M., S. Balazadeh, T. Tohge, A. Erban, P. Giavalisco, J. Kopka, B. Mueller-Roeber, A. R. Fernie and R. Hoefgen (2013). "Comprehensive dissection of spatio-temporal metabolic shifts in primary, secondary and lipid metabolism during developmental senescence in *Arabidopsis thaliana*." Plant Physiology.
- Wichern, F., J. Mayer, R. Joergensen and T. Müller (2010). "Evaluation of the wick method for in situ ¹³C and ¹⁵N labelling of annual plants using sugar-urea mixtures." Plant and Soil **329**(1-2): 105-115.
- Wickman, F. E. (1952). "Variations in the relative abundance of the carbon isotopes in plants." Geochimica et Cosmochimica Acta **2**(4): 243-254.
- Wittmann, C. and E. Heinzle (1999). "Mass spectrometry for metabolic flux analysis." Biotechnology and Bioengineering **62**(6): 739-750.

Wood, L., N. W. Gray, Z. Zhou, M. E. Greenberg and G. M. G. Shepherd (2009). "Synaptic Circuit Abnormalities of Motor-Frontal Layer 2/3 Pyramidal Neurons in an RNA Interference Model of Methyl-CpG-Binding Protein 2 Deficiency." The Journal of Neuroscience **29**(40): 12440-12448.

Wormit, A., S. M. Butt, I. Chairam, J. F. McKenna, A. Nunes-Nesi, L. Kjaer, K. O'Donnelly, A. R. Fernie, R. Woscholski, M. C. L. Barter and T. Hamann (2012). "Osmosensitive Changes of Carbohydrate Metabolism in Response to Cellulose Biosynthesis Inhibition." Plant Physiology **159**(1): 105-117.

Wright, K. M. and K. J. Oparka (1997). "Metabolic inhibitors induce symplastic movement of solutes from the transport phloem of *Arabidopsis* roots." Journal of Experimental Botany **48**(10): 1807-1814.

Zaas, A. K., G. Liao, J. W. Chien, C. Weinberg, D. Shore, S. S. Giles, K. A. Marr, J. Usuka, L. H. Burch, L. Perera, J. R. Perfect, G. Peltz and D. A. Schwartz (2008). "Plasminogen Alleles Influence Susceptibility to Invasive Aspergillosis." PLoS Genet **4**(6): e1000101.

Zhang, Y., M. A. Equiza, Q. Zheng and M. T. Tyree (2011). "Factors controlling plasticity of leaf morphology in *Robinia pseudoacacia*: III. biophysical constraints on leaf expansion under long-term water stress." Physiologia Plantarum **143**(4): 367-374.

Zook, M. and R. Hammerschmidt (1997). "Origin of the Thiazole Ring of Camalexin, a Phytoalexin from *Arabidopsis thaliana*." Plant Physiology **113**(2): 463-468.

Zuther, E., K. Buchel, M. Hundertmark, M. Stitt, D. K. Hinch and A. G. Heyer (2004). "The role of raffinose in the cold acclimation response of *Arabidopsis thaliana*." FEBS Lett **576**(1-2): 169-173.